A THERMODYNAMIC STUDY OF METHANE MULTILAYERS ADSORBED ON GRAPHITE

Thesis by

Jeffrey John Hamilton

In Partial Fulfillment of the Requirements

for the Degree of

Doctor of Philosophy

California Institute of Technology

Pasadena, California

1983

(Submitted May 23, 1983)

Acknowledgments

By definition, thesis advisors are those who give advice. Finding himself faced with this charge, David Goodstein has acquitted himself quite well, for not only has he given advice freely, but it has been so consistently timely and incisive that a measure of sound judgment has no doubt rubbed off on his wayward student. For this I gladly thank him.

Furthermore, in a project such as this the contributions of many individuals are necessarily apparent. Accordingly, I must extend my sincere thanks to all members of the Caltech Low Temperature Physics group, past and present, for the help they have given me along the way. I am especially mindful of the work of Edward Boud, and member-at-large Milton Cole.

I have had help in other ways too, namely through the intangible bonds of freindship. Thus, the contributions of my parents, John and Catherine Hamilton; the H. R. Gregory family of Pasadena, and the usual party of weekend adventurers are all in there somewhere, even if not readily visible.

This work was supported in part by a grant from the Department of Energy, DE-AM03-76SF000767.

Abstract

Thermodynamic measurements of the properties of methane adsorbed on graphite have been made in the range, roughly, of 1-6 molecular layers and 64-105 K. Interpreting the results in the context of current models, a tentative conclusion that layer by layer critical points occur at approximately constant temperature near 78 K is drawn. A line of melting transitions extending from the bulk triple point, T_t=90.66 K, into the multilayer region at temperatures near 90 K is also observed, and while these transitions do not appear to be first order, there is an associated change in entropy. This change in entropy gradually diminishes, and vanishes entirely at about two layers. It is not clear how this line of transitions ends, but it is thermodynamically forbidden from ending in a critical point. Finally, the Landau potential has been constructed and tabulated as a function of its proper variables, namely temperature and chemical potential. This gives a complete thermodynamic description of the methane film in the range studied.

Table of Contents

List of Figures

Chapter 1. INTRODUCTION AND HISTORICAL MOTIVATION

Order and Disorder

The field of low temperature physics (or, if you will, condensed matter physics) has a rich and illustrious history whose exact moment of birth is difficult to pinpoint. Certainly, an early milestone would be Faraday's accidental liquefaction of chlorine gas in 1823. Though his discovery came about by chance, Faraday nevertheless was quick to realize its significance, and in doing so started a chain of events which culminated in Kammerlingh-Onnes' liquefaction of helium in 1908. Since then a rich industry (academic as well as commercial) has built up to the point where it is hard to imagine any substance, metal or insulator, element or compound, which has not been at some time melted, boiled, frozen, compressed, pondered about, or otherwise probed at length in order to determine its thermal characteristics. Through all of this multitude of investigation, one theme has come up time and again: namely, what is the difference between an ordered state and a disordered state?

Order, though easy enough to recognize when present, is difficult to define in rigorous terms. Certainly, one element in this description is entropy. Ordered states, it seems, have low entropy. Thus, we can say that a solid is ordered while a liquid is disordered because in changing a solid to a liquid at fixed pressure one must add a known amount of entropy per particle to break up the crystalline lattice. (Furthermore, the addition of this entropy - i.e. heat -

does *not* raise the temperature at the melting transition; it simply "randomizes" the substance.)

However, entropy cannot be the only consideration because there is a certain class of phenomena (critical phase transitions) in which the entropy *does not change* in going through the transition. Thus, a superconductor close to its transition temperature (T_c), for example, has the same entropy whether it is in the "disordered" state (just above T_c), or the "ordered" state (just below T_c). Moreover, since the entropy of metals at temperatures near 10 K is very low anyway, one might say that normal metals are "almost as ordered" as superconductors despite their striking conductive differences.

This brings us to another complication. Order, in fact, is relative. In comparing a solid to a liquid we conclude that the solid is ordered and the liquid disordered. Yet in comparing the same liquid to a gas we would conclude that the liquid is ordered and the gas disordered. Thus, it appears that order depends in some way on the structural symmetries (using "structure" in a generalized sense) of the medium in question. Solids clearly have the positional structure symmetries of the crystalline lattice. Liquids, on the other hand, have a greater symmetry (being isotropic) but a less well defined structure. Nevertheless, they do have more structure than gases which, in the limit of infinite temperature, have no structure whatsoever.

So then, if we cool a liquid to its point of solidification, we lose the symmetries of rotational and translational invariance. (They are replaced by the point group symmetries of the crystalline lattice which are countable in number.) However, since space is isotropic, this fact must be reflected in the possible states in which solids can exist. Indeed, we find that the isotropy of space is "restored" because there is a uniformly distributed family of possible positions and orientations for crystalline lattices, and for reasons which are

governed by extraneous details, the solid has chosen but one member of this family. Thus, whenever a symmetry is spontaneously broken, we attribute this to the emergence of order. (It should be noted, however, that nature has afforded us with some cases in which the ordered state is the more symmetrical one; these, though, are in contrast to the general rule.)

Two-Dimensional Thermodynamics

The world we live in is, of course, three dimensional. Yet the language we use to describe the physical laws of this world (that is to say, the language of mathematics) is one which need not be tied to a particular dimensionality in any way. Thus, it came about that in considering three-dimensional solids, Peierls and Landau independently realized that the type of order we usually associate with a crystalline lattice could not exist in a two-dimensional universe. It turns out that in a three-dimensional crystal the position of an atom at the origin is correlated with the positions of all the other atoms, including those which are infinitely far away. This causes x-rays, for example, to scatter coherently in certain directions and produce sharp Bragg diffraction peaks. In a two-dimensional crystal, however, the position of the atom at the origin is correlated only with the positions of its neighboring atoms, and as we move infinitely far away we find that the atoms have lost all information about the position of the one at the origin. Bogoliubov and others then followed with similar arguments to show that the types of order we associate with superconductors, superfluids, ferromagnets, and other systems are also excluded from a two-dimensional world. Thus, there arose a very interesting question: since certain types of order are impossible in two-dimensions, does this mean that their corresponding *ordered states* are also forbidden? For a long time, many people assumed that the answer was *yes*. In other words, they felt that two-dimensional solids, superfluids,

superconductors, and so on, really could not exist. However, this view appeared to contradict the third law of thermodynamics which holds that all matter becomes ordered as the temperature approaches absolute zero. (Dimensionality plays no role in the third law.) This paradox has now been resolved, owing to various theoretical and experimental advances made since the 1960's. The answer now appears to be that, in principle, two-dimensional ordered states *can* exist, but that we must be more careful in the way we define order.

The reader may well appreciate the nature of theoretical advances made in the field of two-dimensional thermodynamics, but given the fact that the world is three-dimensional, how can experiments shed light on the subject? The answer is simple: we study systems of atoms and molecules which are adsorbed onto the surface of a substrate, and for the most part are constrained to move about on a two-dimensional surface. Molecules in such systems are bound to the substrates with energies typically of the order of tens or hundreds of milli-electron-volts (meV) and are said to be "physisorbed". They are free in many ways to move about on the surface as if they were in an ideal two-dimensional plane (although the surface properties can sometimes have profound effects). Distinct from this type of situation is that of the "chemisorbed" molecules. These are bound to the substrates with energies of 1 eV or so, and are often locked into place unable to move about. Chemisorbed molecules can be highly reactive, and are of interest to those, for example, who study surface catalysis. Physisorbed molecules, on the other hand, are chemically inert and (save for subtle influences) do no change - or are not changed by - the substrate. In what follows, we will consider only physisorbed molecular systems. Furthermore, in making this choice we will focus our attention on the three classical states of matter: solids, liquids, and gases. Such exotic states as superconductivity and superfluidity will no longer play a role in our discussion.

One would say that the experimental situation took a quantum leap in the late 1960's with the introduction of a specific substrate: exfoliated graphite. Previous work had been done on such substrates as titanium dioxide (jeweler's rouge), porous glass, sintered copper, and various forms of carbon black. In all cases, it is desired to have the substrate take the form of a highly interconnected three-dimensional network in order to expose the largest area possible to the adsorption molecules. A substrate possessing a large internal surface area is mandatory since the thermal signals from the adsorbed film must stand out clearly above those of the background. These background signals come from the body of the experimental cell - a bulk item - and can dwarf any signals from the film unless an exceptionally large area substrate is used. Exfoliated graphite, happily, meets this challenge and provides an internal surface area of about 20 m^2 per gram. However, its most striking feature is not its surface area, but rather its homogeneity. Substrates in the past all had the disadvantage that they exposed adsorption sites to the molecules which were highly non-uniform in binding energy and surface structure. Exfoliated graphite, on the other hand, is prepared in such a way that it exposes large areas of the (0001) basal plane for adsorption. Thus, the molecules see large patches of a smooth surface in which the number of binding sites with energies radically different from the average is only a few per cent.

This exceptional surface uniformity produced two striking effects in adsorption isotherm vapor pressure studies which had been seen before only with poor resolution. The first was the observance of sharp layer formation as the number of molecules on the surface was gradually increased. In other words, after the molecules had filled up a single uniform layer one molecule thick, a second similar layer would abruptly begin to form on top of the first. When the second layer was full, a third would form, and so on until as many as six or seven layers were

seen on the surface. In all the previous studies, the layers would be indistinct, smeared into one another, and demonstrate no more than a general increase in adsorbed film thickness as molecules were deposited. The second effect was most clearly seen in the first monolayer, which is exactly where we would expect the molecules to take on two-dimensional behavior. A plot of the number adsorbed versus the film's chemical potential (of which the pressure of the three-dimensional gas in equilibrium with it was a measure), would show jump discontinuities in various regimes. These discontinuities were strikingly reminiscent of those found in similar plots for bulk substances in regions of two-phase coexistence. Thus, it appeared that the molecules in single absorbed monolayer formed self-condensed "liquids", tenuous "gases", and even what seemed to be "solids" all in a two-dimensional world.

This indeed turned out to be the case. The submonolayer films had their own solid-liquid-gas phase diagrams in direct correspondence to their bulk counterparts. The liquid-gas portion even came complete with a two-dimensional critical temperature. However, proving that this was the case took a great deal of ingenuity and hard work. The answer was provided independently by two types of other experiments. In the first type neutrons (for example) were scattered from the absorbed molecules. It was shown that the two-dimensional (2D) solid was indeed rigid and incompressible; the 2D liquid mobile, but still incompressible, and the 2D gas mobile and compressible. The second type of experiment was at once more elegant and more powerful. It could be used with any adsorbent (not just those with good neutron scattering cross-sections), and yielded a wealth of information beyond simple questions of surface mobility. Experiments of this type used what shall be called now and hereafter the "thermodynamic technique".

Basically, the thermodynamic technique consists of making two types of measurements (heat capacity and vapor pressure) over a wide range of coverage and temperature. From this information we can obtain a complete thermodynamic description of the states of the absorbed system. This description will yield all response functions (compressibilities, and heat capacities among them) which demarcate phase boundaries, and other quantities such as binding energies and spreading pressures (the 2D analog to real pressure). Moreover, working in conjunction with certain theories, the thermodynamic technique can even address questions of the relative order of the various states.

Adding the Third Dimension

Since the late 1960's a great deal of work has been done in the area of two-dimensional thermodynamics. Now that the existence of two-dimensional ordered states has gained widespread acceptance, it would seem that the objections of Bogoliubov et al. have been laid to rest. But have they? Certainly, if we now examine the question on a deeper level the paradox is still there. Given that 2D ordered states are fundamentally different from their 3D counterparts (at least in the way their order is defined), how does this difference manifest itself as one makes a transition from a bulk type of material to a two-dimensional type? That is, what form does order take in a two-layer film? a three-layer film? and so on?

This is precisely the question we hope to address, and in attempting to find at least a partial answer, we shall employ the thermodynamic technique.

The specific system which has been chosen for study is methane gas adsorbed onto exfoliated graphite. The reasons for this choice are numerous, and will be detailed in the next chapter, but one in particular should be mentioned here. As was implied above, the two types of experiments, surface

mobility probes and thermodynamic measurements, can complement each other very nicely. In the case of methane, an NMR study can reveal information about its dynamical state on the graphite surface, and this can be compared to the thermodynamic information at hand. It is intended that the NMR measurements will be made in a companion study, and that the two sets of data will be combined at a future date.

Chapter 2. EXPERIMENTAL APPARATUS AND METHODS

The Methane-Graphite System

The methane molecule, CH_4, is arranged with four hydrogen atoms at the points of a regular tetrahedron, and a carbon atom at the body center. The C-H distance is 1.091 Å, and the electron cloud extends to a radius of about 1.8 Å. Because of its structure, the potential energy between two molecules a distance r apart is well represented by a spherical form compared to other polyatomic molecules. Parameters to fit this potential to the Lennard-Jones 6-12 form exist, but due to the molecule's "proton skeleton", its hard core is more repulsive than an r^{-12} dependence would have it. Consequently, the best simple form for the intermolecular potential is a 6-20 potential with a hard core diameter of 3.559 Å and a well depth of 217 K† [1].

In free space the methane molecule is a spherical rotator possessing a moment of inertia of 5.313×10^{-40} g-cm^2. This corresponds to a quantum rotational energy level of $\hbar^2/Ik_B$ = 15.16 K. The consequences of methane's rotational states are easily seen in the bulk phase diagram where, at a temperature of 20.5 K, it undergoes a solid-solid phase transition. In this change of state, the structural form remains the same (an FCC lattice both above and below the transition), but the individual molecules begin to rotate *in situ*. Below 20.5 K the solid is called the "β-phase", and above it is called the "α-phase", so that 20.5 K on the equilibrium coexistence vapor pressure curve represents the β-α-gas triple point. Not only has this β-α transition been seen in bulk, but it has been

† Intrinsic energies for the most part will be expressed in kelvins (1 K = 1.3806×10^{-16} ergs). These will include temperatures, chemical potentials, and binding energies.

found in quasi-two-dimensional films as well [2].

However in our case we will be devoting more attention to the upper triple point (α-liquid-gas), where melting occurs at a temperature of 90.66 K and a pressure of 87.5 torr, and to the liquid-gas critical point (190.6 K at 45.6 atm).

The substrate used in this experiment is known as Grafoil.† It is prepared from natural graphite crystals by allowing vapors to permeate the spaces between the hexagonal basal planes. Rapid heating causes the vapors to expand, thereby disintegrating the crystal into a large number of platelets which expose their basal planes to the environment. The platelets are typically 3 μm in diameter, and 100 Å thick (corresponding to about 33 planes). From there, the platelets are compressed into sheets typically ten-thousandths of an inch thick, and this final product is of commercial interest as a gasket material. We used an expanded form of Grafoil, known as "Grafoil foam" in which the sheets had not yet been compressed to their final thickness. The density of Grafoil in this form is only 7% of the bulk solid density (2.25 g/cm^3), meaning that a typical distance between platelets is 0.5 μm. (Bear in mind, however, that the platelets' edges come into contact, so that an interconnected three-dimensional framework is established.)

The basal plane of graphite has a honeycomb structure with a carbon atom at each of the six vertices of each hexagon. The distance between centers of adjacent hexagons is 2.459 Å [3], and the centers themselves form a triangular lattice. Under certain conditions an adsorbed film will have its atoms in a set geometrical arrangement with respect to these lattice sites, at which time the film is said to be "registered" or "commensurate". Registry allows the calibration of the adsorption surface area to high accuracy. If a gas handling

† *Grafoil* is a registered trademark of the Union Carbide Corporation.

apparatus gives us the number of adsorbed atoms to 0.1% (more about this later), and if the film is known to be registered (say, at a density of one atom for every three hexagons) then the total area is easily obtained to the same accuracy because the area of each hexagon is known to be 5.236 $Å^2$. Finally, the last graphite dimension of importance is the distance between planes, namely 3.354 Å [3].

Previous adsorption studies of methane on exfoliated graphite have concentrated on the submonolayer regime, and have been of four types. These are vapor pressure isotherms [4–7], neutron scattering [8–10], nuclear magnetic resonance (NMR) [11,12], and heat capacities [13]. According to the combined intelligence of these studies, the first layer phase diagram looks something like that shown in Fig. 1. The details of Fig. 1 are, of course, subject to reinterpretation, but broadly speaking there is a 2D solid-liquid-gas triple point near 57 K, a 2D liquid-gas critical point near 75 K, various commensurate-incommensurate phase boundaries, and a solid-liquid coexistence region of small but finite thickness. (It is not known how this melting curve ends at high temperatures.) The commensurate solid has the structure of one methane molecule per three hexagons, with the molecules situated in a hexagonal super lattice rotated by 30° from the underlying basal plane symmetry direction. This structure is called the "$(\sqrt{3}\times\sqrt{3})R30°$" structure, where $\sqrt{3}$ signifies the methane/hexagon lattice constant ratio. Because there is one molecule per three hexagons, this phenomenon is called "one-third ordering", and the coverage at which it occurs is $N_{1/3}$.

A typical binding energy (that is, isosteric heat of adsorption) of a methane molecule to the graphite substrate is 1500 K [14], and this compares to about 1300 K which is the cohesive energy of solid methane. Such quantities give an indication of the vapor pressure of gas in equilibrium with a film. The upshot of

Figure 1. Methane First Layer Phase Diagram

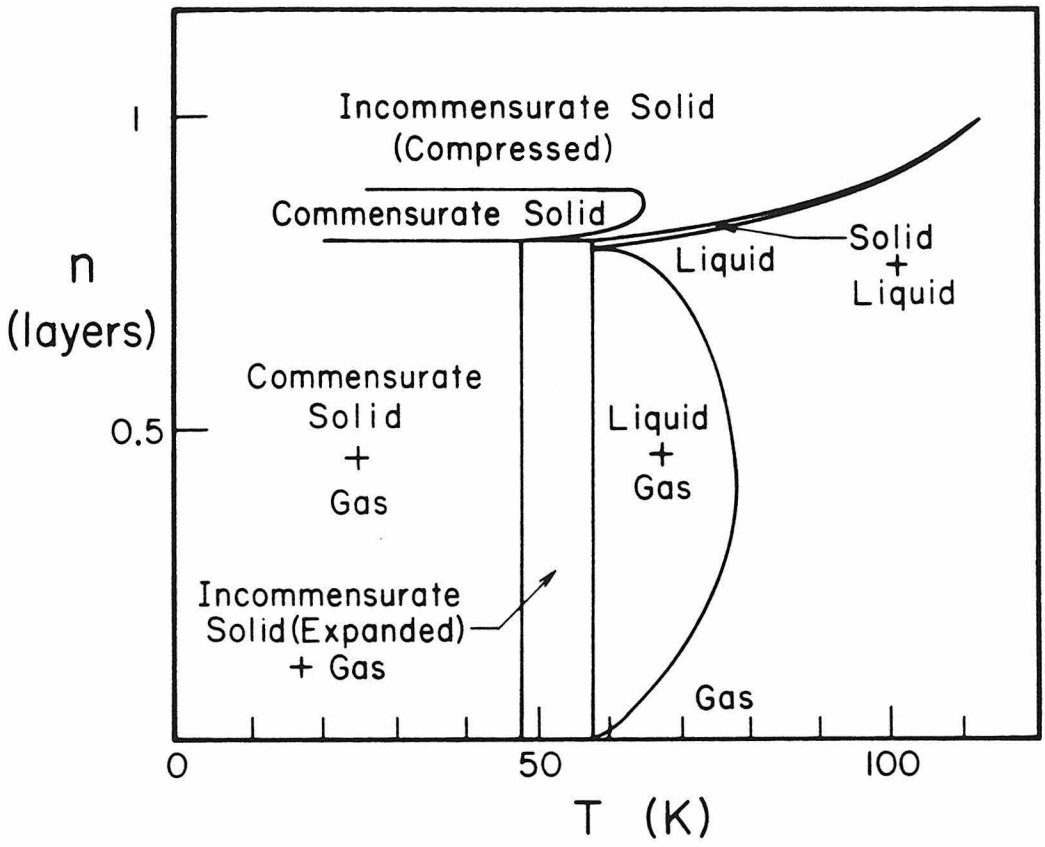

the difference between these two quantities is that vapor pressures of a sub-monolayer film are about one-thousandth of that of the saturated bulk vapor pressure. In cases where the temperature is near 77 K, these pressures are of the order of tens of millitorr and tens of torr respectively. As we shall see later, this will have a profound influence on keeping the film in thermal equilibrium.

Experimental Apparatus and Techniques

An adiabatic calorimeter cryostat was constructed as shown in Fig. 2. The heart of the cryostat is an aluminum cell filled with the Grafoil substrate and attached to a one meter long inlet tube whose inner diameter is 2 mm. Aluminum was chosen over copper (a more traditional material) because of the cell's high internal volume (80.4 cm^3). Grafoil foam, being much less dense than regular Grafoil, was used because its open structure facilitates an even mass distribution when adsorbate molecules are introduced into the cell. This property proved crucial to the attainment of thermal equilibrium, and necessitated the cell's large volume. In order to keep the background heat capacity small, the cell wall dimensions had to be so thin that a copper cell would have been prohibitively fragile. Aluminum, though a worse conductor than copper, has a much lower heat capacity per unit volume and permitted the construction of a light yet robust cell.

The finished cell contains about 20 g of aluminum, 13 g of graphite, and less than 1 g of other materials. It is cylindrical in shape, roughly 3 cm in diameter and 10 cm high, and has a wall thickness of 0.25 mm (0.010 inch). For strength there are circular ribs at one inch intervals along the length of the cell body. These ribs (three in all) are about 1 mm thick, and 1 mm wide. The top and bottom are thicker than the body wall, and a rib along the bottom houses two resistance thermometers: one platinum and one germanium.

Figure 2. The Experimental Apparatus

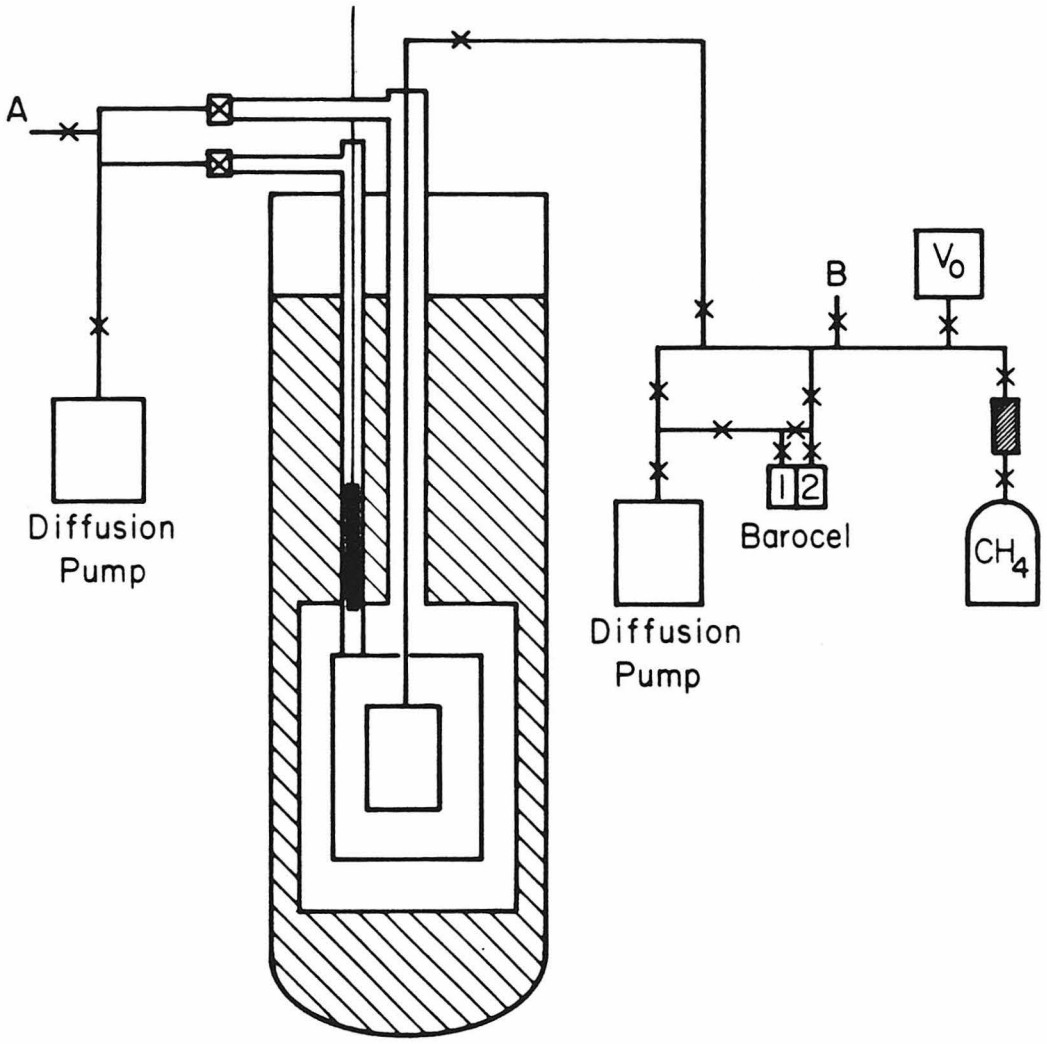

One disadvantage to working with aluminum is that it cannot be sealed vacuum tight by soldering. Consequently, after the graphite was packed in, the cap of the cell was joined to the main body by using six miniature stainless steel screws to compress an indium o-ring seal. (This seal had been provided when the cell was originally machined.) A miniature threaded flange for the screws formed a lip at the top of the cell body, and thus the screws are a permanent part of the completed cell.

Prior to this, a 1 mm diameter stainless steel tube had been force-fit through a hole in the center of the the cell cap. This tube is about one inch in length, and stycast epoxy was applied to both sides of the joint where the tube protruded. This formed a vacuum tight neck to which the 2 mm diameter inlet tube could be conveniently soldered. When the cell was finished, an 800 Ω length of evanohm wire was wound around the cell's exterior and glued in place. (Here again the traditional choice of glue - GE 7031 varnish - had to be discarded because it would not adhere to the aluminum. A suitable substitute was found to be Duco Cement thinned with acetone.) This wire is the heating element used to raise the cell's temperature. The inlet tube neck also has a heater wire (80 Ω) as does the rest of the length of the inlet tube (its heater being independent of the neck's).

Prior to its placement in the cell, the Grafoil was heated to a temperature of 800° C inside a chamber evacuated by a liquid nitrogen trapped diffusion pump. It was held this way for a number of hours in order to drive out any remnant impurities on the basal plane surfaces. In being transferred to the cell, the Grafoil was, of course, exposed to air. However repeated flushings with helium gas and pumping down to the 10^{-6} torr range when the cell was complete insured a clean substrate by the time an experiment was attempted. The Grafoil took the form of twenty disks one inch in diameter and a quarter inch thick.

These were press fit into the cell to insure good thermal contact. The Grafoil completely filled the internal volume of the cell, but as solid graphite comprises only 7% of the space occupied, this left a dead volume in the cell of 80.4 cm^3. Finally, at this point a stiff wire was used to poke holes through the disks to aid in the distribution of gas molecules throughout the cell.

Given that aluminum does not conduct heat as well as copper, there was some question as to what the thermal response of the cell would be when calorimetric measurements were made. Using thermal conductivity data from the National Bureau of Standards (NBS), it was estimated that heat could distribute itself throughout the metallic part of the cell on a time scale always less than 45 seconds. However, the metallic part of the cell comprises, in effect, only the outer surface, and it took a longer time for the heat to make its way into the cell's interior. The time scale for this step was found empirically (the NBS does not have data for Grafoil) to be three minutes at 80 K or so. Thus, after ten or fifteen minutes one could be sure that the heat from a heat pulse would be uniformly distributed throughout the cell.

One can now appreciate the need for thermal isolation if the cell is expected not to gain or lose any heat while the temperature becomes uniform. If absolute heat capacity measurements are to be made to an accuracy near 0.1%, then heat leaks must not alter the cell's temperature by more than a few millidegrees (for a 1 K rise in temperature) during the fifteen minutes or so which the experimenter waits. True thermal isolation is impossible, of course, but various features of the cryostat allow a working procedure which can compensate for heat leaks. As shown in Fig. 2, the cell is suspended in a vacuum isolation can which allows the cell's temperature to be raised above that of the bath. If the cell's temperature becomes too high, however, heat can escape through radiation to the colder inner surface of the vacuum can. To replace this

heat, a constant current can be made to flow through the heater wires on the inlet tube. However, this only compensates for the heat lost from above, and further measures are needed to protect the sides and bottom of the cell. Thus, (see Fig. 2), the cell is completely surrounded by a radiation shield† whose temperature can be independently manipulated. Typically, the shield's temperature is kept to within 1 K of the cell's, thereby minimizing the radiation loss. The shield is also made of aluminum, but it has a top plate made of copper which acts as a support buttress and from which the cell is suspended. Connected to the shield's top is a mechanical heat switch [15], which pierces the vacuum can at the top. The temperature of the shield can be manipulated in two ways. Either it can be set to a specific temperature using a self-balancing bridge arrangement, or it can use the signal from a four-junction chromel-alumel difference thermocouple to follow the temperature of the cell. (The reference junctions were attached to the cell, and the measuring junctions to the shield.) In the experiment, both modes of operation were employed with equal success, and thermometers on the cell and shield permit calorimetric measurements of this type in the range of 1-300 K.

Meanwhile, the top of the vacuum can is extended, in effect, to the top of the cryostat by a thin walled stainless steel tube one-half inch in diameter. Through this tube passes the cell's inlet fill tube, as well as some twenty-four electrical leads for the thermometers and heaters. Teflon spacers along the length of the fill tube prevented it from touching the sides of the outer tube which is always in intimate contact with the bath. Moreover, the electrical leads were thermally and mechanically anchored where they emerged in the interior of the vacuum can.

† The shield is called an "adiabatic shield", where the term *adiabatic* refers to the fact that no heat enters or leaves the cell during a measurement. Quantum-mechanically speaking, there is nothing "adiabatic" about it at all.

It is apparent from Fig. 2 that two independent high vacuum systems are used when an experiment is in progress. The vacuums in both systems are maintained by liquid-nitrogen trapped oil diffusion pumps capable of maintaining pressures in the 10^{-7} to 10^{-6} torr range.

The first vacuum system envelops the second inside the cryostat, and is used to maintain thermal isolation from the bath. Helium exchange gas can be administered through port A in order to bring all the components inside the vacuum can to the bath temperature at the beginning of a run. The gas is then pumped out when thermal isolation is desired.

The second vacuum system plays a more crucial role in measurement process, and it is the mechanism by which methane gas is put into the cell. Its main features, apart from the diffusion pump, are a two-liter calibrated volume (V_0), and a Barocel capacitive manometer [16]. The Barocel has an electronic readout which displays 4½ digits of precision, and these 4½ digits can be used to graduate a full scale of 1000, 100, 10, or 1 torr. Thus, the smallest change detectable in a pressure reading is 0.01% of full scale, and this corresponds to 0.1 millitorr on the lowest scale. The Barocel's sensor head contains two chambers, and the readout gives the difference in pressure between chamber 2 and chamber 1 (as labelled in Fig. 2). In all cases chamber 1 was kept evacuated so that the reading was, in effect, an absolute measure of the pressure in chamber 2. The volume of V_0 was found by filling it with water and measuring the water's volume with a graduated cylinder. The value was found to be 2015 cm^3 with an overall accuracy of ±0.05% (about 1 cm^3 total). When this (dry) calibrated volume was connected to the rest of the system, it permitted the computation of all the other volumes by gas expansion. In this way, the volumes of connecting tubing, the Barocel chambers, open valves, and the experimental cell were all found.

Precise amounts of methane gas (or other gases introduced through port B) could then be metered into the cell. The total volume of the system was known to within 0.1%, and the pressure could be read to 0.01%, thus the ideal gas law could be used to compute the number of gas atoms in the system to a similar accuracy of 0.1%[a]. When the gas molecules entered the cell (some of them, no doubt, being adsorbed on the graphite surface), the total amount in the cell could be computed simply by subtracting off the amount in the part of the system at room temperature. Once the amount in the cell was known, a determination was made of the *surface excess* [17], or (in effect) the amount adsorbed onto the surface. This number is equal to the total number in the cell minus the number that would be in the vapor if only the vapor filled the entire volume of the cell (at the temperature and pressure in question). In practice, this number differs from the "true" amount on the surface by only a few parts in 10^4 owing to the condensed nature of the film and the highly tenuous nature of the vapor[b].

This might seem an unduly complicated way to define a thermodynamic quantity, but in fact it is the best and simplest way. The volume occupied by the film is unmeasurable in practice and undefinable in principle. (Where does the "film" end and the "vapor" begin?) The surface excess, however, is exactly defined, easily measured, and subject to no philosophical complications. Bearing this in mind, we shall from now on speak of the "surface excess" and the "amount adsorbed" as one and the same thing.

---

a) Actually, corrections were made for nonidealities. The second virial correction was at all times equal to or less than 0.1% if the total, and the third was utterly negligible. The second virial coefficient, $B(T)$, was computed for methane by assuming that molecular interactions were of the Lennard-Jones type with a hard core diameter of 3.817 Å, and a well-depth of 148.2 K.

b) Of all the molecules in the cell, perhaps 1% might be in the vapor and 99% in the film. But although the film contains 99% of the atoms, it might occupy only 1% of the available volume, being contained within the first few monolayers of the surface. Thus, the difference between the surface excess and the "true number in the film", is that 1% of 1% which would be in the volume occupied by the film if only the film were not there.

Now having a way to administer known amounts of gas into the cell, it was a straightforward task to make thermodynamic measurements. The first order of business was to develop a procedure to avoid pressure gradients within the cell. This problem can arise whenever conditions are such that the gas mean free path is greater than the spacings between individual graphite platelets. Consequently, whenever molecules were admitted to or removed from the cell, the temperature was raised until the pressure was high enough to guarantee that all the molecules were evenly distributed. The cell was then cooled gradually (usually overnight) to its final working temperature.

Furthermore, because the thermodynamic behavior of the helium/Grafoil system has been so thoroughly studied [18,19], it was a simple matter to measure the substrate surface area. A 4.2 K helium isotherm [20] yielded a value of the one-third-ordering coverage of $N_{1/3} = 77.3 \pm 0.26$ STPCC†, corresponding to an area of 326 ± 1.4 m^2. A surface area this large made it impossible to obtain reliable pressure measurements in the submonolayer regime for methane because of the molecular distribution problems mentioned above. Thus, the lower coverage limit for measuring methane film vapor pressures is just under one monolayer.

Now let us turn our attention to heat capacity measurements and the methods by which they were made. Both the platinum and germanium resistance thermometers were calibrated against a diode thermometer from Lake Shore Cryotronics [21]. Primarily, the platinum thermometer is for use above 25 K, and the germanium thermometer below. In all of the measurements reported in Chap. 4, only the platinum thermometer was used. The background (empty cell) heat capacity was measured in the range of 60-110 K, and was found to

† 1 STPCC = 2.6869×10^{19} molecules.

compare very well with an estimate based on the assumption that the cell consisted of 20.6 g of aluminum, 13 g of graphite, 0.4 g of indium, and 0.6 g of iron. This estimate was derived from NBS tables listing the specific heats of various materials. In fact, the measured values were consistently higher than the estimate by about 4%, and this difference can easily be attributed to the heat capacity of the heater and thermometers, something which was not contained in the NBS tables. Typically, this background measurement varied smoothly from 5.5 J/K at 60 K to 12 J/K at 100 K with an uncertainity of ±0.2% or less. Once this background signal was known, a variable knot B-spline fit was made in order to pass a smooth curve through the data points. Then, a computer subroutine was written to provide this curve, on demand, when given any value of the temperature within the measured range.

Now when methane was introduced to the cell, heat capacity measurements were made following a straightforward procedure. First, the temperature of the cell and shield were stabilized so that the cell's temperature drifted by no more than 0.1 K per hour. Simultaneously plotted on a strip chart recorder were (a) the off-null reading from the thermometer bridge [22], (b) the film vapor pressure (when measurable), and (c) an on/off signal indicating whether current was flowing through the cell heater or not. Second, a four-terminal measurement of the cell heater wire's resistance was made and the value written on the chart recording. Third, the heater was turned on for a period of 10-20 seconds and during this time the voltage across the heater was recorded. The time duration of the heat pulse was measured in units of 10 μsec by a frequency counter operating at 100 KHz, and this too was recorded. While the heater was on, the settings for the shield's temperature were changed to accommodate the cell's temperature rise (typically 1 K), and the bridge balance arm decade resistance re-adjusted for an approximate null at the new temperature. Since the bridge

was at an exact null before the heat pulse, the original balance arm reading was a measure of the cell's initial temperature. As was mentioned above, it took ten to fifteen minutes for the added heat to penetrate to the interior of the cell, and this manifested itself on the chart recording as a continuously variable temperature drift rate. When the drift rate had stabilized, the off-null reading was extrapolated back to the center of the heat pulse (the initial drift rate having also been extrapolated) and the final balance arm value was recorded. Since the bridge was not precisely on balance, the deviations from null were calibrated by changing the decade resistance by a fixed amount and noting the resultant pen deflection on the chart recorder. The off-null signal measured at the center of the heat pulse (calibrated against the known deflection) plus the final value of the balance arm then yielded a value for the cell's final temperature. Temperature differences calculated in this way (final minus initial) were known to better than 2 mK out of 1 K. Finally, the pressure readings were also extrapolated to the center of the heat pulse, and recorded.

Operationally, the total heat capacity is easily derived from all these measurements. Simply put it is $\Delta Q/\Delta T$ where ΔQ is the amount of heat added and ΔT the cell's temperature rise. ΔQ is easily evaluated as $V^2\Delta t/R$ (V the voltage across the heater, R the heater resistance, and Δt the time duration of the heat pulse), but this heat has gone to a number of places and we want to know only that amount which went into the film.

Of the basic measurement, $\Delta Q/\Delta T$, the background heat capacity is immediately subtracted off. This leaves a contribution due entirely to the methane, which however has three parts. One part is from the film, one part is from the vapor, and one part is from the desorption of molecules from the surface. Of these, we are only interested in the first. We can easily calculate the vapor's contribution by assuming it is a nearly ideal gas at constant volume. Moreover,

the contribution from desorption can be determined if we know q_d, the differential heat of adsorption [23,24]. This quantity is measured, in effect, by measuring film vapor pressures on a dense grid in the temperature-coverage plane. This forms part of the data presented in Chap. 4, and so it was possible to correct the raw heat capacities for desorption. The specific way in which q_d was calculated will be described in the next section.

Of the total signal, the background heat capacity accounted for, typically, 90-95%. The contributions from the vapor were small, but the desorption corrections could be as much as 50% of what remained. Consequently, when these effects were subtracted out, the 0.2% scatter in the total signal was duly magnified. Notice also that even though film heat capacities can be corrected for desorption, it does not mean that they are isosteric. For a fixed amount of methane in the system, desorption causes the coverage to decrease with increasing temperature. Thus, while the correction above makes each point locally isosteric, isostericity is not maintained in going from point to point. To obtain truly isosteric data, a grid of heat capacity measurements in the coverage-temperature plane is required so that interpolation to constant-coverage values is possible.

Thermodynamic Analysis and Technique

The fundamental purpose of the thermodynamic technique is to obtain an energy function in terms of its proper variables. These variables for any system come in conjugate pairs: entropy (S) and temperature (T); volume (V) and pressure (P); number of atoms (N) and chemical potential (μ). The first variable in each pair is an extrinsic quantity (proportional to the amount of material present), and the second is an intrinsic quantity (independent of the amount of material present) and, at equilibrium, is constant throughout the entire volume

(at least in systems of uniform density). The energy functions (or thermodynamic potentials) in terms of their proper variables are given here:

$$E(S,V,N) \quad (energy)$$
$$F(T,V,N) = E - TS \quad (Helmholtz\ free\ energy)$$
$$G(T,P,N) = F + PV \quad (Gibbs\ free\ energy)$$
$$H(S,P,N) = E + PV \quad (enthalpy)$$

Changes of the potentials are related to changes in their proper variables by way of the variables' conjugates. Thus:

$$\begin{aligned} dE &= TdS - PdV + \mu dN \\ dF &= -SdT - PdV + \mu dN \\ dG &= -SdT + VdP = d(\mu N) \\ dH &= TdS + VdP + \mu dN \end{aligned} \qquad (1)$$

Having $F(T,V,N)$, therefore, gives us complete thermodynamic information since we can find the entropy, pressure, and chemical potential by differentiation:

$$S = -\left(\frac{\partial F}{\partial T}\right)_{N,V}$$

$$P = -\left(\frac{\partial F}{\partial V}\right)_{N,T} \qquad (2)$$

$$\mu = \left(\frac{\partial F}{\partial N}\right)_{T,V}$$

Clearly, the information contained in Eqs. 1 is four-fold redundant, and this permits us to find relations among the variables by equating crossed derivatives of the various differentials. For example,

$$\frac{\partial^2 G}{\partial T \partial P} = \frac{\partial^2 G}{\partial P \partial T}$$

or

$$-\left(\frac{\partial S}{\partial P}\right)_T = \left(\frac{\partial V}{\partial T}\right)_P.$$

These relations are the Maxwell relations, and are very useful for converting a thermodynamic description from one set of proper variables to another.

However, Maxwell relations never give the derivative of a variable with respect to its pair conjugate. Such quantities are known as response functions, and have a fundamental link to the physics of the system. Their measurement, of course, is of prime importance to an experimental program such as ours, but having a complete thermodynamic description they can be obtained from the differentiation of Eqs. 2 (for example). Of the common response functions, two have special names; $\partial S/\partial T$ (or $T\partial S/\partial T$) is the heat capacity and $\partial V/\partial P$ (or $-V^{-1}\partial V/\partial P$) is the compressibility. With the other conjugate pair, μ and N, the ratio $\partial N/\partial \mu$ is largely ignored because it is directly related to the other response functions in a uniform system. To wit,

$$\frac{1}{N}\left(\frac{\partial N}{\partial \mu}\right)_{T,V} = \frac{N}{V}\kappa_T$$

and

$$\frac{1}{N}\left(\frac{\partial N}{\partial \mu}\right)_{S,P} = \frac{N}{TS^2}C_P$$

where κ_T is the isothermal compressibility, and C_P is the heat capacity at constant pressure. (The response function $N^{-1}(\partial N/\partial \mu)$ is defined so that (a) it is the derivative of the extrinsic variable with respect to the intrinsic variable, (b)

it is always positive, and (c) both numbers of the conjugate pair appear either in the numerator or denominator.)

However, in systems in an external potential, neither the pressure nor density are uniform. Here the chemical potential asserts its superiority as a thermodynamic variable since it remains uniform even though external force fields are present. In the case of adsorption studies, the atoms feel the van der Waals attraction to the substrate and these forces (though short range) have a profound influence on the density and pressure profiles throughout the system. (They, of course, are responsible for the sharp separation into a thin film and a tenuous gas.) But since we only have access to the temperature, pressure at the mouth of the cell, and total number of molecules, we cannot possibly ascertain the density or pressure profiles.†

Here, were it not for the chemical potential, we would face a dilemma. All of the energy functions in Eqs. 1 are functions of density or pressure:

$$E(S,V,N) = N\,e(S/N,N/V)$$
$$F(T,V,N) = N\,f(T,N/V)$$
$$G(T,P,N) = N\,\mu(T,P)$$
$$H(S,P,N) = N\,h(S/N,P)$$

Consequently, we need to use a different thermodynamic potential whose proper variables are T, V, and μ. Such a quantity is the Landau potential, Ω [25]:

$$\Omega(T,V,\mu) = F - \mu N$$
$$d\Omega = -SdT - PdV - Nd\mu\ .$$

† From now on it should be clear that any measurements of "pressure" refer to the pressure at the mouth of the cell, or in effect, the pressure infinitely far from the substrate where the van der Waals forces have died off.

In uniform systems, $\Omega = -PV$, but PV work has no meaning for an adsorbed film. Moreover, the cell's volume is constant so we can set $dV = 0$ in the above equation. Furthermore, we will have three different species i of methane in the cell, so we have:

$$d\Omega_i = -S_i dT - N_i d\mu, \tag{3}$$

(where i can be o for the total system, g for the gas, and suppressed for the film). It is not necessary, of course, to label T and μ with subscripts since they are uniform throughout the cell in equilibrium.

Here it can be seen that the response function $N^{-1}(\partial N / \partial \mu)$ becomes important in its own right, and perhaps deserves a name of its own.†

Since the chemical potential of the gas is equal to that of the film, we can obtain its value by using the nearly-ideal gas formula

$$\mu = k_B T \ln \left[\frac{1}{k} \left(\frac{2\pi\hbar^2}{mk} \right)^{3/2} \frac{P}{T^{5/2}} \right] + B(T)P + \mu_{rot} \tag{4}$$

where $B(T)$ is second virial coefficient of methane (see footnote (a), p. 19), and μ_{rot} is the contribution from methane's rotational energy levels. (This includes the nuclear spin degeneracy terms as well. See Appendix 1 for details.) With P in torr and μ and T in kelvins this becomes

$$\mu = T \ln (8.0292 \times 10^{-4} P / T^{5/2}) + B(T)P + \mu_{rot}.$$

With measurements of the pressure, the number in the gas is easily computed:

$$N_g = \frac{PV}{kT} \left[1 - B(T) \frac{P}{kT} \right]$$

† Since generalized response functions are referred to as "susceptibilities" [26], one might call it the "chemical susceptibility".

(where V is the full dead volume of the cell: 80.4 cm^3) whereupon $N = N_o - N_g$. Because there is a temperature gradient along the length of the fill tube, a thermomolecular correction is applied to the pressure readings (at room temperature) to infer the true pressure in the cold cell [27]. In most cases this correction is negligible and the room temperature reading can be taken as a true measure of the pressure at the cold end of the fill tube.

To obtain the data in Chap. 4, heat capacity measurements were made at various coverages from 65 - 105 K, and vapor pressure isotherms (coverage vs. pressure) were made from 78 - 96 K at precise 1 K temperature intervals. Thus, the basic data set contains a wealth of information in the N-T plane. The coverages, N, for the most part span the range of 1 - 6 monolayers.

The Landau potential is obtained by integrating Eqs. 3 and 4 at constant T:

$$\Omega(N,T) = - \int_{-\infty}^{\mu(N)} N(T,\mu)\, d\mu \quad , \tag{5}$$

a relation known as the Gibbs-Bangham equation. (In the data analysis μ as a function of N and T is inverted to obtain N as a function of T and μ.) The lower limit of the integral corresponds to N=0. Having $\Omega(N,T)$ allows us to find the entropy from Eq. 3 by performing a numerical differentiation of the data:

$$S = - \left[\frac{\partial \Omega}{\partial T}\right]_N - N \left[\frac{\partial \mu}{\partial T}\right]_N .$$

In principle, a further differentiation is possible to get the heat capacity, so the separate heat capacity measurements appear to be redundant. However, a double-differentiation of numerical data is virtually impossible, given the inherent scatter, so the heat capacity measurements turned out to be valuable in their own right. In fact, they turned out to be essential for the completion of the thermodynamic analysis, as shall be described below.

As was mentioned in the previous section, knowning μ on a dense N-T grid made it possible to correct the heat capacity measurements for desorption. The total signal (minus the background) can be written as [24]:

$$C_X = C_N + C_{V_g} - q_d \left[\frac{dN}{dT}\right]_X$$

where "X" denotes the experimental conditions, C_N the heat capacity of the film at constant N, and C_{V_g} the heat capacity of the gas at constant volume. Our conditions X were constant N_{TOT} (the number of molecules in the entire system), constant A (substrate area), but variable N and P. The heat of desorption is [24]:

$$q_d = \frac{3}{2}k_B T + T\left[\frac{\partial \mu}{\partial T}\right]_N - \mu - 2PT\left[\frac{dB}{dT}\right] + k_B e_{rot}$$

where e_{rot} is the rotational energy per molecule as defined in Appendix 1. In this expression, all quantities are measured during a heat capacity run (providing that one monitors the pressure) except for $(\partial\mu/\partial T)_N$. At low enough pressures this can be approximated by the known quantity $(\partial\mu/\partial T)_X$, but for us this was not always sufficient. However, since the isotherm measurements provided μ independently on a dense N-T grid, we could interpolate these values to find $(\partial\mu/\partial T)_N$, and hence q_d.

Now that we are able to extract the true film heat capacity from the raw heat capacity measurements, we can complete our thermodynamic analysis. We wish to integrate Eq. 5 from zero coverage, yet we have information only about coverages above one layer. Thus, there is a gap in our data set from zero to one layer which we must span. Fortunately, this gap has already been filled by Thomy and Duval [4], and because of the high reproducibility of the exfoliated graphite surface it was an easy matter to merge our data with theirs. In order

Figure 3. 80 K Isotherm: Caltech and Thomy & Duval Data Combined

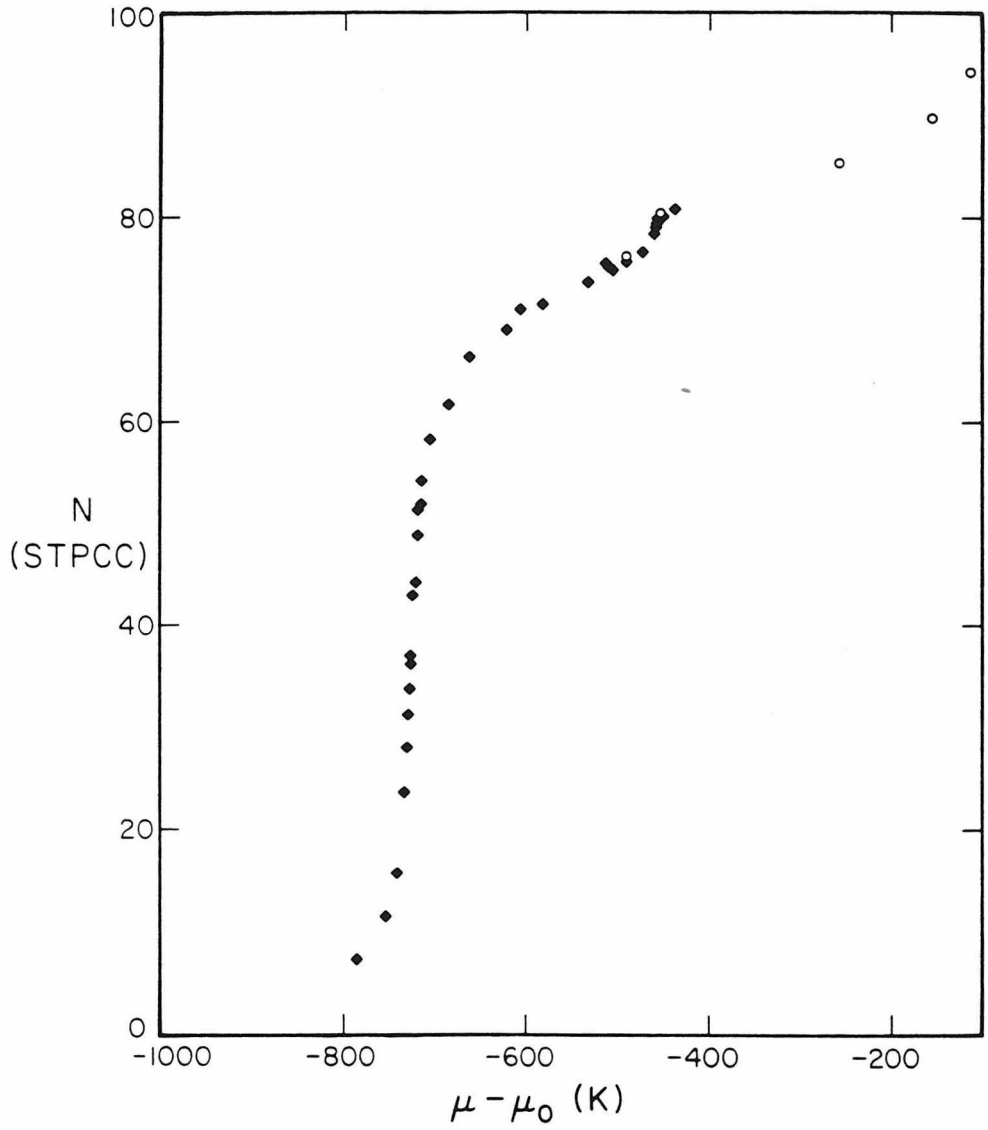

to do this, we had to measure V_{B1}, the coverage at the "knee" in the first layer part of a methane isotherm. From the data presented in Chap. 4, we find this to be 83.3 STPCC, and a plot of the combined data for T = 80 K is shown in Fig. 3. (Here the circles represent Caltech data, and we have measured the chemical potential relative to its bulk value, which was obtained from Eq. 4 by substituting for P values of the bulk saturated vapor pressure, P_o [28].) V_{B1} is, in effect, a measure of the substrate's monolayer capacity. However, later authors [9,12] have chosen to define one methane monolayer at an inflection point in the isotherm, i.e. at a coverage 9% higher than V_{B1}. Defined in that way our own monolayer is 90.9 STPCC, and this correlates very well with our independently measured value of $N_{1/3}$ (77.3 STPCC), known to be about 85% of a monolayer [5,9,12].

However, our data and theirs overlap only for temperatures between 78 and 84 K, and here the necessity of independent heat capacity measurements becomes apparent. Where the data overlap we can get all the desired information by integrating Eq. 5. But to extend this information out of the 78 - 84 K range (especially to 90 K or so where interesting processes take place), we need the entropy. This will allow us to integrate upwards in temperature at constant coverage according to:

$$\Omega(N,T) = \Omega(N,T_o) - \int_{T_o}^{T} S(N,T')dT'$$

where T_o lies in the range of 78 - 84 K. The entropy outside the 78 - 84 K range can be gotten by integrating the heat capacity at the same coverage, or:

$$S(N,T) = S(N,T_o) + \int_{T_o}^{T} \frac{C(N,T')}{T'}dT' \quad .$$

Having done this integration for one coverage, we can then integrate upwards or downwards in coverage using Eq. 5 modified for a different starting point than

$N=0$, viz.

$$\Omega(N,T) = -\int_{\mu(N')}^{\mu(N)} N(\mu,T)d\mu + \Omega(N',T) \quad (T = const.) \quad .$$

(Ω is an extrinsic quantity, so $\Omega(N=0,T) = 0$.)

It is clear that this operation can be performed starting with any coverage where a line of heat capacity measurements versus temperature exists. Furthermore, if such lines exist for more than one coverage, then we have redundant information. Therefore, we can check the self-consistency of the data by carrying out this procedure at least twice, using two different starting coverages. (This was done, and the two sets of thermal quantities agreed to within 1%.)

Finally, all heat capacity measurements discussed so far have been taken at constant substrate area, A. Obviously, there is no other way to take data, but for questions on the nature of phase transitions it is more desirable to have heat capacity at constant spreading pressure, φ [18,24]. Spreading pressure is the two-dimensional analog to real pressure, namely the force per unit *length* needed to keep the area from changing. A change in the area produces a corresponding amount of work:

$$dW = -\varphi dA \quad .$$

The thermodynamic analysis allows us to convert from C_A to C_φ (equivalent to converting from C_V to C_P in bulk) by [24]

$$C_\varphi = C_A + \left[\frac{S/N - (\partial S/\partial N)_T}{(\partial\Omega/\partial N)_T}\right]\left[\frac{\partial\Omega}{\partial T}\right]_N \quad .$$

Chapter 3. CLASSES OF FILM BEHAVIOR

Wetting and Roughening

Before presenting the data in detail, it will be instructive to consider the various forms of behavior an adsorbed film can exhibit. Some of these forms have already been mentioned; to wit, films can be liquids, gases, commensurate solids, and incommensurate solids (with or without the bulk lattice structure). Moreover, these forms can coexist in two-phase regions, and in the case of polyatomic molecules, can display orientational properties different from their bulk counterparts. However, here the story is far from complete because it has been tacitly assumed that a sandwich-planar geometry (substrate-film-vapor) exists at all times. In other words, that the film is *completely wetted.* Anyone who has ever seen a drop of water bead up on a piece of oilcloth can appreciate the idea that adsorbed films might not always be completely wetted, but perhaps partially wetted or completely beaded instead.

Films are, after all, surface phenomena. Three elements (substrate, film, vapor) always coexist, and the interplay between them can be intricate and subtle. Meniscus and capillary types of behavior should be expected in general, and if they do not exist it is because of an especially strong atom-substrate attraction. Having three elements, the interfaces between them can take three forms: film-substrate, film-vapor, and vapor-substrate. Each interface has its own surface tension, γ, and the relationship between these quantities determines whether or not the films wet [29].

Dash [30] has considered such types of behavior, and has classified them into three categories according to how the bulk state is reached as molecules are

continuously let into the cell:

(I) Films of uniform thickness build up until they are as thick as bulk samples.

(II) Bulk nucleation abruptly takes place after the adsorption of a few uniform layers.

(III) Bulk nucleation takes place with no preadsorbed layers.

(Clearly, class III is a limiting case of class II where the number of preadsorbed layers becomes zero.) According to our present language (which is to say, that of Pandit, Schick, and Wortis [17]), class I corresponds to complete wetting, class III to complete beading, and class II to an intermediate case known as "incomplete" or "partial" wetting.

Thermodynamic equilibrium states are those of minimum free energy ($E-TS$), and contributions to both the energy and entropy terms are made by the various surface tensions γ_{fv} (film-vapor), γ_{fs} (film-substrate), and γ_{sv} (substrate-vapor). To minimize the energy term, small interfacial areas are favored. However, having three connecting interfaces means that one's area can decrease only at the expense of the others. Furthermore, minimization of the entropy term causes a tendency for larger interfacial areas, and equilibrium states reflect compromises among all these effects. In general, the film will be beaded (partially or otherwise) and the angle of contact between the three interfaces where they meet is governed by γ_{fv}, γ_{fs}, and γ_{sv} [29].

Entropy always increases with temperature, and for a given interface it means that γ will decrease [29]. At high enough temperatures the γ's are so weakened that large increases in interfacial areas can easily be accommodated at no cost to the free energy. In other words, the increase of energy is more than counterbalanced by the increase of entropy, resulting in a net lowering of the overall free energy. At a certain temperature, T_w, the energy advantages of

beading are lost to the entropy advantages of wetting, so the contact angle drops to zero and the film becomes wetted. T_w is, of course, referred to as the *wetting temperature*, and in cases where the films are wetted at all temperatures we say that $T_w = 0$. In wetting transitions, then, beaded states are considered to be the ordered states, and the change from beading to wetting can be gradual or abrupt.

Now in all of our discussion of interfaces, we never addressed the character of the interface itself. By and large, interfaces can be of two types: rough and smooth. "Roughness" and "smoothness" have nothing to do with surface preparation in this context, but rather with the position of the free interface. According to the usual definition, an interface is said to be *smooth* when fluctuations in its position remain finite as one considers parts of the interface infinitely far from the origin. On the other hand, if the fluctuations diverge, then the interface is said to be *rough*. (Consequences of this definition with regard to multilayer films will be discussed in the next section.) We would say then that solids are (for the most part!) smooth, and liquids are rough, perhaps in contrast to our usual notions of them.

In principle, however, even though liquids are always rough, there is no guarantee that solids are always smooth. (Roughness in a solid shows up as an inability of the surface to support crystal facets [31,32].) Presumably, a solid could be smooth below a certain temperature, T_R, and rough above it. T_R would thus mark the *roughening transition*, and because its existence depends on having an interface, it would show up in bulk samples *only along a solid-fluid coexistence line*.

In adsorbed films, of course, the substrate is assumed to be a smooth solid so that the film-substrate and substrate-vapor interfaces are also smooth. Moreover, the film-vapor interface is stabilized by the substrate potential, and

so fluctuations in its position cannot diverge [33]. However, whether or not the film-vapor interface can have other attributes of rough surfaces is still an open question, and it will be taken up later.

So then, we find a number of phase transitions which films can support: wet/beaded, commensurate/incommensurate, the usual solid/liquid/gas transitions, and perhaps a rough/smooth type of transition as well. The relationship between all these effects will have to be considered carefully.

A Review of Current Ideas on Film Behavior

The recent flurry of interest in multilayer films has been due to various theoretical treatments of the problem based on certain model systems [17,34–42]. Of these, the most comprehensive is Ref. 17 by Pandit, Schick and Wortis (hereafter referred to as *PSW*), based on a lattice gas model suggested by de Oliveira and Griffiths [34]. In this model, space is permeated by a lattice of discrete sites, at any one of which there can be zero or one atom. The lattice is only semi-infinite, however, being bounded by a solid wall substrate, and any given atom will feel a potential from both this substrate and the atom's nearest neighbors. If atom i feels an attractive potential v_{ij} from its neighbors j (the repulsion part being substituted by the fact that no two atoms can occupy the same site), and an attractive potential u_i from the substrate, then the ratio of the strengths of these potentials, $|u|/|v|$, will play an important part in determining the behavior of the film. One reason for the popularity of this model, apart from its apparent simplicity, is that its Hamiltonian is isomorphic to that of the Ising problem (providing that the potential v_{ij} is restricted to nearest neighbors only). In this picture, a filled lattice site corresponds to spin up, an empty site to spin down, and the substrate potential to a magnetic field applied only at the boundary of the system. Thus, the entire body of knowledge already

at hand for Ising systems can be applied to multilayer adsorption with no more than a simple renaming of the variables.

Although the crudeness of this model is self evident, it nevertheless portrays certain *classes* of behavior which should also be present in real systems. For example, if $|u|/|v| \gg 1$ (that is, the substrate much more attractive than the interatomic potential), then the film will show complete wetting at all temperatures. On the other hand, different ratios of $|u|/|v|$ allow non-wetting below T_w and wetting above T_w, or even in the case of a very weak substrate, a phenomenon known as "drying". If all of space is filled with atoms, and one begins to remove them one at a time, drying occurs if the removed atoms are those near the substrate surface. Bear in mind that the substrate is always attractive, but in the case of drying it is energetically more favorable to remove an atom from the surface region rather than the interior of the lattice. Drying and wetting are complementary phenomena in which all qualitative behavior is the same but for a change of atoms into holes and vice versa. However, since there is no experimental work related to drying, it will no longer play a role in our discussion. A further fine-tuning of $|u|/|v|$ even shows different forms of wetting corresponding to Dash's type II or type III. Thus, this model appears to encompass all the categories of wetting phenomena.

Experimentally, wetting transitions have been seen in liquid systems [43,44], as well as the following adsorption systems: ammonia [45] and ethylene [46] on graphite, and krypton on the cleavage face of calcium iodide [47]. (This last case does not show a wetting transition *per se*, but a transition involving increased layering.) Other references to unpublished work are given in PSW. In the present case of methane on graphite, there is no experimental evidence of a wetting transition. (See Chap. 4.) Vapor pressure measurements in the 5-6 layer range show that the film remains wetted down to at least 64 K, and heat

capacity measurements of the rotational transition [2] indicate wetting down to 20 K or so. (A submonolayer methane film has been shown to wet down to 10 K [45], but it is likely that a submonolayer film of any substance will always wet unless the substance is strictly of type III.) Since methane is the focus of our study, we need not consider the problem of wetting in any further detail, except for a brief discussion in Chap. 5 of how to detect it using the thermodynamic analysis.

The bulk limit of the model (corresponding to infinite film thickness) displays a critical point at which the difference between distinct condensed and dilute phases disappears. Because of the structure imposed artificially by the lattice, there is no way to tell whether the condensed phase corresponds to a solid or a liquid. (The shear stress is not calculable.) So, one glaring drawback is the absence of a phase transition between two condensed phases such as those found in real substances. In other words, the bulk coexistence line possesses a critical point, but no triple point. However, the bulk limit does contain a roughening transition, so there is a T_R less than T_c which will play an important role in our analysis.

Despite its drawbacks, the model does achieve a number of successes - most notably with regard to thin multilayer films. To begin with, the strict monolayer case reduces to the standard 2D lattice-gas/Ising-model. It has a well known critical temperature, $T_c(1)$ (the 1 meaning "first layer"), and a 2D condensed/dilute coexistence region below $T_c(1)$. Moreover, it is known that the 1D surface which separates the two phases is always rough. If further layers are added on top of the first, then the system will possess two-phase coexistence regions which disappear, for n layers, at a certain critical temperature $T_c(n)$. The two phases in coexistence are regions where, in the n^{th} layer, the atoms either clump together in self-condensed patches, or else they exist as individual

unbound particles. Above $T_c(n)$, these distinct regions no longer exist, but the atoms spread out uniformly over the n^{th} layer. (Bear in mind, however, that even though the distinction between phases can be seen merely by looking at the n^{th} layer, the transition at $T_c(n)$ involves the entire film.)

These facts have important consequences for vapor pressure isotherms. If the amount adsorbed is plotted versus the chemical potential at constant temperature, then there will be a vertical jump in the curve whenever N falls in one of the two-phase regions. (That is, a range of N's corresponding to changing from the density of one phase to the other will exist at the same μ.) A strictly vertical step corresponds to a first order phase transition, and hence these jumps are called "layering transitions." Clearly, layering transitions will show up only in isotherms where the temperature is less than at least one of the $T_c(n)$'s. Isotherms above the $T_c(n)$'s are said to be "supercritical," and although they might have step-like structure, the step risers will not be strictly vertical. An isotherm whose temperature falls above some of the T_c's, but below the others will then exhibit both vertical and non-vertical steps. Since the $T_c(n)$'s tend to increase with n, this means that the low coverage steps will be non-vertical, and the high coverage steps vertical.

This prediction is somewhat counter-intuitive to those familiar with the experimentally measured isotherms of, say, Ref. 4. An example of such an isotherm from our own data is shown in Fig. 4. Here coverage is plotted against pressure (related to the chemical potential by Eq. 4), and distinct steps in the second and higher layers are seen. Whether or not they are strictly vertical is a quantitative question, but (though unresolvable in the figure) the higher layer steps are definitely less vertical than the lower ones. Before the lattice-gas model, the explanation for the smearing of the high-N steps was thermal promotion. That is, as the number of layers increases, then the differences in their

Figure 4. 77.4 K Isotherm: Coverage vs. Pressure

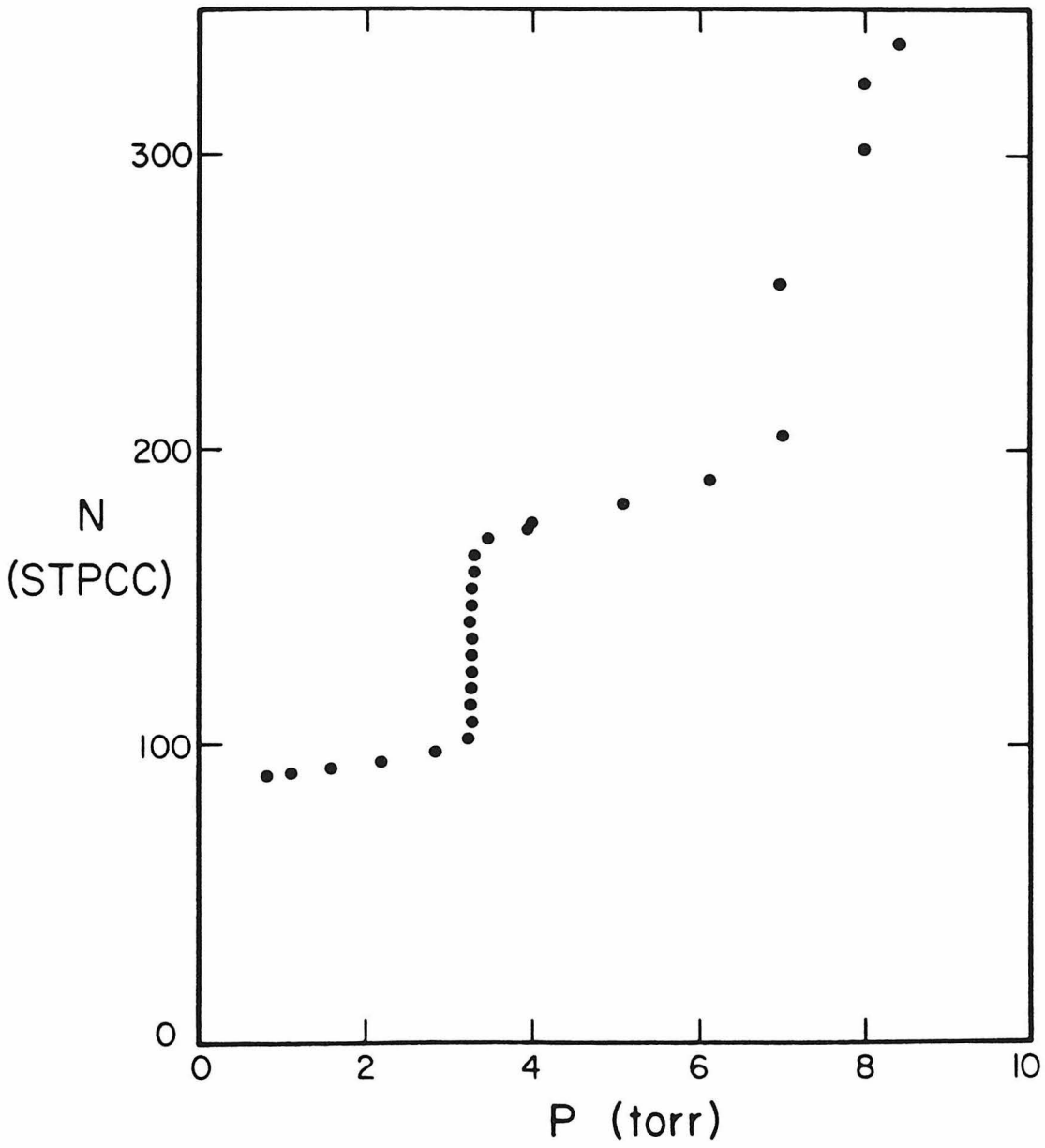

binding energies become small compared to $k_B T$, and a molecule is less likely to be localized in any one particular layer. Certainly, isotherms for lower temperatures are known to show sharper steps.

Note that the two explanations for non-verticality are radically different. In the lattice-gas model, verticality is destroyed by behavior in one layer only (the n^{th}), whereas thermal promotion involves the behavior of many layers, namely all those whose binding energies are within $k_B T$ of each other. Notice also that that strict verticality can be eliminated by binding energy variations across the substrate [48]. (In this case, the identification of the critical point from vapor pressure isotherms can be be a tricky business, and is discussed in more detail in Appendix 2.)

One can re-examine the experimental data of Refs. 4-7, or that of Putnam and Fort [49] in more detail to see if the higher coverage steps are indeed more vertical. However, even without the complications of substrate inhomogeneity, one can draw different conclusions depending on how one handles the data. In Chap. 4 we will consider this question in detail.

The fact that $T_c(n)$ increases monotonically with n is a consequence of the collective attraction of ever increasing amounts of adatoms. (Also, Rauber, Klein, and Cole [50] have pointed out that differences in substrate screening between the first and higher layers produce a similar effect, although this is not contained in the PSW model.) This increase is not without bound, however, since $T_c(n)$ approaches a limiting value as $n \to \infty$. In the original model of de Oliveira and Griffiths, $T_c(\infty)$ is just the bulk T_c. However, since their model is a mean-field calculation, it omits the effects of the roughening transition. They argued that when these are properly included, then $T_c(\infty)$ should be T_R. Subsequent and more sophisticated calculations by others [39-41] support this conjecture. Moreover, they predict that the shapes of the two-phase regions in the N-T

plane should be "blunt-nosed" instead of rounded, and for this reason it may make sense to call these "layering transitions" since the jump in n is always about one layer. (In other words, the leading edge of the two-phase region, though rounded in principle, should remain in the vicinity of $T_c(n)$, and hence T_R.) An examination of the data presented in Chap. 4 will lead us to a similar conclusion.

At first glance, why the bulk roughening transition should influence the quasi-2D liquid gas critical behavior in the layers is a mystery. After all, the phenomena seem dissimilar. But there is a connection, and it is provided by the realization that the steady buildup of layers indicated by the layering transitions amounts to the buildup of a crystal facet. As the thickness of the film increases, the differences in binding energies among the layers become much less than $k_B T$, so that the buildup of such a facet can take place only if the temperature is less than T_R. (In principle, all the facets have different T_R's, so strictly speaking, it must be less than the specific T_R for the facet in question.) Thus, for films of sufficient thickness, we do no expect to see any sharp layering transitions above T_R.

However, there are other attributes to rough surfaces apart from their inability to support crystal facets. One, which has already been mentioned, is the divergence in correlations of fluctuations of the surface's position between points ever farther apart. Since the substrate potential stabilizes the surface of a film, these correlations can no longer diverge. Similar phenomena are familiar from everyday experience. Water in a glass, for example looks smooth to the naked eye because its surface is stabilized by gravity (an effect left out of the usual definition of roughness). And yet since water is clearly a liquid, its surface, though smooth in terms of positional fluctuations, must have other properties of roughness.

One such property might concern its microscopic area (that is, the area of the surface computed on an atomic scale). Its *geometric* area (the area computed by averaging surface fluctuations over a macroscopic scale) is minimized by surface tension, and is a much different quantity. In the lattice-gas/Ising model, the roughening transition is signaled not only by the divergence in correlations, but by the spontaneous generation of edge defects on the surface. (Below T_R the number of these defects is suppressed by the Boltzmann factor, but above T_R their entropy lowers the free energy, and they can exist freely throughout the area of the surface.) Presumably, at T_R, the spontaneous generation of these defects will cause a discontinuity in the surface's microscopic area, or in one of its derivatives.

Moreover, surface roughness may be related to the phenomenon of surface plasticity, an effect which presumably plays an important role in the sintering process. (A plastic surface, of course, would not return to its original position if displaced parallel to itself, unlike an elastic surface.) So of all the characteristics of a rough surface: a delocalized position, a high microscopic area (caused by the abundance of edge defects), and a plastic response to shear stresses, a multilayer adsorbed film above T_R certainly does not have the first, but it might have the others.

Experimentally, roughening transitions have been seen both at solid-liquid [31] and solid-gas [32] interfaces. Moreover, the phenomenon of surface plasticity has been well known to metallurgists for decades, and it is known to occur at temperatures on the order of 85% of the triple temperature. Roughening has never been seen in bulk methane, but in Chap. 4 we will present evidence that there is a roughening temperature of about 78 K, or 85% of T_t (90.66 K). Moreover, this evidence is present in films as thin as 4-6 layers.

The model considers the behavior of surface tension, as it is a fundamental quantity in determining whether or not a film will wet. In our experiments we do not measure the surface tension directly, but we do measure φ, the spreading pressure. (See Chap. 2.) How these quantities are related will be discussed in Chap. 4.

In those areas where the model makes physically simplistic assumptions, work has been done to make it more sophisticated. For example, Saam [41] has considered systems with commensurate/incommensurate transitions, and Weeks [39] has relaxed the strict lattice conditions in favor of the atoms occupying lattice sites on average, while having continuously variable positions. The most serious drawback to the model, however, is its lack of a bulk triple point. In real physical systems, does the triple point replace T_R? The answer (as we have already hinted for methane) appears to be *no*. Moreover, a treatment of a Potts lattice-gas model by Ebner [38] draws the same conclusion. However, in the case of ethylene on graphite [46], the triple point seems to coincide with $T_{\mathcal{W}}$, and perhaps, therefore, T_R.

The model is at its best in defining classes of behavior for multilayer films. As we shall see in the next chapter, the actual behavior of methane layers adsorbed on graphite is richer and more complex than the situations the model considers. Nevertheless, there appears to be agreement on some fundamental points.

Chapter 4. EXPERIMENTAL RESULTS AND DISCUSSION

Basic Heat Capacities and Isotherms

In this chapter two tentative conclusions concerning methane multilayers on graphite will be put forth on the basis of the data taken according to the methods of Chap. 2. Both should be regarded as hypotheses, looking on these data as a preliminary survey, and subject to experimental verification by future, independent, and more detailed measurements.

The first conclusion is that the layer by layer critical temperature, $T_c(n)$, is roughly independent of n in the range $1 \lesssim n \lesssim 6$ with $T_c(n) \approx 78$ K. (This sort of behavior, in fact, has been predicted by some of the more sophisticated treatments of the lattice-gas problem [34,36–38].) If this result is extrapolated to infinite n, then in the context of the PSW model, it implies a roughening transition in bulk methane at about the same temperature.

The second is that the melting transition descends from bulk coexistence into the multilayer film region at nearly constant temperature, $T_m(N) \approx T_t$. The entropy change associated with this transition decreases smoothly, reaching zero at roughly two layers. It is not entirely clear how the transition "closes" (that is, how the phase boundary links up with some other one), but it does not appear to be first order in the multilayer region.

The data from which these conclusions have been drawn can be seen as follows. Figure 5 is a map showing the region surveyed in this study. Broadly speaking, there are data from nine heat capacity runs extending from 65 to 100 K for films between ½ and 2½ layers, and four runs between 4 and 6 layers, and vapor pressure data from 78 to 96 K between ½ and 6 layers. To anchor this grid

Figure 5. Surveyed Regions in the $N-T$ Plane

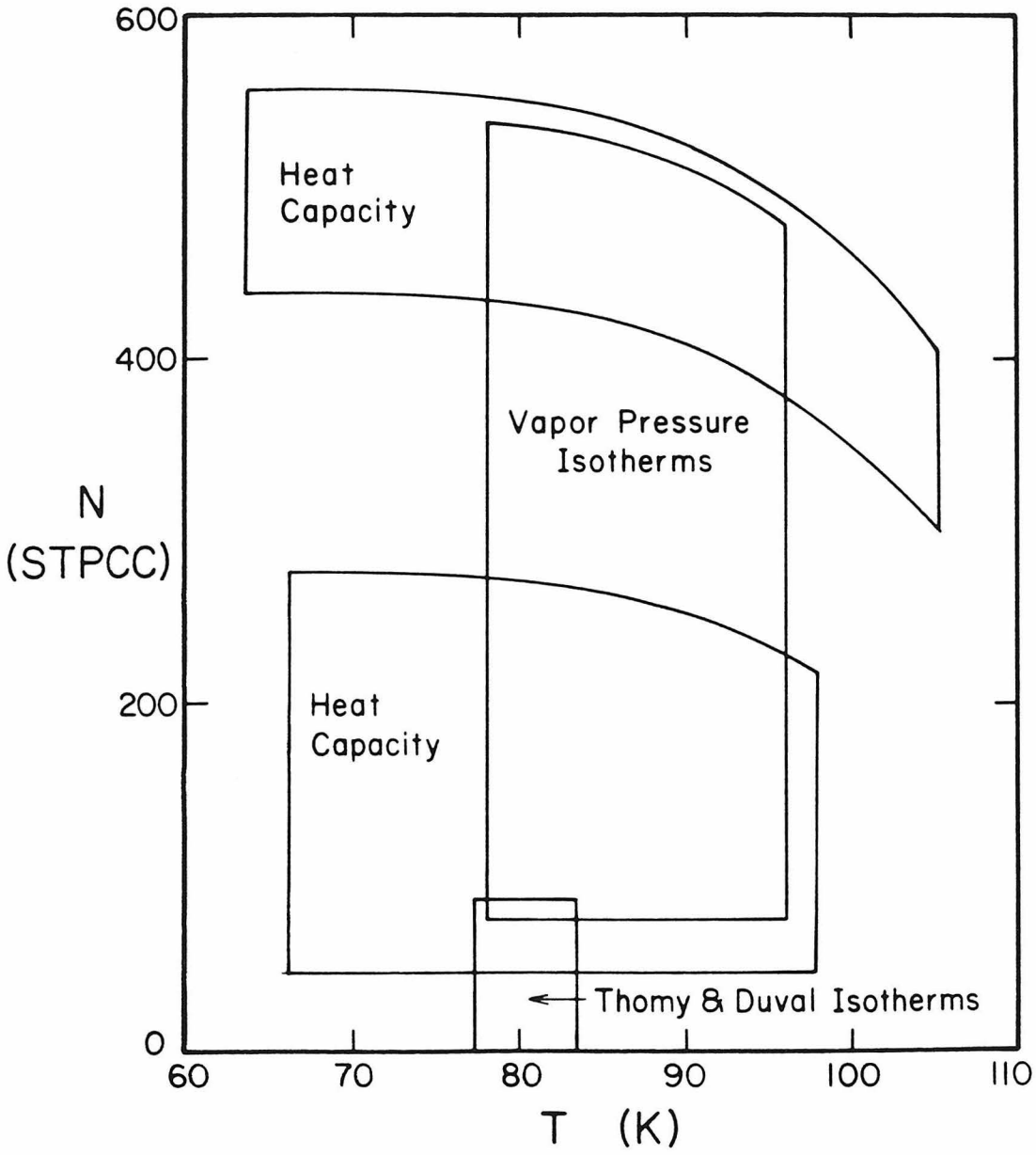

to zero coverage, the adsorption isotherm data (on exfoliated graphite) of Thomy and Duval were used in the region below one layer, and from 77 to 84 K. This overlapped both the heat capacity and vapor pressure data.

The data on which our analysis is based are shown in Figs. 6 and 7. In Fig. 6 we see the total heat capacity of the film. These are nonisosteric data, the coverage decreasing with increasing temperature. They must subsequently be interpolated to give isosteric values, or corrected by thermodynamic means to give the specific heat at constant intensive quantities, such as that at constant spreading pressure, C_φ. Note from Fig. 5 that there is a 1½ layer gap between the upper and lower sets of heat capacities. This gap shows up in Fig. 6 as well, and can be filled in using the tables of Appendix 3 (see p. 140). The coverages of Fig. 6 range from ½ to 2½ layers, spaced at roughly one-third of a layer, and from 4 to 6 layers spaced at half a layer. The spacings can be seen more easily in Fig. 11 below. Figure 7 shows vapor pressure data displayed in the form of coverage vs. chemical potential. Recall that one nominal monolayer is 90.9 STPCC. The plots are actually straight line segments passing through some 750 experimental points whose symbols have been suppressed for the sake of clarity, and the arrow indicates a possible phase transition in the second layer, about which more will be said below.

There are 19 isotherms in all, spaced at precise 1 K intervals from 78 to 96 K. We can recall from Fig. 1 that the first layer liquid-gas critical temperature is approximately 75 K. If this represents the thin film limit of our system, then the opposite limiting case is bulk coexistence. On the bulk coexistence curve, the triple point separating solid and liquid phases is at 90.66 K, and so the isotherm data span a temperature region between $T_c(1)$, the first layer critical point, and beyond T_t, the bulk triple point.

Figure 6. Total Film Heat Capacity

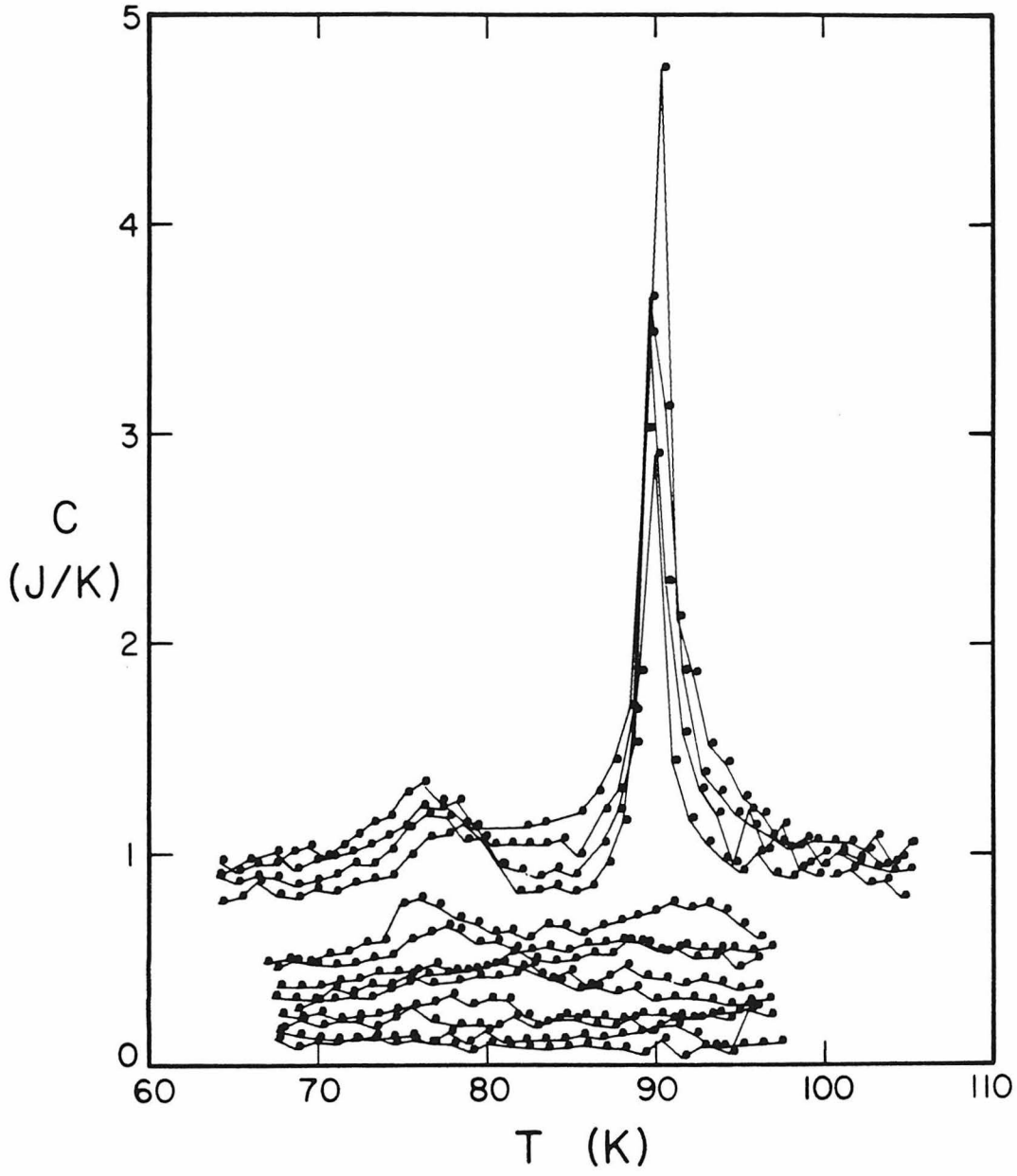

Figure 7. Vapor Pressure Isotherms: N vs. μ

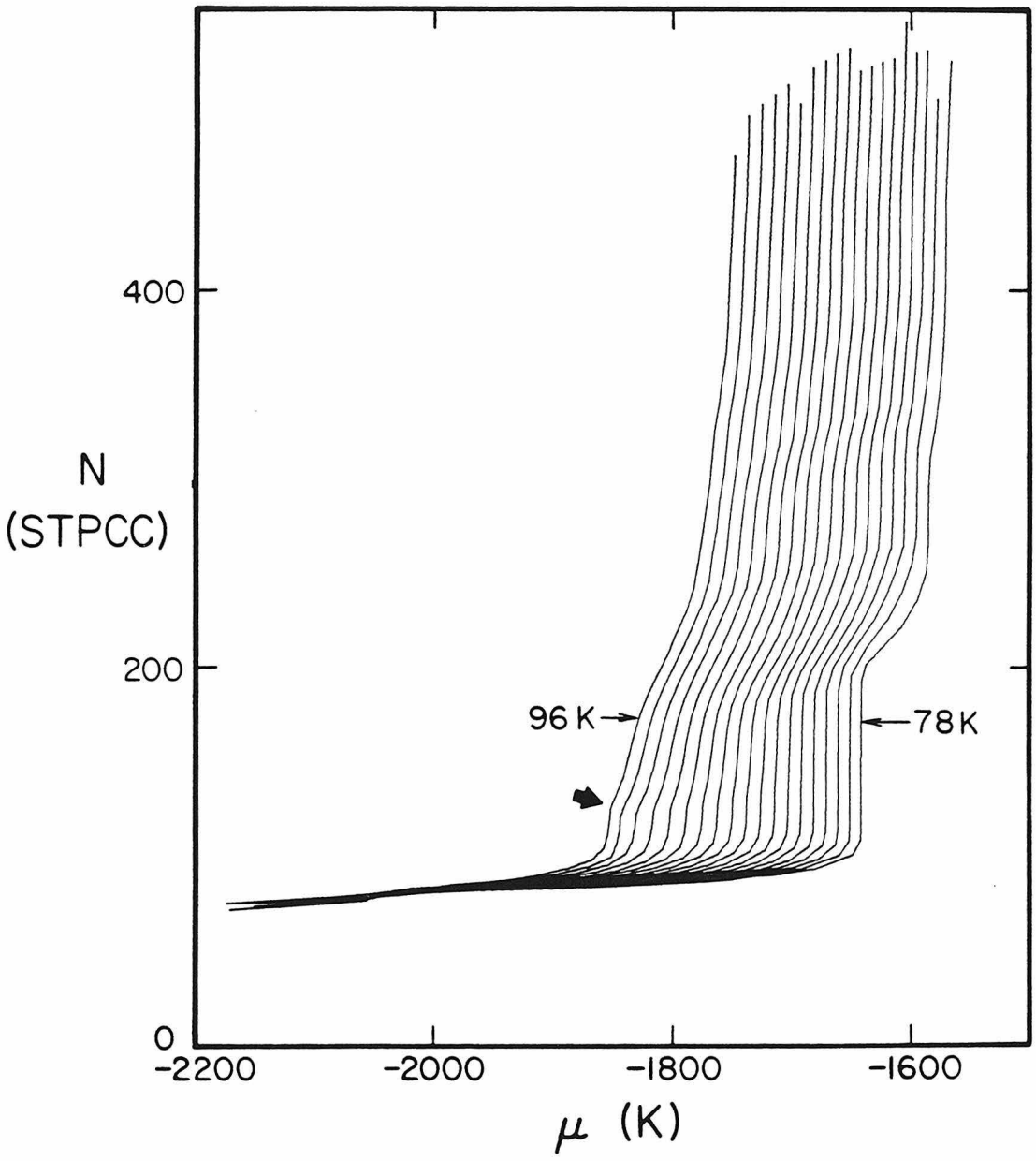

Evidence for the two principal conclusions tentatively put forth is easily seen in the data of Figs. 6 and 7. The most prominent feature of the heat capacity curves is a sharp peak in the thicker films at $T_p \approx 90$ K. The peak gets smaller as the film becomes thinner, but it does so at nearly constant temperature, and there is still a vestige of it to be seen at about 2½ layers. (A linear extrapolation of peak height vs. coverage shows that it would disappear entirely at about 2.1 layers.)

The heat capacity at bulk coexistence has a δ-function infinity at T_t=90.66 K because at that point the system temperature does not change until the heat of fusion has been provided. It is natural to assume that the sharp peaks in Fig. 6 are remnants of this triple point behavior, the area under the peak being associated with the entropy of melting. However, the peaks are clearly not δ-functions, nor do they have the "mesa-like" shape one would expect of essentially constant coverage heat capacities at a first order phase transition in a thin film [51].

Some years ago, a number of groups [52] carried out studies of the heat capacity of multilayer films near the bulk triple point in a variety of systems. The general trend of the results was that the bulk triple point δ-function became broadened and its maximum moved to lower temperature as the film became thinner. By contrast, in the present study, neither the width of the peak nor its temperature appear to change with film thickness. We believe this difference from the earlier studies to be due to the much greater uniformity of the graphite substrate we have used. The situation seems closely analogous to that of multilayer heat capacities for helium near the bulk lambda transition: Bretz [53] reported heat capacity anomalies of constant width and temperature (but declining height with film thickness) for helium on graphite near the temperature of the lambda transition, whereas earlier studies on other substrates gave results

strikingly similar to the early melting point data cited above [54].

On the other hand, the present results are very similar to the multilayer heat capacities for nitrogen reported by Chung and Dash [55]. Chung and Dash have interpreted the sharp peak they observed at the temperature of the bulk triple point to mean non-wetted films, the peak being contributed by the melting of beads of bulk matter. We are able to rule out that interpretation by means of the data in Fig. 7: the chemical potential is measurably lower than the coexistence value for all of the data listed in this work. That means no beads of bulk matter could have formed.

Although beading, or non-wetting, can be ruled out as an explanation for the 90 K heat capacity peaks, it is more difficult to rule out an alternative explanation, capillary condensation. Capillary condensation occurs when the effects of surface tension make it profitable to form bulk material in pores and cracks in the substrate before film growth is completed; negative curvature of the bulk-matter/gas interface at the mouth of each pore allows coexistence at pressures below the bulk vapor pressure. The observed heat capacity peaks would then be due to the melting of the bulk matter formed in this way.

The onset and extent of capillary condensation depends on the geometry of suitable imperfections in the substrate which, of course, is unknown. However, we may assume that capillary condensation begins to occur when the film thickness exceeds roughly two layers because that is where the 90 K peaks begin to appear. If we then analyze the entropy change associated with the peaks, we conclude that, in order to account for them, about half the matter absorbed beyond the first two layers must be in capillary condensed bulk form when the nominal coverage is 4½ layers. (The melting entropy of the bulk is 1.24 k_B/molecule. The equivalent of more than a full layer in bulk form would have to melt to account for a peak the size of that in the 4½ layer film.)

The circumstantial evidence does not favor this view. Steps in adsorption isotherms, indicating layer by layer condensation, are approximately the same size up to at least the fifth layer in the methane/graphite system. This may be seen, with rather poor resolution in the thicker films, in our Fig. 10 below. It is seen more clearly in a 77.3 K isotherm by Thomy and Duval [4]. Capillary condensation to the extent necessary to explain our heat capacity peaks is clearly inconsistent with their data in the fifth layer. To be sure, we have used a different substrate, but uncompressed graphite foam should be at least as free of cracks and pores as the exfoliated graphite used by Thomy and Duval.

Thus, although the evidence is not decisive, is is sufficient to lead us to choose against putting forth capillary condensation as the explanation for the behavior we observe at 90 K.

Our tentative conclusion, then, is that melting extends from the bulk triple point down to approximately two layers, in a line at nearly constant temperature. The obvious next question is then, how does it close? Since there can be no path from bulk solid to bulk liquid which does not pass through a phase transition, it is thermodynamically forbidden for this line to end in a critical point. Since it must end on some other phase boundary, which ones are there available? Obvious candidates include the melting curve in the first layer (see Fig. 1), and whatever phase transition (melting for example) might be found in the second layer above $T_c(2)$.

Figure 8 shows some possible phase boundaries in the n-T plane. Bulk melting descends at nearly constant temperature, ending (or becoming invisible) at about $n=2$. On the same scale we see first layer melting (as mapped out by the authors of Refs. 4 (*), 5 (+), 12 (o), and this work, (×)), and a possible phase transition in the second layer. It is not known how - or even if - these lower curves end at high temperature.

Figure 8. Possible Phase Boundaries in the $n-T$ Plane

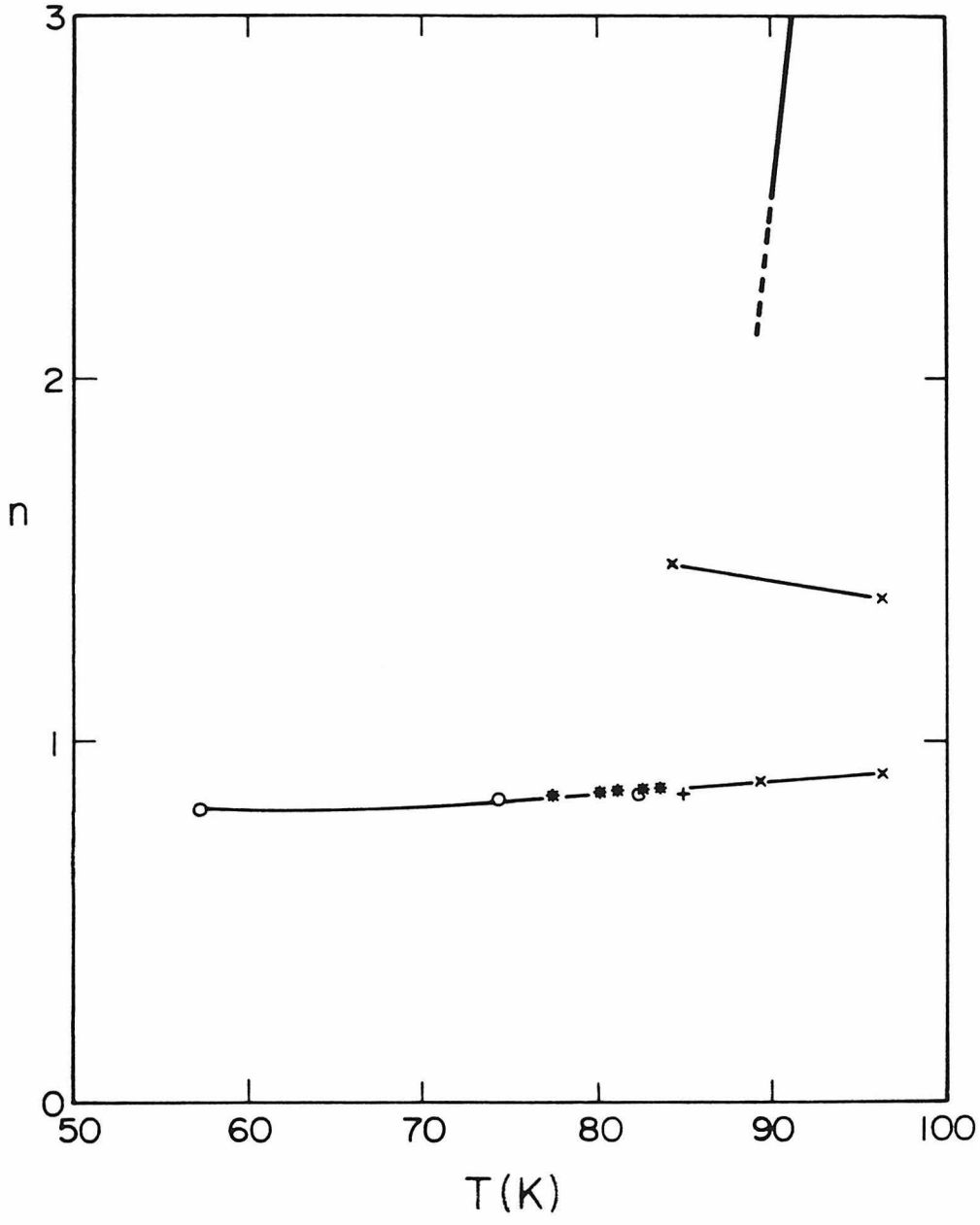

In our vapor pressure data, we observe a series of kinks in the second layer which could be interpreted as a phase boundary. The positions of these kinks are indicated by an arrow in Fig. 7, and their locus is plotted in Fig. 8 noted by the upper symbols ×. (They can perhaps be seen most easily, however, in Fig. 13 below.) If it is a phase transition, it could, for example, be the melting of the second layer. It occurs at roughly 1 plus 1/3 layers, which seems a rather low density for melting to occur, but of course many kinds of transitions in thin films have been conjectured (orientational order-disorder, for example).

We do not observe, then, the extension of the bulk melting to close on a known transition. It seems to end rather far from first layer melting. It is closer to, but not known to arrive at a possible transition of unknown nature in the second layer. An additional possibility is that it becomes a "thermodynamically invisible" melting transition of the type suggested by Kosterlitz and Thouless, Halperin and Nelson, and Young (hereafter referred to as KTHNY) [56].

Our second conclusion concerns $T_c(n)$. In the data of Fig. 7, one easily sees vertical, or nearly vertical steps (N increasing at constant μ) in the second and third layers at 78 K, becoming slightly less vertical at higher temperature. At the same time, there is a bump in each heat capacity from roughly 2 to 5 layers at about 78 K. We would propose that this behavior results from a $T_c(n)$ at about that same temperature for n up to at least 5, and perhaps 6.

The PSW model suggests that $T_c(n)$ will vary smoothly from $T_c(1)$ to T_R, the bulk roughening temperature, as $n \to \infty$. One intriguing possibility is that T_c will increase with n, with, for example, $T_c(2) > T_c(1)$. In that case, an adsorption isotherm of the type shown in Fig. 7 where $T_c(2) > T > T_c(1)$ should be more vertical in the second (and higher) layers than in the first. This behavior would be somewhat counter-intuitive, as pointed out in Chap. 3, since on the basis of all previous experimental work one generally expects sharper features in the first

Figure 9. Combined Caltech and Thomy & Duval Isotherms: 78 - 84 K

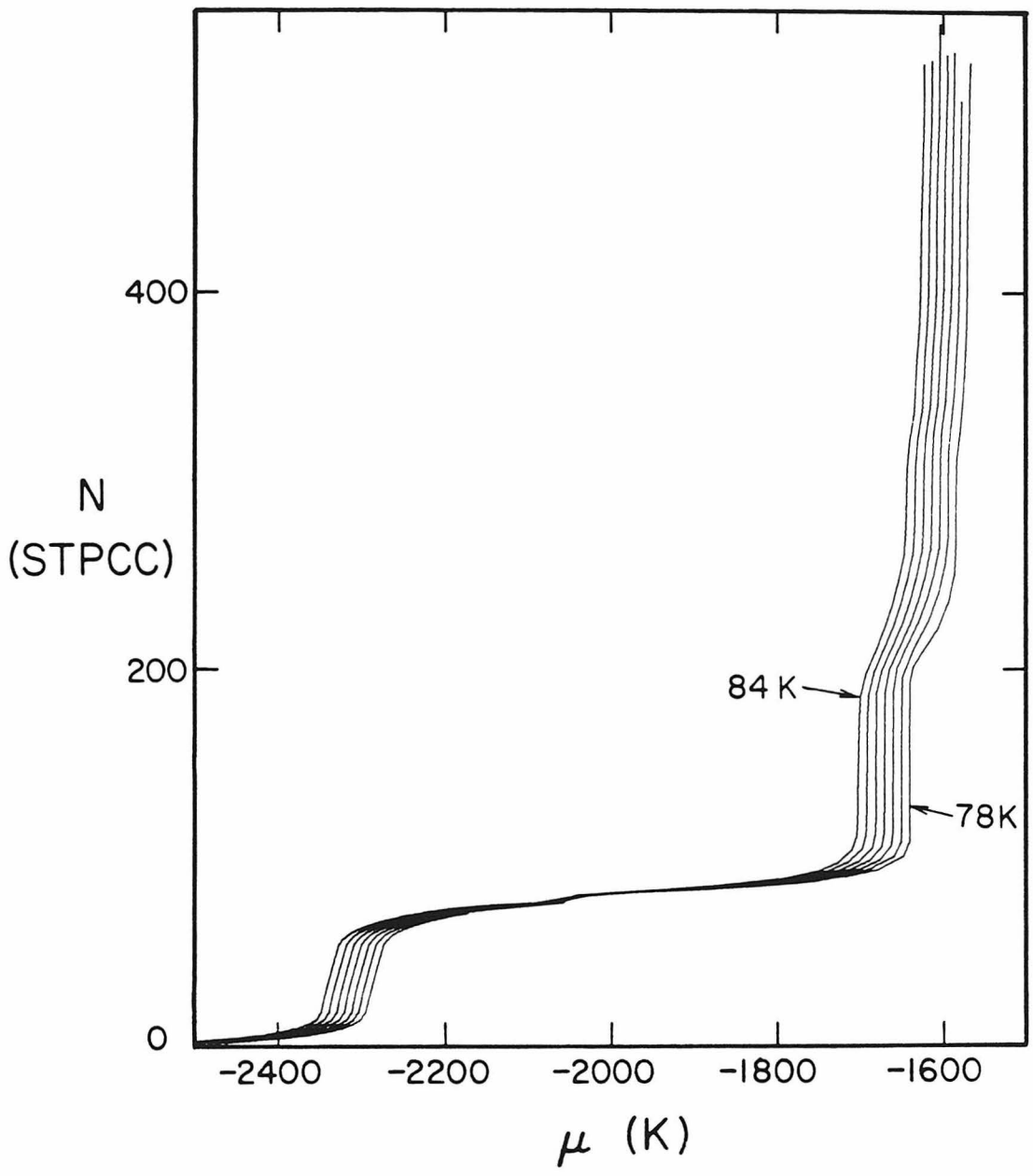

layer than in the higher layers.

To test this idea, we have combined our results with the first layer data of Thomy and Duval, using the proper substrate scaling factor as mentioned in Chap. 2. Isotherms constructed in this way for 78 K $\leq T \leq$ 84 K are shown in Fig. 9. (The Thomy and Duval data have been interpolated to match the temperatures of our survey grid.) One sees what appears to be the predicted behavior, with, for example, the second layer steps being distinctly more vertical than the first.

However, the effect may be an artifact of the way in which the data are presented. The first layer occupies a much larger range of μ than does the second. This tends to stretch out the first layer step, making it appear less vertical, and compress the second layer, making it appear more vertical.

To improve our view of the situation, we may plot the data in a different way, based on an excessively crude model of adsorption. The model is that $\mu(N,T)$ differs from the bulk coexistence value $\mu_o(T)$ only by the van der Waals potential of the substrate. In particular, if we take the van der Waals potential to be α/d^3 where α is a constant and d the film thickness, we have the Frenkel-Halsey-Hill isotherm:

$$\mu-\mu_o = -\alpha/d^3 \quad . \tag{6}$$

This model neglects precisely the interactions which give rise to the critical point behavior we are examining. However, it does suggest that if we plot N vs. $|\mu-\mu_o|^{-1/3}$, we will be giving more nearly equal space on the graph to each layer.

A plot of this kind is shown in Fig. 10 at T=80 K. We see that the first three steps now appear about equally vertical, and there are even vestiges of a fourth step. The smearing out of the steps at higher layers is due to loss of

Figure 10. 80 K Isotherm: N vs. $|\mu-\mu_o|^{-1/3}$

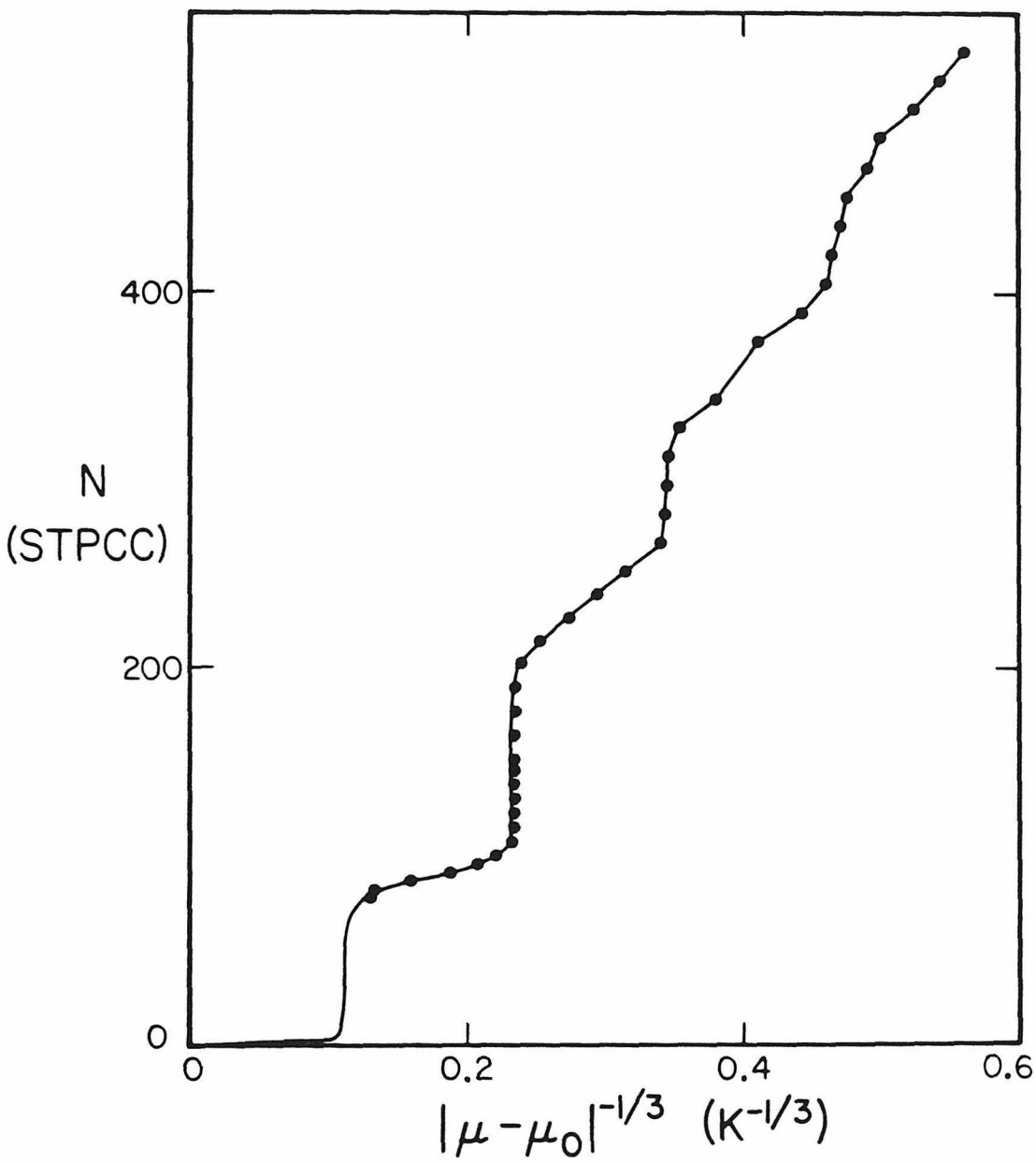

experimental resolution as $\mu \rightarrow \mu_o$. (In Fig. 10 the symbols for Thomy and Duval's points were so numerous that they have been suppressed for clarity. They have already been shown in Fig. 3.)

Analysis of experimental data to choose a precise $T_c(n)$ in each layer is extremely difficult. On an ideally homogeneous surface, a first order phase transition at $T<T_c$ would show up as a truly vertical step in an isotherm. Thus, T_c would be the lowest temperature at which the isotherm has no vertical portion. However, as Dash and Puff have pointed out [48], in a real system, the substrate presents a distribution of binding energies. The condensed phase begins to form on the most strongly binding sites, and as condensation proceeds, the interface between high and low density phases sweeps through the distribution of binding energies of the substrate. Consequently, μ, rather than being constant during condensation at constant T, has a shape that reflects the distribution of binding site energies. (See Appendix 2.) This effect is most clearly seen in data for ^{3}He [57] and ^{4}He [18] on Grafoil, where the 0 K isotherms (N vs. μ) have been reconstructed thermodynamically. At low coverage, the 1/3-registered phase coexists with a two-dimensional vacuum (the two-dimensional vapor pressure being zero). In these cases, the 0 K isotherms are not quite vertical (i.e., μ changes as N is increased) and the results were used to deduce the distribution of binding energies. The important point for this study, however, is that even in a first order coexistence region, isotherms are not expected to be vertical.

When the data plotted in Fig. 7 are examined in numerical form, it is found that the observed steps are never quite vertical. That is to say, there is sufficient experimental resolution to show that $\mu(N_2) > \mu(N_1)$ whenever $N_2 > N_1$. As we have just argued, that is necessary but not sufficient evidence to conclude that we are observing supercritical behavior at all N. It would seem that the

Figure 11. Heat Capacity Trajectories, Possible Two-phase Regions

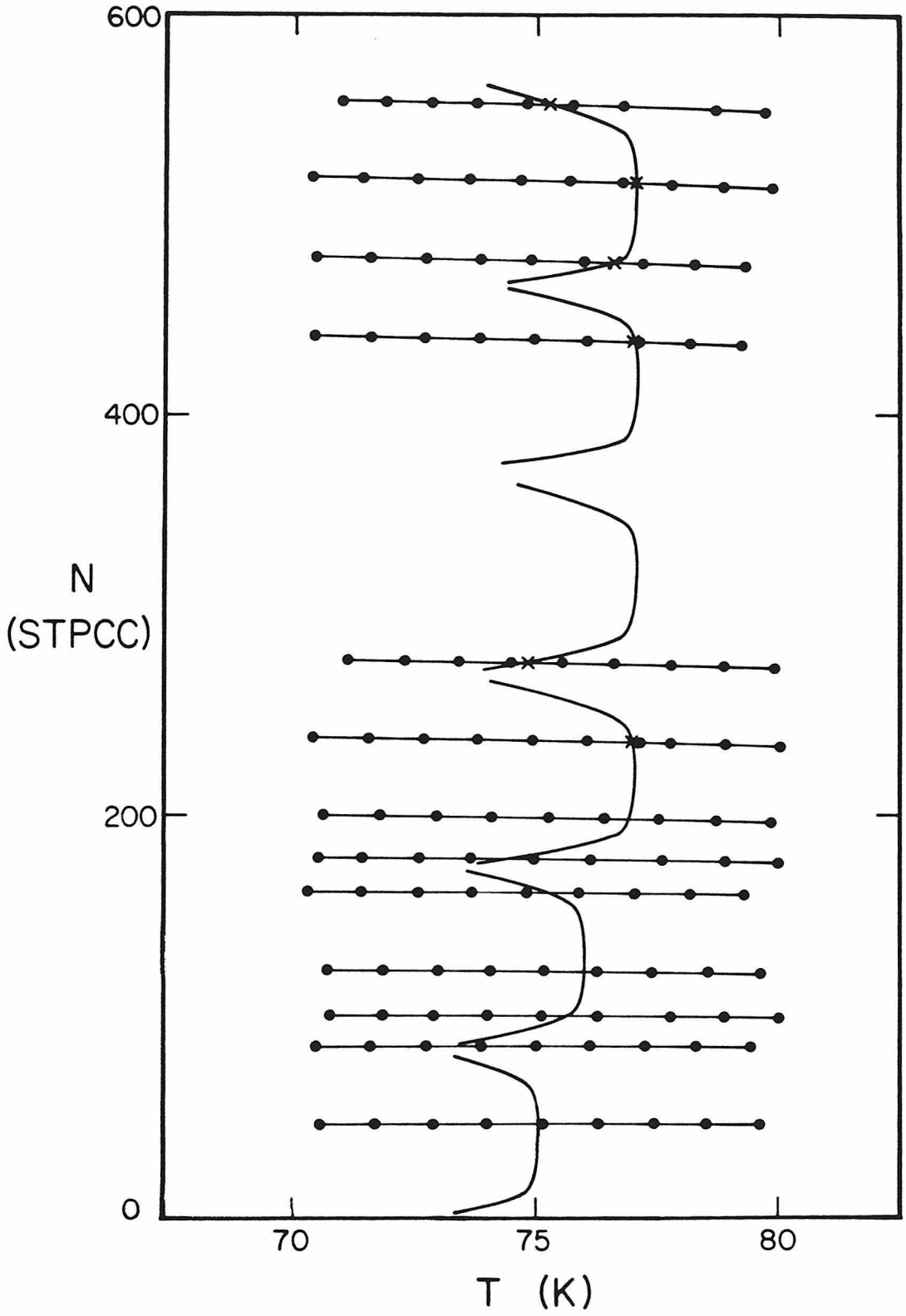

small bumps in the heat capacity curves at $T \approx 78$ K are a better qualitative indication of the situation. We should perhaps interpret them to mean that the shapes of the coexistence curves in each of the first four or five layers is such that one is very likely to pass out of the two-phase region at about 78 K.

If one passes out of a two-phase region along paths such as those sketched in Fig. 11, one expects a heat capacity signal varying from a discontinuity (if the phase boundary is intercepted far from the critical point) to an Ising-like singularity (at the critical point). However, because the two-phase region is one of infinite (two-dimensional) compressibility, inhomogeneities in even the best real substrates may be expected to smear any of these heat capacity signals into something that resembles the bumps seen in Fig. 6 [51]. We can thus propose that the bumps indicate a phase diagram of the kind sketched schematically in Fig. 11.

Now having considered qualitative arguments in favor of the two tentative conclusions put forth, we shall look into some quantitative details relevant to the central points. We shall return in Chap. 5 to discuss briefly some further implications of these conclusions.

Figure 12 shows interpolated specific heats at coverages of 430 and 232 STPCC. This figure makes it clear that whereas the peak at the triple point temperature vanishes dramatically in thinner films, the smaller bump at 78 K is of essentially constant size in the specific heat. If we take the low coverage curve in Fig. 12 as an indication of the background behavior not involved in the melting transition, we can subtract it off and use the remaining large peak to estimate the change in entropy. If we attribute that change to the amount adsorbed in excess of two layers, the result is 0.64 k_B/molecule compared to an entropy of melting of 1.24 k_B/molecule in bulk methane.

Figure 12. Isosteric Specific Heats: 430 and 232 STPCC

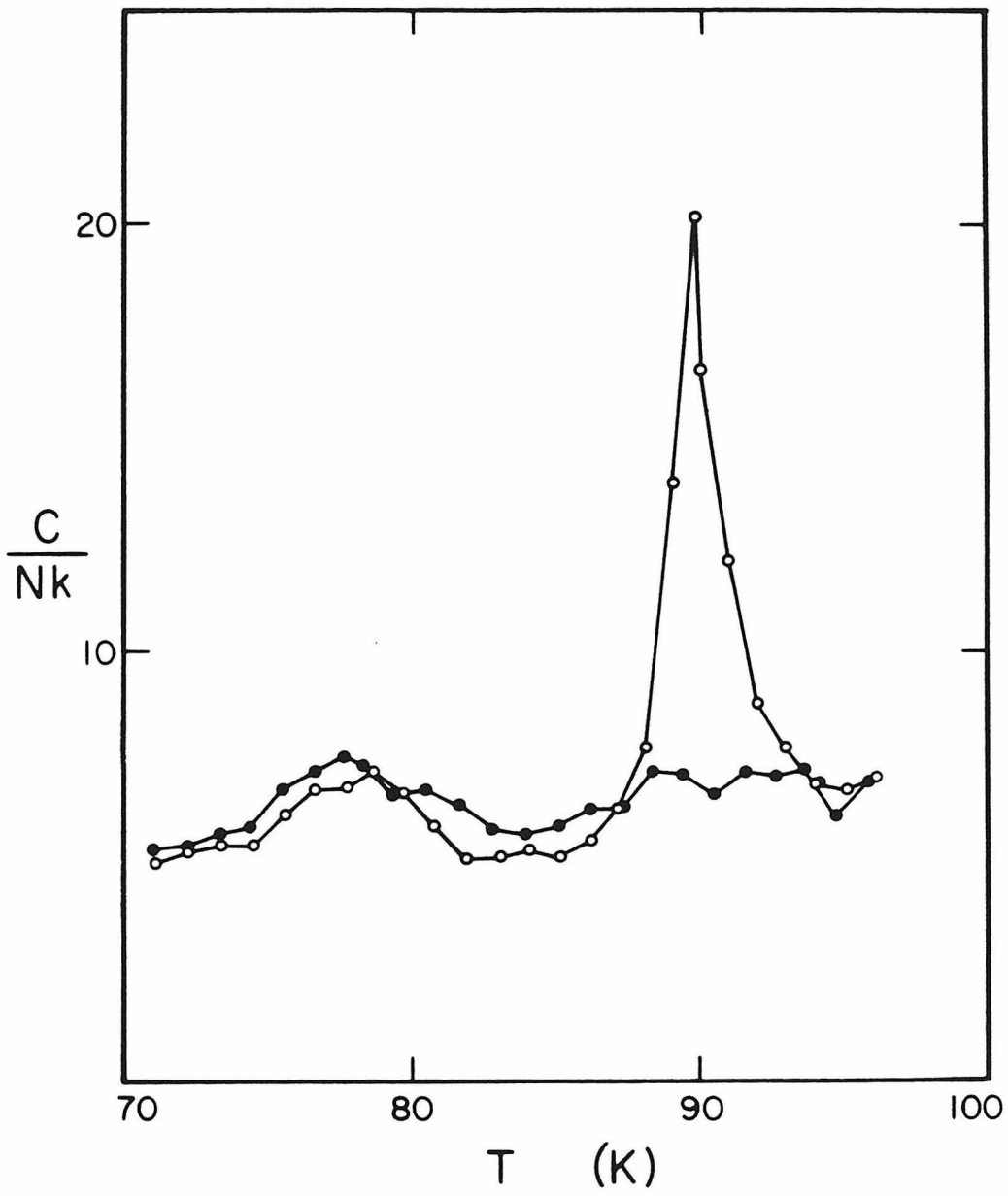

Figure 13. $\mu-\mu_o$ vs. N

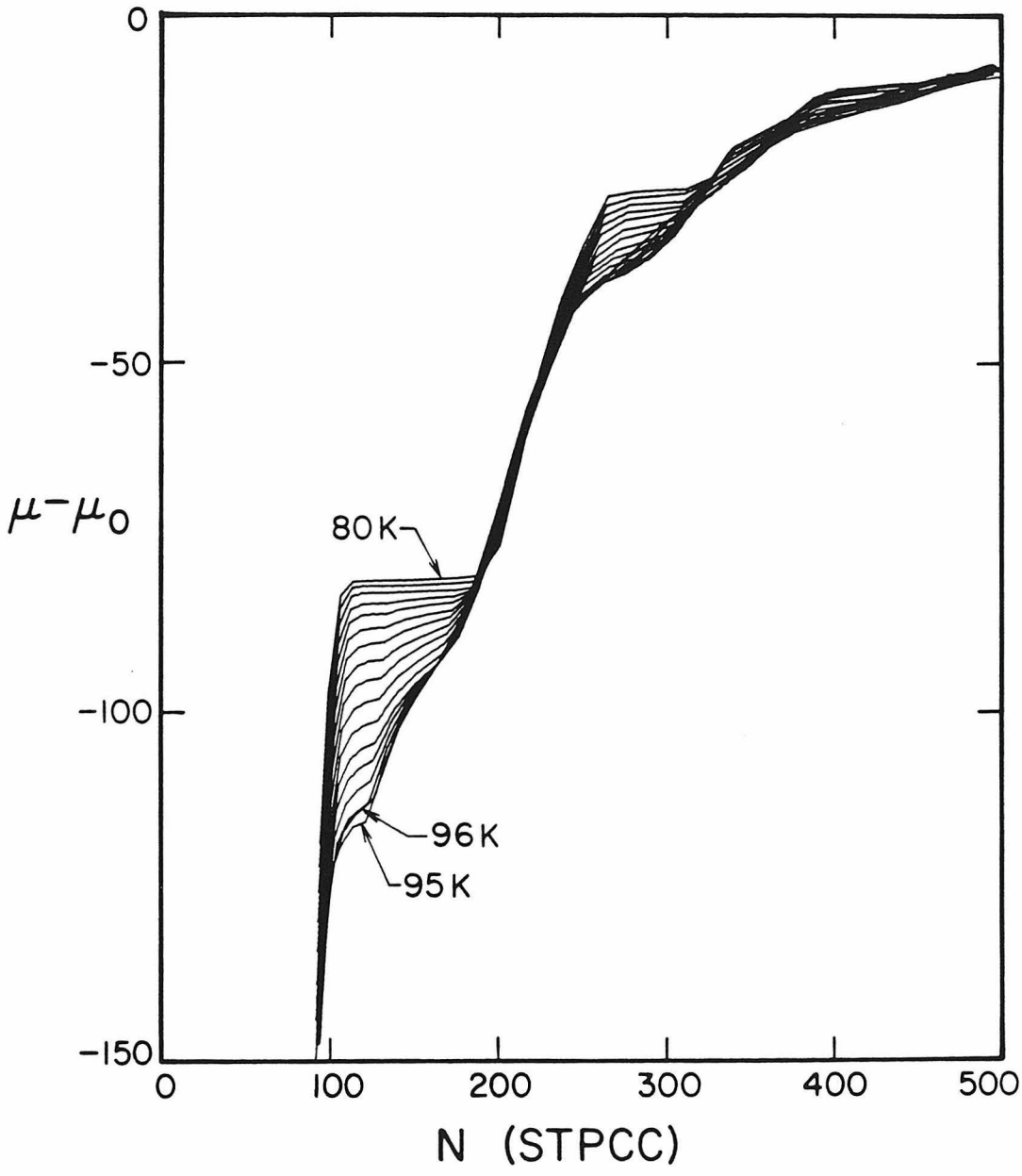

In Fig. 13 we have plotted all our vapor pressure data in the form N vs. $\mu-\mu_o$. This has the effect of collapsing the data onto a nearly universal curve. To put it differently, for many values of N, $\mu-\mu_o$ depends only on N, not T:

$$\mu-\mu_o = f(N) \quad . \tag{7}$$

Equation 6 above suggests a particular model for $f(N)$. It is easy to show that a thermodynamic consequence of Eq. 7 is:

$$\left(\frac{\partial S}{\partial N}\right)_T = s_b - v_b \frac{dP_o}{dT} \tag{8}$$

where $(\partial S/\partial N)_T$ is the partial molar entropy of the film, v_b the specific volume, and P_o the saturated vapor pressure of the bulk condensed phase at coexistence. To the extent that the second term can be ignored (it is roughly 0.01% of the first), every molecule added to the film has the entropy of a molecule in the bulk. Thus, the coalescing of the isotherms in Fig. 13 means that the essential thermal behavior of the film is that of the bulk, and the curve that remains, $f(N)$, is indeed due to the van der Waals potential of the substrate.

There are, however, prominent regions in Fig. 13 where the isotherms do not coalesce. These are precisely the regions where the thermal behavior of the system is dominated by layer by layer condensation, which is characteristic of the thin film nature of the system and not similar to the behavior of the bulk.

If Eq. 7 is not satisfied perfectly, in other words, if $f(N)$ does have some dependence on T, then the difference between $(\partial S/\partial N)_T$ and s_b is given by $(\partial f/\partial T)_N$. To examine the quantitative significance of the apparent coalescing of the curves in Fig. 13, $(\partial f/\partial T)_N$ has been computed from the numerical data at three coverages where the curves in Fig. 13 seem to coincide. The results are shown in Fig. 14, with the coverages 371 (△), 218.5 (○), and 87.5 (■) STPCC. Although these derivatives were computed in the "worst" possible way (i.e. finite

Figure 14. $(\partial f / \partial T)_N$ vs. T

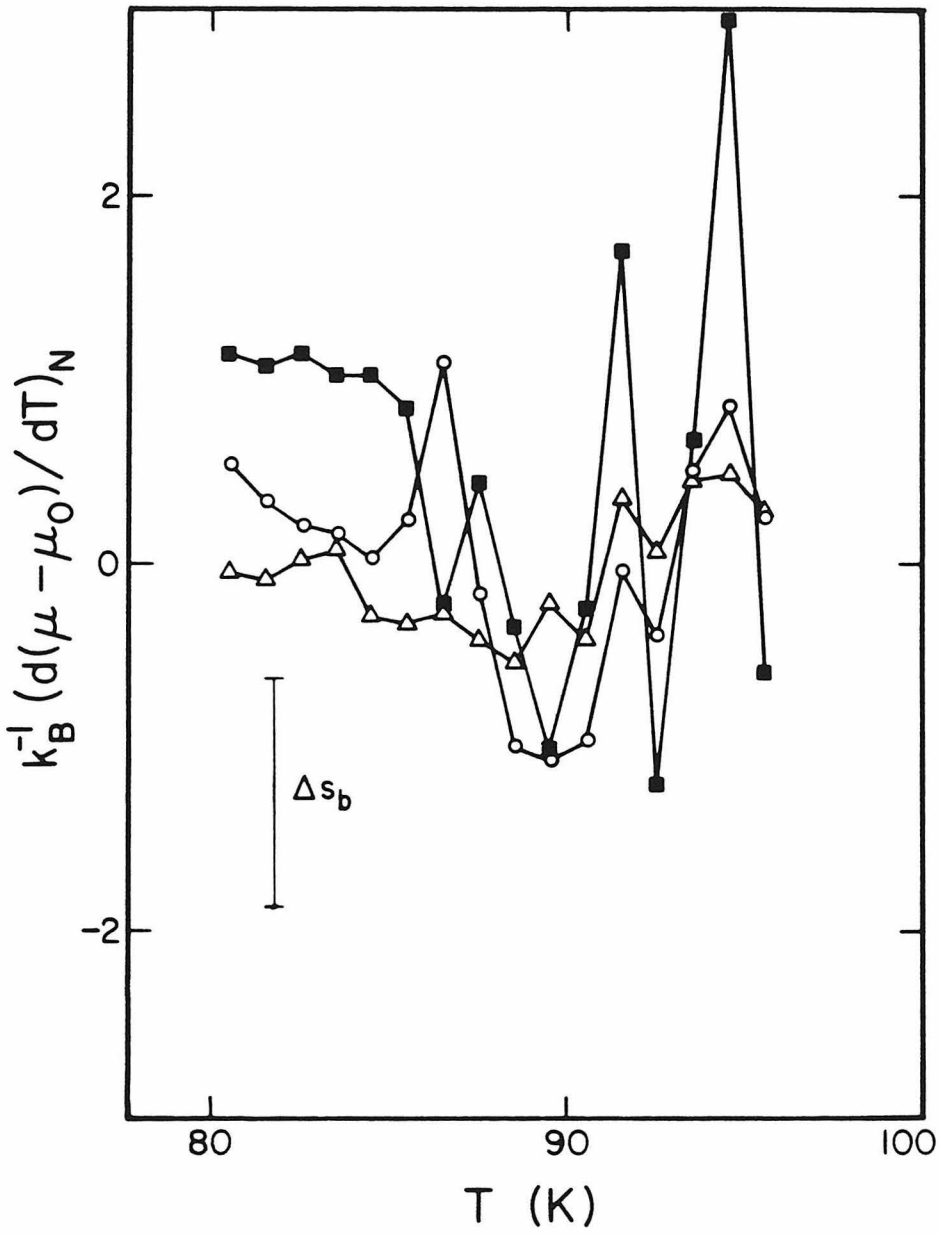

difference derivatives of unsmoothed data), it is important to note that the scatter in this measurement is comparable to the change in entropy of the bulk when it melts, and reflects little more than the limit of experimental resolution. The significance of this observation is that the coalescing of the isotherms cannot be taken to mean that thin films are solid-like below T_t and liquid-like above. Measurements of $\mu(N,T)$ by means of vapor pressure are not sufficiently sensitive to detect that difference. On the other hand, it is precisely that difference which shows up as the very large spike in the heat capacity in the thicker films at T_t.

To summarize this discussion, layer by layer condensation is seen clearly in the data for $\mu(N,T)$, but only weakly in the heat capacity - it would not be possible to offer an interpretation of the small heat capacity bumps at 78 K without guidance from the vapor pressure data. Conversely, the effects of bulk melting are seen vividly in the heat capacity data, but are essentially undetectable in $\mu(N,T)$. Both kinds of data are needed to survey the behavior of adsorbed systems.

Thermodynamic Analysis

Having taken a look at directly measured quantities, chemical potentials and heat capacities, we are now in a position to see if anything more can be gleaned by doing the complete thermodynamic analysis. The answer, briefly, is *yes* in principle, but in this particular case our efforts might not always bear fruit due to the coarseness of our survey grid.

The key to the whole analysis is the construction of the Landau potential, Ω, as a function of its proper variables, T and μ. This has been done according to the methods described in Chap. 2, and the results have been tabulated in the second table of Appendix 3. From the Landau potential we can immediately get

the spreading pressure, $\varphi = -\Omega / A$, where A is the area of the substrate (326 m^2). We can also convert heat capacities from C_A to C_φ, and consider questions pertaining to lateral compressibilities.

One such question, for example, is, Does the monolayer melt in a first order phase transition? The isotherm measurements of Larher [5] do indicate that the transition is first order, but unfortunately our present data are not sufficiently dense or sensitive to shed any light on the discussion. These data, of course, constitute a sweeping survey of a broad region, and armed with this survey, we can direct more detailed future studies to specific areas of interest. The monolayer melting curve would be one such area, but we would need to resolve details on a scale of 0.1 layer or better. The spacing between the heat capacity coverages of Fig. 6 is at least half a layer, of which only one coverage is in the submonolayer regime. (This run, by the way, shows no structure above the experimental resolution.) On the other hand, if we had more detailed information we could form 2D isochors, as was done for the helium monolayer by Elgin and Goodstein [18], and answer the question definitively.

In analyzing the vapor pressure data near the monolayer melting region, however, we can make a somewhat unexpected observation concerning the shape of the phase boundary in the μ-T plane. If the chemical potential (relative to bulk) on the transition line is compared to its corresponding melting temperature, T_m, then the relationship is found to be linear over a range of at least 20 K:

$$(\mu - \mu_0)_m = -1385.2 + (11.507)\, T_m$$

This is shown graphically in Fig. 15 where the data have been taken from Refs. 4 (▪), 5 (▫), and this work (▲). The significance of this observation is unknown.

Figure 15. $(\mu-\mu_o)_m$ vs. T_m in the First Layer

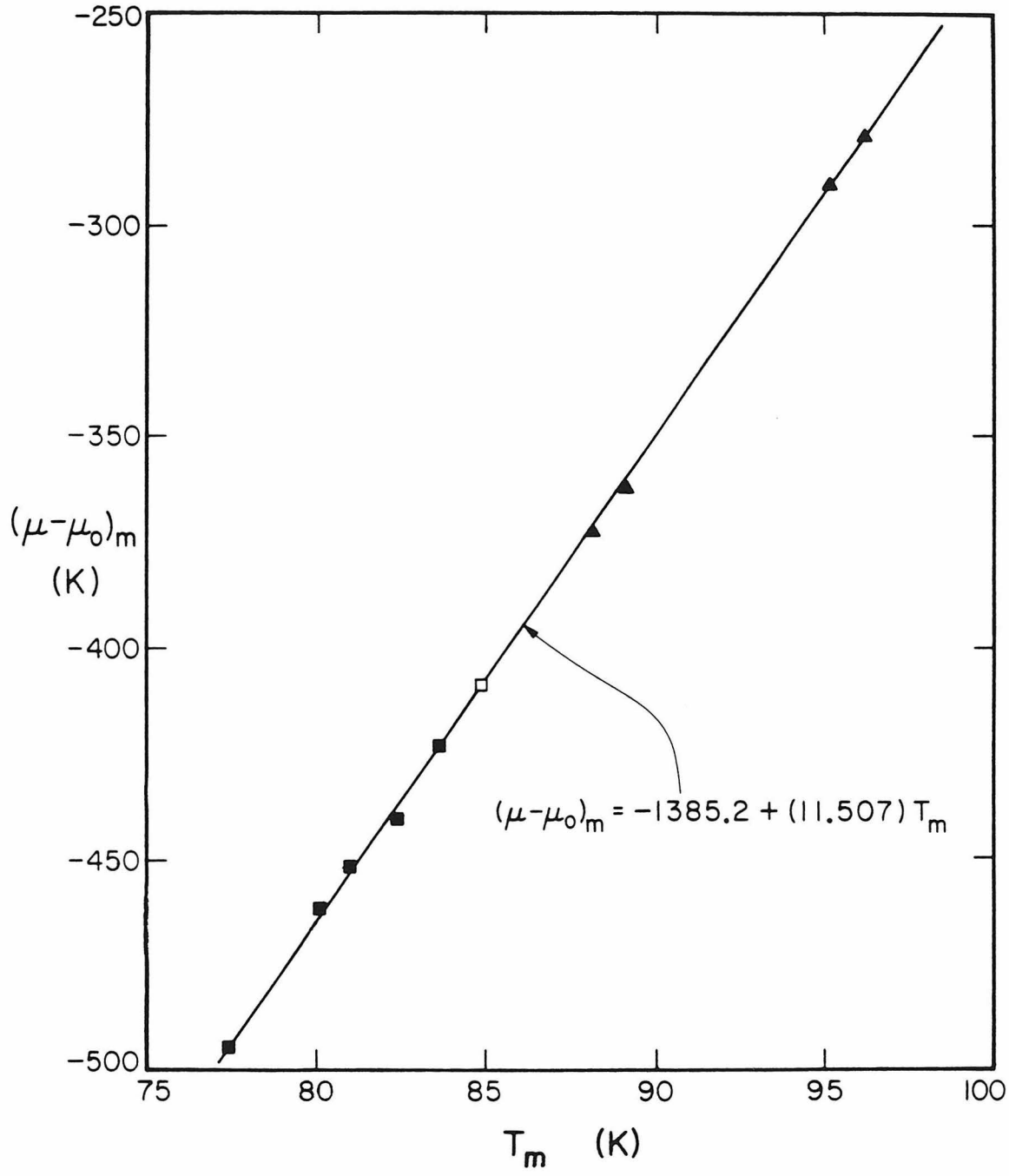

Meanwhile, what do we get from a knowledge of φ? In and of themselves, the data in Appendix 3 tell us mainly that φ becomes independent of N for thick films. This is to be expected since φ is mainly $V(\bar{P}-P)/A$, where $\bar{P}$ is the volume average pressure throughout the cell. The local pressure is different from P only in the first few layers where the van der Waals attractions are strong. So, once these layers are filled up, there will be no more contributions to φ if molecules are subsequently added. The shapes of the isotherms in Fig. 7 bear this out: N becomes independent of μ as $\mu \to \mu_o$, and the corresponding contributions to the integral in Eq. 5 are small.

One reason φ is interesting is that it is an intrinsic quantity. (It is essentially the thermodynamic conjugate variable to A.) As such, it can be used to map out phase boundaries on a φ-T plot where two-phase "regions" collapse into lines much as they would for a bulk substance on a P-T plot. We can convert our measured heat capacities, C_A, to C_φ to see if, for example, the 90 K peaks of Fig. 6 get sharper. (In bulk substances, the equivalent operation would be to convert C_V to C_P in order to see a mesa-like step at coexistence change into a δ-function spike whose area is the latent heat of the transition.)

However, it turns out that using the formula on p. 32 to convert C_A to C_φ tells us very little. Because as φ becomes independent of N, we have $(\partial\Omega/\partial N)_T \to 0$, and C_φ becomes infinite *at all temperatures*. Does this mean that some cataclysmic thermodynamic upheaval is taking place? No, it simply means that as the film thickness increases to near bulk proportions, the presence of the first few layers becomes unimportant and C_φ becomes C_P at coexistence. (The film is always in equilibrium with its vapor.) But C_P at coexistence is no less than the δ-function infinity mentioned above, corresponding in this case to crossing the saturated vapor pressure curve at any random point. Thus it reflects only the bulk condensed-state/vapor latent heat, and not the latent

heat between two condensed states at 90 K.

Given this impasse, we could construct C such that some other intrinsic variable were held constant (μ or $\mu-\mu_0$ for example). The tables of Appendix 3 could certainly be used for this purpose (albeit with the coarse data grid resolution problems already discussed, and with the realization that the results would no longer be isosteric), but the data as they stand may need only little "manipulation" to decide such questions anyway. To begin with, we have been somewhat loose in our definition of C_A, and must now be more precise. The heat capacities pictured in Fig. 6 (and subsequently listed in Appendix 3) can be considered to have been taken under the following conditions. First, N is held constant, and A is of course constant. (The non-isosteric raw data have been corrected as described in Chap. 2 to bring this about.) Furthermore, the thickness of the film, d, takes on whatever value it needs to maintain a free surface in equilibrium with its vapor. Thus, at all times $d = d(N,T)$, and is for us unmeasurable. Now if we call these conditions "Y" (not to confuse them with the conditions "X" of Chap. 2), then we can relate C_Y (formerly "C_A") to the true heat capacity at constant volume (i.e. at fixed N, A, *and* d):

$$C_Y = C_V + T\left(\frac{\partial S}{\partial V}\right)_T\left(\frac{\partial V}{\partial T}\right)_Y \quad .$$

where V is Ad and $(\partial V)_Y = A(\partial d)_Y$. The message of this equation is clear: for the submonolayer, where the molecules are strongly bound to the surface, $d(N,T)$ is independent of temperature (being merely the width of one molecule), so $(\partial V/\partial T)_Y = 0$ and C_Y and C_V are one and the same thing. It then makes sense to convert C_A to C_φ to probe the sharpness of the phase transition, and reiterates the fact that the submonolayer regime is where the concept of φ is most meaningful. However, for a multilayer film, $d(N,T)$ takes on a temperature dependence roughly determined by the bulk coefficient of thermal expansion. Thus,

for thick enough films, C_Y becomes C_{SAT}, or, the bulk heat capacity along the saturated vapor pressure curve. Converting to C_φ (i.e. C_P) yields no information, as mentioned above, but since C_{SAT} already contains a spike at the triple point, no conversion is necessary. For films of intermediate thickness, then, it is not really clear how C_Y must be altered to make it reflect conditions of constant intrinsic variable and constant N.

As pointed out in Chap. 3, a great deal of thought is devoted to the film surface tension in the PSW model. Here the thermodynamic technique can be of use. First, it is important to realize that surface tension, γ, and spreading pressure, φ, are not the same thing. Spreading pressure is a thermodynamic quantity pertaining to the entire film, and causes the film to expand if its boundaries are relaxed. On the other hand, surface tension deals with behavior only at the surfaces of the film (both the substrate and vapor interfaces) and causes the film to contract if its boundaries are relaxed. Explicitly,

$$\varphi = A^{-1} \int_0^N N \, d\mu \qquad (T = const.)$$

from Eq. 5, and

$$\gamma = \gamma_{fs} + \gamma_{fv} = -A^{-1} \int_0^N N \, d(\mu - \mu_o)$$

from Ref. 29. (The minus sign means simply that φ and γ act in opposite directions.) Since T is held constant during the integration, $\mu_o(T)$ is merely an additive constant in the second expression. The two integrals become the same, therefore, but for the difference in sign. Formally, this amounts to saying that the surface excess formalism described in Chap. 2 leaves us with only interfacial contributions to the Landau potential in the case of a fully wetted film. The quantity γ_{fs} has never been measured for the methane/graphite system, but if

γ_{fv} could be obtained independently by conventional means, then the tables in Appendix 3 would allow us to find γ_{fs} and thus make an important fundamental measurement.

Finally, the thermodynamic technique can be used to extend our knowledge of μ into regions where the pressure is unmeasurably low [18]. An attempt was made to do this for temperatures below 78 K in order to see, for example, if the layering isotherm steps become more vertical. Again the coarseness of the survey grid caused the results to be of questionable value (unfortunately one needs to know $(\partial S/\partial N)_T$ which is sensitive to the separations in heat capacity coverages), but there did seem to be a general trend to more verticality as the temperature decreased.

The main conclusion of this section is that the thermodynamic technique can provide valuable information on a number of topics of fundamental importance. Given the ideal situation of having perfectly accurate data on an infinitely dense grid in the N-T plane, there would be no thermodynamic quantity which could not be obtained from the analysis. However, in the present situation, the data grid corresponds to a preliminary "first pass" survey of a broad region of interest, and is necessarily coarse. Even at that, it is not without merit, and moreover points the way to future interesting investigations.

Chapter 5. CONCLUSIONS

This survey of multilayer methane films adsorbed on graphite was undertaken to probe the thermodynamic behavior of a system whose dimensionality is somehow intermediate between two and three dimensions. Of particular interest is the melting transition which occurs on the equilibrium vapor curve at the triple point, 90.66 K. The PSW model of multilayer adsorption suggested other possible effects at T_w and T_R, of which we found evidence of the latter.

We set out to survey a temperature region between $T_c(1)$, the first layer critical temperature, and T_t, the bulk triple point. According to the PSW model, $T_c(1)$ should be the first in a series of transitions $T_c(n)$, with $T_c(\infty) = T_R$ the roughening transition, and T_t is the upper limit of possible roughening temperatures. Thus the survey could be expected to give interesting results, provided methane wets graphite in this temperature interval.

All of the data we present are at $\mu < \mu_o$, which is to say, in a fully wetted film. Of course methane on graphite might have a finite wetting temperature T_w below the range we have studied (future measurements will investigate this point). It is also possible that methane begins to bead up in films of more than about 6 layers, but this seems exceedingly unlikely.

Beading up means that beads of bulk matter coexist with a uniformly adsorbed film. For this to occur, it is necessary that the film be in a state of higher intrinsic free energy than the bulk in order to balance its lower van der Waals potential. However, the evidence presented in this report shows that a five layer film is so similar to the bulk that it melts at nearly the same temperature. Thus the conditions necessary for beading up do not seem to be present.

The traditional method of detecting beading is to see how $\mu(N, T)$ intersects the μ_o axis [17]. But if beading does occur in methane films below 64 K, there is

no hope of detecting it by making direct vapor pressure measurements. One would have to use the thermodynamic technique to extend, by new heat capacity measurements below 64 K, knowledge of the chemical potential to such low temperatures. The tables of Appendix 3 could be used as a starting point for this effort. It is also possible that a thermodynamic signature of wetting could be found in the heat capacity measurements themselves, providing that the solid film could be maintained in true equilibrium (as opposed to a metastable thermodynamic state) during the measurement.

Meanwhile, we have evidence for layering transitions that there is a $T_c(n) \approx 78$ K independent of n for the first five or six layers. If we boldly extrapolate n from six to infinity, this implies a roughening transition at the interface between bulk solid methane and its vapor at $T \approx 78$ K.

The melting transition seems to extend from the bulk triple point into the multilayer region at essentially constant temperature. It does not appear to be first order in films of five layers and less. The entropy associated with melting (i.e. the area under the heat capacity peak we associate with melting) becomes smaller as the film becomes thinner, vanishing altogether at about two layers. This effect does not appear to be due to capillary condensation.

This is somewhat surprising since one can argue that if the melting transition extends into the multilayer region at *exactly* T_t, then it should be truly first order. The argument is this: the two film states, solid and liquid, each possess their own chemical potential which is a function of N and T. Since chemical potential is no more than free energy per particle, the film will be in the state of lowest μ, whether that be $\mu_s(N,T)$ or $\mu_l(N,T)$. The temperature at which these quantities are equal, T^*, is the transition temperature where the system jumps from one state to the other. If we consider μ to be fixed at the transition, we have:

$$\mu^* = \mu_s(N_s, T^*) = \mu_l(N_l, T^*)$$

where $N_s - N_l$ reflects the difference in densities (if any) between the two states s and l. (One can imagine adding or removing particles at fixed μ to effect the transition at T^*. Since $N_s - N_l$ is the amount added, a non-zero result indicates a first order transition.) Now if the transition occurs at exactly the triple temperature we would have

$$\mu_s^*(N_s, T_t) = \mu_l^*(N_l, T_t)$$

in which both quantities μ_s^* and μ_l^* *are functions of N only*. Since they cannot be the same function (otherwise there would be no difference between the s and l phases), N_s cannot be equal to N_l and the transition is first order.

So it seems paradoxical that the melting transition in these films is at constant temperature (~90 K) and yet not first order. Of course the real question involves the degree to which T^* can vary and yet *appear* to be unchanging in a plot such as Fig. 6. A close investigation of the data reveals that the peak temperatures do shift downward with lower coverages, but a resolution of the peaks' true positions to better than 1 K is difficult. Moreover, if a 4 layer film happened to melt, say, at 89 K, then all the films between 4 layers and bulk would melt somewhere between 89 and 90.66 K, and the transition line would appear nearly isothermal in a plot where the axes are linear in N and T. The situation is reminiscent of looking for strictly vertical isotherm steps in a plot of N vs. μ. One has to handle the data properly to draw the right conclusion.

Isothermal or not, the melting transition must close in some way because it should not be possible to follow any thermodynamic path from solid to liquid without passing through a phase boundary. However, the data show only a phase transition that becomes successively weaker until it disappears into the experimental scatter. It does not appear to end on the first layer melting curve, but

there is some evidence of a phase transition in the second layer which might provide a way for the extension of the triple point to close. Alternatively it might end on a thermodynamically invisible transition as suggested by KTHNY.

In summary, the complete thermodynamic analysis of the data presented here has enabled us to put forth hypotheses, suggested by these data, but requiring independent future measurements to test them.

Epilogue

Since we seem to have raised more questions than we have answered, we are perhaps no closer to discerning the difference between order and disorder than we were in Chap. 1. However, it has become clear - from the work of KTHNY, for example - that phase transitions in themselves do not have to be associated with discontinuities in thermodynamic properties (the classical way of identifying them). More to the point, they involve different *classes* of elementary excitations of the system in question. Whatever these excitations are (be they phonons, dislocations, broken Cooper pairs, or spin waves), whenever the dominant type of excitation in a system changes from one class to another, we can identify this as a phase transition. The other known properties of phase transitions (thermodynamic discontinuities, alterations in structure, and changes in symmetry) all fall into line, and we can say at this point that the order of the system has undergone a fundamental change.

Appendix 1. THE ROTATIONAL STATES OF THE METHANE MOLECULE

Methane is a spherical rotator so that its rotational energy levels are $\hbar^2 J(J+1)/2I$ where $J = 0,1,2, \cdots$. (See p. 151 of Ref. 25.) Thus, the molecule possesses a partition function of

$$Z_{rot} = \sum_{J=0}^{\infty} \sigma_J \, e^{-\hbar^2 J(J+1)/2IkT}.$$

The difficulty in evaluating this sum is figuring out the degeneracy, σ_J, of each J state on account of the nuclear spin of the molecule's protons. First of all, for each independent state of angular momentum J, there are $(2J+1)$ orientations in space. Thus we can write

$$Z_{rot} = \sum_{J=0}^{\infty} d_J \, (2J+1) \, e^{-\hbar^2 J(J+1)/2IkT}$$

where $d_J = \sigma_J/(2J+1)$ and is the number of independent states of angular momentum J.

Each of the four protons has a nuclear spin ½, so that there are $4^2 = 16$ possible nuclear spin states (each spin having two possible orientations $i_z = \pm$ ½). Of these states the total nuclear spin can be $S=2$ (5 states), $S=1$ (3 families giving 9 states in all), or $S=0$ (2 families for 2 states). However, the identical nature of the four protons places restrictions on how many of the nuclear spin states S can take on an angular momentum J. If we call this number n_S^J (an integer), then we have

$$d_J = \sum_{S=0}^{2} n_S^J \, (2S+1).$$

The numbers n_S^J for J up to 4 are given in p. 151 of Ref. 25, and following their same reasoning, we can complete the table:

Values of n_S^J				
J	S=0	S=1	S=2	d_J
0	0	0	1	5
1	0	1	0	3
2	2	1	0	5
3	0	2	1	11
4	2	2	1	13
5	2	3	0	11
6	2	3	2	21
7	4	4	1	21
8	4	4	1	21
9	2	5	2	27
10	4	5	2	29
11	4	6	1	27
J+12	n_0^J+4	n_1^J+6	n_2^J+2	d_J+32

Because each term J is related to $J+12$, we can write

$$\sum_{J=0}^{\infty}(J) = \sum_{n=0}^{\infty}\sum_{J'=0}^{11}(J'+12n)$$

and accordingly replace the dummy index J' with J. Thus

$$Z_{rot} = \sum_{n=0}^{\infty}\sum_{J=0}^{11}[2(12n+J)+1]\,(d_J+32n)\,e^{-\frac{\hbar^2}{2IkT}(12n+J)(12n+J+1)}$$

$$= 5 + 9e^{-T_r/T} + 25e^{-3T_r/T} + 77e^{-6T_r/T} + 117e^{-10T_r/T} + \cdots$$

where $T_r = \hbar^2/Ik_B$ = 15.160 K. (This differs from the expression in Ref. 25 by a factor of 16: we wish to include the 16-fold nuclear spin degeneracy in this partition sum.) In the classical limit we have

$$Z_{rot} = \frac{16}{12}\sqrt{\pi}\left(\frac{2IkT}{\hbar^2}\right)^{3/2}, \qquad T >> T_r\ .$$

This is to be expected since $\sqrt{\pi}(2IkT/\hbar^2)^{3/2}$ is the partition function of a classical sphere and the factor of 16/12 comes about due to quantum degeneracy†. The factor of 16 has already been mentioned as a consequence of the 16 spin states, and the factor 1/12 comes about because of the identical nature of the protons. For each orientation of the methane molecule there are 12 equivalent orientations brought about by symmetry operations. These 12 orientations must be counted as a single quantum state, and not 12 separate states as would be the case if the protons were distinguishable.

The consequences of the rotational energy levels are easily seen on the thermodynamic functions of the gaseous molecules. In particular, for a gas consisting of N_g molecules we have

$$Z_{rot}(total) = Z_{rot}^{N_g}$$

giving the free energy as

$$F_{rot} = -kT \ln Z_{rot}^{N_g}$$

$$= -N_g kT \ln Z_{rot}$$

The rotational contributions to the entropy, chemical potential, and heat capacity are easily calculated:

$$S_{rot} = -\left(\frac{\partial F_{rot}}{\partial T}\right)_{N_g} = \frac{N_g kT}{Z_{rot}} \frac{dZ_{rot}}{dT} + N_g k_B \ln Z_{rot}$$

$$C_{rot} = T\left(\frac{\partial S_{rot}}{\partial T}\right)_{N_g} = \frac{N_g kT}{Z_{rot}}\left[2\frac{dZ_{rot}}{dT} - \frac{T}{Z_{rot}}\frac{dZ_{rot}}{dT} + T\frac{d^2Z_{rot}}{dT^2}\right]$$

† The appearance of Planck's constant, h, in a classical expression is due to the way we have divided phase space into cells. Since classical mechanics permits the size of the cells to be anything, there is no contradiction in terms if we choose the one size required by quantum mechanics, namely h^3.

$$\mu_{rot} = \left(\frac{\partial F}{\partial N_g}\right)_T = -k_B T \ln Z_{rot} = \frac{F_{rot}}{N_g}$$

with $E_{rot} = F_{rot} + TS_{rot}$.

The contribution per molecule can be gotten by dividing by $N_g k_B$:

$$f_{rot} = F_{rot} / N_g k_B = \mu_{rot} / k_B$$
$$s_{rot} = S_{rot} / N_g k_B$$
$$e_{rot} = E_{rot} / N_g k_B$$
$$c_{rot} = C_{rot} / N_g k_B$$

In the classical limit (putting T_r as 15.160 K) we have

$$Z_{cl} = (6.68434)\,(T/15.16)^{3/2}$$
$$f_{cl} = -(1.89977)T - (3/2)T \ln (T/15.16)$$
$$s_{cl} = 3.9977 + (3/2) \ln (T/15.16)$$
$$e_{cl} = (3/2)T$$
$$c_{cl} = 3/2$$

For reducing the data presented in Chap. 4, computer subroutines were written to provide values of μ_{rot}, c_{rot}, and s_{rot} on demand. In all of the calculations, the partition sum was truncated after the first twenty-four terms.

As an example of these calculations, c_{rot} is shown plotted as a function of temperature in Fig. A1. There is a peak of 1.838 at a temperature of 25.143 K, and this is close to the 20.5 K rotational transition temperature seen in the bulk solid.

Figure A1. Rotational Specific Heat of the Methane Molecule

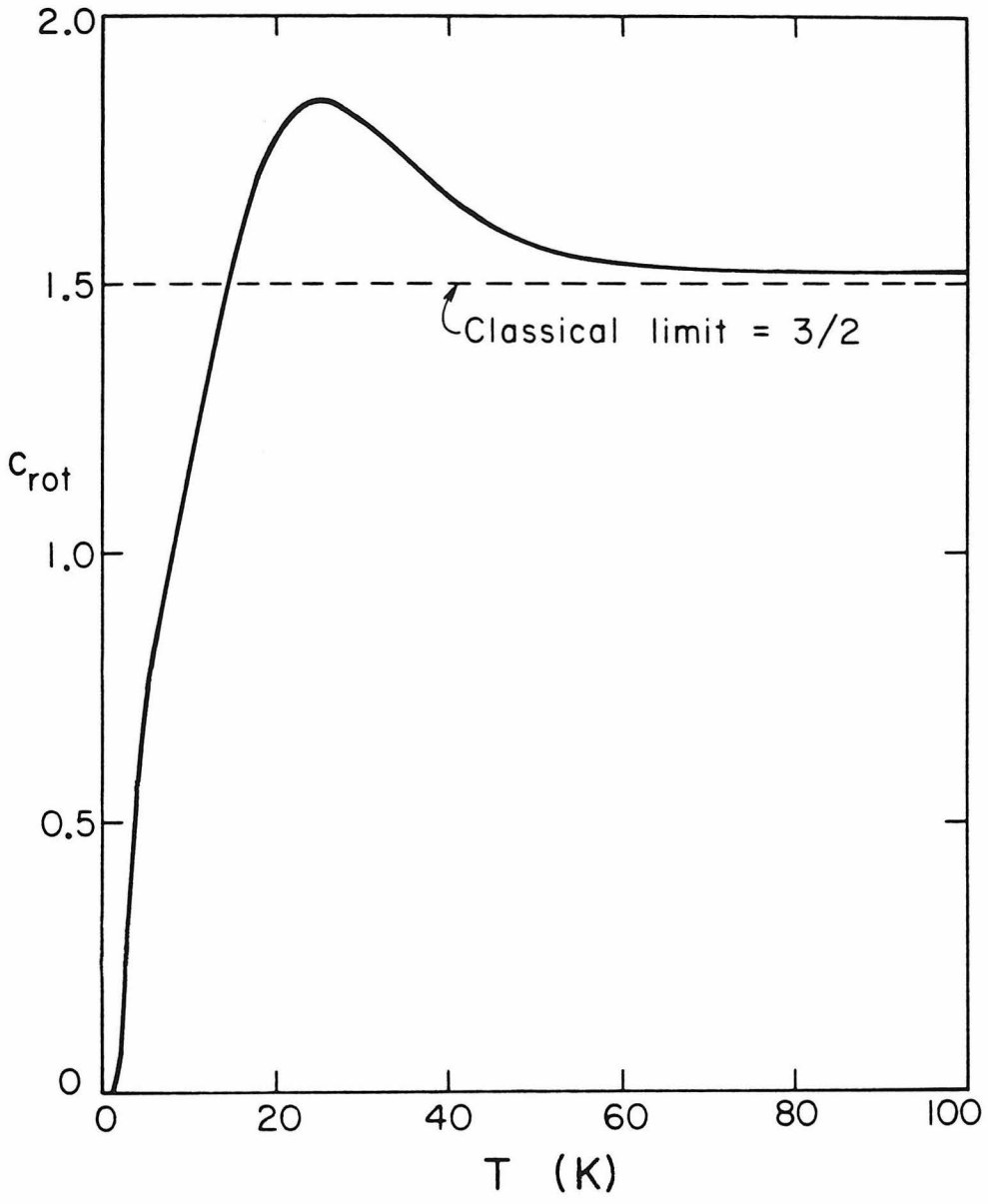

Appendix 2. CRITICAL POINTS AND VAPOR PRESSURE ISOTHERMS

In monolayer adsorption studies, a standard technique for identifying 2D liquid/gas critical points is the use of μ-N data plotted along an isotherm [17]. (Usually vapor pressure is plotted instead of μ, but these are trivially related by Eq. 4.) A first order phase transition shows up as a vertical discontinuity in the plot of N vs. μ, and this indicates a two-phase coexistence region between two film states of different areal density, $n=N/A$ (where A is the area of the substrate). The size of this coexistence region is simply $\Delta n_{coex} = n_2 - n_1$, where the two phases are labelled 1 and 2. This quantity is temperature dependent, and in some cases may shrink to zero at a critical temperature, T_c. Thus, the isotherm at T_c shows a vertical jump of zero width (i.e. a vertical inflection point) at density $n_c = n_1 = n_2$, and higher temperature isotherms show no vertical jumps whatsoever.

However, the picture is complicated if the molecules see a nonuniform distribution of binding site energies over the face of the substrate. In this case we can define a positional parameter y for which $\hat{y}$ points in the direction of $\nabla_{\|}u$, where u is the substrate potential, and $\nabla_{\|}$ denotes the gradient in directions parallel to the surface. (That is, if contours of constant u were drawn looking down from above, $\hat{y}$ would be perpendicular to them at each point.) The chemical potential is still uniform throughout the area A (and, in fact, throughout the entire cell), so we have

$$\mu = \mu_{th}(T, n(y)) + u(y) = const.$$

where μ_{th} is the "thermodynamic part" of μ, and $n(y)$ is the local density governed by the substance's equation of state. (Note that if $u(y)$ is uniform,

then it simply reverts to an additive constant.) We can let $y=0$ correspond to the strongest energy binding site, and $y=h$ correspond to the weakest. Thus, in a two-phase coexistence region, the condensed phase (phase 2) will begin to collect first at $y=0$, and as more molecules are added to the surface, the 1D interface between phases 1 and 2 will sweep through y from 0 to h. However, this process no longer occurs at constant μ since we have $\mu_{th}(T,n_1) = \mu_{th}(T,n_2) = \mu_{coex}(T)$ at the interface. Therefore, the two-phase region begins at $\mu_1 = \mu_{coex}(T)+u(0)$ and ends at $\mu_2 = \mu_{coex}(T)+u(h)$, and the range of chemical potential is independent of temperature: $\mu_2-\mu_1 = u(h)-u(0)$.

Since this occurs over a range of μ, the two-phase region no longer appears vertical on an isotherm plot. How, then, are we to identify the critical point? The answer turns out to be simple in principle, but difficult in practice because it demands much higher resolution from the experimental data. To begin with, we must realize that the density profile, $n(y)$, is unmeasurable. At any given time, all we know is N, the number of molecules on the surface, and A. Hence, we only know the average density, $\bar{n} = N/A$, where $\bar{n}$ is like any other averaged quantity $\bar{g}$:

$$\bar{g} = \frac{1}{h}\int_0^h g(y)dy.$$

The isotherm, then, is simply a plot of $\bar{n}$ vs. μ, and instead of strict vertical steps, there will be breaks in the slope $(\partial\bar{n}/\partial\mu)_T$ at the points μ_1 and μ_2. Moreover, the shape of the curve $\bar{n}$ vs. μ between μ_1 and μ_2 will reflect the shape of the energy distribution $u(y)$. (Strict verticality, of course, means that $u(y)=constant$.) Thus, T_c can be identified when the curve $\bar{n}$ vs. μ contains no breaks in slope.

Basically we have phase 1 (the dilute phase) below μ_1, phase 2 above μ_2, and two-phase coexistence between μ_1 and μ_2. Thus, if $\vartheta(x)$ is the step function, we

have

$$\bar{n}(T,\mu) = \vartheta(\mu_1-\mu)\bar{n}_1(T,\mu) + \vartheta(\mu-\mu_2)\bar{n}_2(T,\mu) + \vartheta(\mu-\mu_1)\vartheta(\mu_2-\mu)\bar{n}_{12}(T,\mu)$$

where

$$\bar{n}_{12}(T,\mu) = \frac{1}{h}\left[\int_0^{y(\mu)} n_2(T,\mu,y')dy' + \int_{y(\mu)}^{h} n_1(T,\mu,y')dy'\right]$$

and takes account of the fact that at coexistence, the boundary between phases 1 and 2 will be at some position y which is dependent on the chemical potential. (Namely, $y = u^{-1}[\mu-\mu_{coex}(T)]$.) The derivative $(\partial\bar{n}/\partial\mu)_T$ is related to the compressibility (see Chap. 2), and is found to be

$$\left(\frac{\partial\bar{n}}{\partial\mu}\right)_T = \left[\vartheta(\mu_1-\mu)\left(\frac{\partial\bar{n}_1}{\partial\mu}\right)_T + \vartheta(\mu-\mu_2)\left(\frac{\partial\bar{n}_2}{\partial\mu}\right)_T + \vartheta(\mu-\mu_1)\vartheta(\mu_2-\mu)\left(\overline{\frac{\partial n_{12}}{\partial\mu}}\right)_T\right]$$

$$+ \vartheta(\mu-\mu_1)\vartheta(\mu_2-\mu)\frac{1}{h}\left(\frac{\partial y}{\partial\mu}\right)_T\Bigg|_{\mu}\Delta n_{coex}(T)$$

where

$$\overline{\frac{\partial n_{12}}{\partial\mu}} = \frac{1}{h}\left[\int_0^{y}\left(\frac{\partial n_2}{\partial\mu}\right)_{T,y'}dy' + \int_{y}^{h}\left(\frac{\partial n_1}{\partial\mu}\right)_{T,y'}dy'\right].$$

Despite the presence of the ϑ-functions, the quantity in square brackets is continuous, but the trailing term is a mesa-like step giving discontinuities at μ_1 and μ_2. The magnitude of this step is proportional to the slope of the interface profile (y vs. μ), and to $\Delta n_{coex}(T)$. Thus, at T_c, where there are no longer two solutions to the equation of state, $\Delta n_{coex} = 0$ and the discontinuities go away.

As for the interface profile $y(\mu)$, we have $(\partial y/\partial\mu)_T = (du/dy)^{-1}$, evaluated at μ. In principle, given data of sufficient resolution, du/dy (and hence $u(y)$) can be reconstructed from the mesa-like part of $(\partial\bar{n}/\partial\mu)_T$ providing one has a

way of subtracting off the continuous part. The fact that du/dy is reflected in the $\bar{n}$ vs. μ curve led Dash and Puff [48] to suggest that there will be no discontinuity in slope upon entering or exiting the two-phase region. (They claim that the "corners" of the isotherm step will be rounded because of the shape of the $u(y)$ distribution at the high and low energy ends.) That this is not the case is seen clearly in the expression for $(\partial\bar{n}/\partial\mu)_T$. However, if $u(y)$ has a high energy (i.e. strong binding) tail extending to infinity, this could suppress μ_1 to $-\infty$. Thus, from the first molecule to go on the surface, there will be at least some of phase 2 present, and we would (in effect) always be in the two-phase region as long as μ is less than μ_2. However, even in this extreme case there will be a slope discontinuity at μ_2.

The best temperature to work with for extracting $u(y)$ is clearly $T=0$. Here phase 1 is simply a 2D vacuum, and all molecules will congregate in patches of phase 2. The thermodynamic technique is required in order to obtain values of μ at $T=0$, but this has been done for the cases of ^{3}He and ^{4}He on Grafoil, and the function $u(y)$ has been duly extracted [57].

Since the differentiation of experimental data is a difficult task even under the best of circumstances, it surely means that in order to identify T_c from $\bar{n}$-μ isotherms we must abandon the discrete point measurements of, say, Ref. 4. Our purpose would be better served by a continuous measurement technique such as that reported by Rouquerol et. al. [58]

Appendix 3. NUMERICAL TABLES OF THE DATA

Listed here in numerical form are the data presented graphically in Chap. 4. The nineteen vapor pressure isotherms are presented twice, as are the thirteen heat capacity runs of Fig. 6. The first listing of isotherms gives film number (N), number in the cell (N_o), number in the cell plus fill tube (N_{tot}), pressure (P), absolute chemical potential (μ), and chemical potential relative to the bulk (μ-μ_o). (The number N_{tot} is given in case future experiments are done with the cell valve closed off. In such cases the cell would be inaccessible to the Barocel, but the pressure could be discerned by using these tables.) The second isotherm listing gives N, μ, $(\partial\mu/\partial T)_N$, $(\partial\mu/\partial N)_T$, Landau potential ($\Omega$), and entropy ($S$). Thus we have Ω and its proper derivatives given as functions of T and N. Note that the 78 K and 79 K isotherms are not as reliable as the others. (They were taken early, before the technique had been finalized.) Numerical differentiation of these data below 80 K is therefore doubtful.

In some columns, decimal places are given beyond the experimental resolution in order to accommodate a wide range of values throughout the table. Moreover, any number listed as "10000.00" or "9999.9990" should be regarded as infinite. The units of these listings are:

Number - STPCC (1 STPCC = 2.6869×10^{19} molecules)

Temperature and chemical potential - Kelvins

Pressure - Torr

Landau potential - STPCC-K (1 STPCC-K = 3.7095×10^{-4} J)

Entropy - STPCC-k_B.

Recall that one nominal monolayer is 90.9 STPCC.

ISOTHERM: T = 78 K.

Point	N	N_o	N_{tot}	P	μ	$\mu-\mu_o$
1	522.48	526.25	526.34	10.1798	-1566.61	-4.12
2	507.53	511.23	511.32	9.9898	-1568.08	-5.58
3	492.47	496.13	496.21	9.8698	-1569.02	-6.53
4	477.33	480.95	481.04	9.7548	-1569.93	-7.44
5	462.22	465.80	465.88	9.6428	-1570.83	-8.34
6	447.11	450.65	450.74	9.5478	-1571.60	-9.11
7	431.91	435.44	435.53	9.5268	-1571.78	-9.28
8	416.76	420.28	420.36	9.4808	-1572.04	-9.55
9	401.61	405.12	405.21	9.4678	-1572.15	-9.65
10	386.47	389.96	390.04	9.4028	-1572.68	-10.19
11	371.38	374.81	374.89	9.2458	-1574.00	-11.50
12	356.31	359.66	359.74	9.0528	-1575.64	-13.15
13	341.27	344.52	344.60	8.7768	-1578.05	-15.56
14	326.26	329.39	329.46	8.4188	-1581.30	-18.80
15	311.16	314.13	314.20	8.0028	-1585.25	-22.75
16	296.02	298.95	299.02	7.8828	-1586.43	-23.93
17	280.81	283.73	283.80	7.8718	-1586.53	-24.04
18	265.63	268.55	268.62	7.8628	-1586.62	-24.13
19	250.52	253.38	253.45	7.7108	-1588.14	-25.65
20	235.69	238.28	238.34	7.0048	-1595.63	-33.13
21	221.23	223.42	223.47	5.9127	-1608.84	-46.35
22	211.00	212.80	212.84	4.8697	-1623.97	-61.47
23	201.34	202.84	202.87	4.0546	-1638.25	-75.76
24	192.75	194.18	194.21	3.8626	-1642.03	-79.54
25	183.84	185.27	185.30	3.8526	-1642.23	-79.74
26	175.16	176.59	176.62	3.8426	-1642.44	-79.94
27	165.87	167.29	167.33	3.8376	-1642.54	-80.04
28	157.07	158.49	158.53	3.8356	-1642.58	-80.09
29	148.37	149.79	149.83	3.8296	-1642.70	-80.21
30	123.69	125.12	125.15	3.8229	-1642.80	-80.31
31	115.89	117.31	117.34	3.8207	-1642.83	-80.34
32	108.25	109.67	109.70	3.8186	-1642.86	-80.37
33	100.66	101.96	101.99	3.5004	-1649.64	-87.15
34	93.55	94.43	94.45	2.3805	-1679.71	-117.21
35	90.08	90.64	90.65	1.4967	-1715.89	-153.40
36	89.44	89.91	89.92	1.2497	-1730.03	-167.53
37	87.62	87.96	87.97	.9354	-1752.63	-190.13
38	86.60	86.86	86.87	.7118	-1773.86	-211.37
39	86.13	86.36	86.37	.6096	-1786.02	-223.53
40	84.74	84.87	84.87	.3502	-1829.24	-266.75
41	83.22	83.29	83.29	.1731	-1884.21	-321.72
42	81.75	81.77	81.77	.0541	-1974.94	-412.45
43	80.11	80.12	80.12	.0279	-2026.71	-464.22
44	77.90	77.91	77.91	.0197	-2053.93	-491.43
45	76.38	76.39	76.39	.0188	-2057.52	-495.03
46	74.76	74.76	74.76	.0120	-2092.66	-530.17
47	71.71	71.71	71.71	.0044	-2171.52	-609.03
48	70.54	70.54	70.54	.0042	-2174.77	-612.28
49	69.94	69.95	69.95	.0038	-2181.79	-619.30
50	69.46	69.46	69.46	.0035	-2188.81	-626.32

T = 78 K (cont.)

Point	N	N_o	N_{tot}	P	μ	$\mu-\mu_o$
51	68.86	68.87	68.87	.0032	-2195.83	-633.33
52	68.10	68.10	68.10	.0029	-2202.84	-640.35
53	67.30	67.30	67.30	.0027	-2209.86	-647.37
54	66.53	66.53	66.53	.0024	-2216.88	-654.39
55	65.66	65.66	65.66	.0022	-2223.90	-661.40
56	64.79	64.79	64.79	.0020	-2230.92	-668.42
57	63.81	63.81	63.81	.0019	-2237.93	-675.44
58	62.66	62.67	62.67	.0017	-2244.95	-682.46
59	61.38	61.38	61.38	.0016	-2251.97	-689.47
60	59.84	59.84	59.84	.0014	-2258.99	-696.49
61	57.47	57.47	57.47	.0013	-2266.00	-703.51
62	54.17	54.17	54.17	.0012	-2273.02	-710.53
63	43.54	43.54	43.54	.0011	-2280.04	-717.54
64	32.39	32.40	32.40	.0010	-2287.05	-724.56
65	17.94	17.94	17.94	.0009	-2294.07	-731.58
66	13.79	13.79	13.79	.0008	-2301.09	-738.60
67	12.05	12.05	12.05	.0008	-2308.11	-745.61
68	10.80	10.80	10.80	.0007	-2315.13	-752.63
69	9.58	9.58	9.58	.0006	-2322.14	-759.65
70	8.92	8.92	8.92	.0006	-2329.16	-766.67
71	8.05	8.05	8.05	.0005	-2336.18	-773.68
72	7.49	7.49	7.49	.0005	-2343.20	-780.70
73	6.90	6.90	6.90	.0004	-2350.21	-787.72
74	6.34	6.34	6.34	.0004	-2357.23	-794.74
75	5.85	5.85	5.85	.0004	-2364.25	-801.75
76	5.50	5.50	5.50	.0003	-2371.26	-808.77
77	5.16	5.16	5.16	.0003	-2378.28	-815.79
78	4.77	4.77	4.77	.0003	-2385.30	-822.81
79	4.39	4.39	4.39	.0003	-2392.32	-829.83
80	4.15	4.15	4.15	.0002	-2399.33	-836.84
81	3.90	3.90	3.90	.0002	-2406.35	-843.86
82	3.66	3.66	3.66	.0002	-2413.37	-850.88
83	3.41	3.41	3.41	.0002	-2420.39	-857.90
84	3.17	3.17	3.17	.0002	-2427.41	-864.91
85	2.96	2.96	2.96	.0001	-2434.42	-871.93
86	2.75	2.75	2.75	.0001	-2441.44	-878.95
87	2.54	2.54	2.54	.0001	-2448.46	-885.97
88	2.37	2.37	2.37	.0001	-2455.48	-892.98
89	2.16	2.16	2.16	.0001	-2462.49	-900.00
90	.00	.00	.00	.0000	-10000.00	-10000.00

ISOTHERM: T = 79 K.

Point	N	N_o	N_{tot}	P	μ	$\mu-\mu_o$
1	501.77	506.01	506.11	11.9265	-1578.03	-6.48
2	485.88	490.11	490.21	11.7815	-1578.99	-7.45
3	470.41	474.62	474.72	11.6604	-1579.81	-8.26
4	454.75	458.95	459.05	11.5479	-1580.58	-9.03
5	438.23	442.42	442.52	11.4776	-1581.06	-9.51
6	422.90	427.09	427.19	11.4319	-1581.39	-9.84
7	407.44	411.60	411.70	11.3609	-1581.88	-10.33
8	392.10	396.22	396.32	11.2689	-1582.52	-10.97
9	376.77	380.81	380.91	11.0459	-1584.10	-12.55
10	361.48	365.42	365.51	10.7568	-1586.19	-14.64
11	346.22	350.03	350.12	10.4078	-1588.80	-17.25
12	331.10	334.76	334.84	9.9818	-1592.09	-20.54
13	315.96	319.46	319.54	9.5508	-1595.58	-24.03
14	300.70	304.18	304.26	9.4988	-1596.01	-24.46
15	285.22	288.69	288.77	9.4918	-1596.07	-24.52
16	269.96	273.43	273.51	9.4638	-1596.30	-24.75
17	254.92	258.23	258.30	9.0318	-1599.99	-28.44
18	240.05	243.05	243.12	8.1688	-1607.91	-36.36
19	225.30	227.86	227.93	7.0198	-1619.88	-48.33
20	210.50	212.55	212.60	5.6007	-1637.71	-66.16
21	195.45	197.19	197.23	4.7343	-1650.98	-79.43
22	175.60	177.32	177.36	4.6954	-1651.63	-80.08
23	160.24	161.95	161.99	4.6872	-1651.77	-80.22
24	144.87	146.58	146.62	4.6791	-1651.90	-80.35
25	123.40	125.11	125.15	4.6769	-1651.93	-80.38
26	115.59	117.30	117.34	4.6602	-1652.20	-80.65
27	107.96	109.66	109.70	4.6398	-1652.55	-81.00
28	100.44	101.97	102.01	4.1797	-1660.80	-89.25
29	93.43	94.47	94.49	2.8342	-1691.48	-119.93
30	90.03	90.69	90.71	1.7967	-1727.48	-155.93
31	89.62	90.23	90.25	1.6712	-1733.22	-161.67
32	87.36	87.76	87.77	1.0764	-1767.97	-196.42
33	86.61	86.93	86.94	.8776	-1784.08	-212.53
34	85.10	85.28	85.29	.4969	-1829.03	-257.48
35	82.72	82.78	82.78	.1534	-1921.89	-350.33
36	81.21	81.23	81.23	.0551	-2002.82	-431.27
37	79.69	79.70	79.70	.0335	-2042.12	-470.57
38	78.13	78.14	78.14	.0306	-2049.14	-477.58
39	76.50	76.51	76.51	.0268	-2059.77	-488.22
40	73.38	73.38	73.38	.0085	-2150.43	-578.88
41	72.38	72.39	72.39	.0079	-2155.76	-584.21
42	72.00	72.00	72.00	.0073	-2162.78	-591.23
43	71.55	71.55	71.55	.0066	-2169.80	-598.25
44	71.13	71.13	71.13	.0061	-2176.81	-605.26
45	70.54	70.54	70.54	.0056	-2183.83	-612.28
46	69.94	69.95	69.95	.0051	-2190.85	-619.30
47	69.46	69.46	69.46	.0047	-2197.87	-626.32
48	68.86	68.87	68.87	.0043	-2204.88	-633.33
49	68.10	68.10	68.10	.0039	-2211.90	-640.35
50	67.30	67.30	67.30	.0036	-2218.92	-647.37

T = 79 K (cont.)

Point	N	N_o	N_{tot}	P	μ	$\mu-\mu_o$
51	66.53	66.53	66.53	.0033	-2225.94	-654.39
52	65.66	65.66	65.66	.0030	-2232.95	-661.40
53	64.79	64.79	64.79	.0027	-2239.97	-668.42
54	63.81	63.82	63.82	.0025	-2246.99	-675.44
55	62.66	62.67	62.67	.0023	-2254.01	-682.46
56	61.38	61.38	61.38	.0021	-2261.02	-689.47
57	59.84	59.84	59.84	.0019	-2268.04	-696.49
58	57.47	57.48	57.48	.0018	-2275.06	-703.51
59	54.17	54.17	54.17	.0016	-2282.08	-710.53
60	43.54	43.54	43.54	.0015	-2289.09	-717.54
61	32.39	32.40	32.40	.0013	-2296.11	-724.56
62	17.94	17.94	17.94	.0012	-2303.13	-731.58
63	13.79	13.79	13.79	.0011	-2310.15	-738.60
64	12.05	12.05	12.05	.0010	-2317.16	-745.61
65	10.80	10.80	10.80	.0009	-2324.18	-752.63
66	9.58	9.58	9.58	.0009	-2331.20	-759.65
67	8.92	8.92	8.92	.0008	-2338.22	-766.67
68	8.05	8.05	8.05	.0007	-2345.23	-773.68
69	7.49	7.49	7.49	.0007	-2352.25	-780.70
70	6.90	6.90	6.90	.0006	-2359.27	-787.72
71	6.34	6.34	6.34	.0006	-2366.29	-794.74
72	5.85	5.85	5.85	.0005	-2373.30	-801.75
73	5.50	5.50	5.50	.0005	-2380.32	-808.77
74	5.16	5.16	5.16	.0004	-2387.34	-815.79
75	4.77	4.77	4.77	.0004	-2394.36	-822.81
76	4.39	4.39	4.39	.0004	-2401.38	-829.83
77	4.15	4.15	4.15	.0003	-2408.39	-836.84
78	3.90	3.90	3.90	.0003	-2415.41	-843.86
79	3.66	3.66	3.66	.0003	-2422.43	-850.88
80	3.41	3.41	3.41	.0002	-2429.45	-857.90
81	3.17	3.17	3.17	.0002	-2436.46	-864.91
82	2.96	2.96	2.96	.0002	-2443.48	-871.93
83	2.75	2.75	2.75	.0002	-2450.50	-878.95
84	2.54	2.54	2.54	.0002	-2457.51	-885.97
85	2.37	2.37	2.37	.0002	-2464.53	-892.98
86	2.16	2.16	2.16	.0001	-2471.55	-900.00
87	.00	.00	.00	.0000	-10000.00	-10000.00

ISOTHERM: T = 80 K.

Point	N	N_o	N_{tot}	P	μ	$\mu-\mu_o$
1	528.05	533.29	533.41	14.4839	-1586.49	-5.84
2	512.42	517.62	517.74	14.3749	-1587.09	-6.44
3	496.89	502.04	502.16	14.2459	-1587.81	-7.16
4	481.54	486.63	486.75	14.0519	-1588.91	-8.26
5	465.06	470.11	470.23	13.9699	-1589.38	-8.72
6	449.62	454.62	454.74	13.8219	-1590.22	-9.57
7	434.13	439.11	439.23	13.7769	-1590.49	-9.83
8	418.62	423.58	423.70	13.7039	-1590.91	-10.26
9	403.12	408.06	408.18	13.6509	-1591.22	-10.57
10	387.66	392.52	392.64	13.4259	-1592.55	-11.90
11	372.40	377.07	377.19	12.9329	-1595.54	-14.88
12	341.68	346.13	346.24	12.3049	-1599.51	-18.86
13	326.53	330.74	330.84	11.6179	-1604.10	-23.45
14	311.17	315.29	315.39	11.3799	-1605.76	-25.11
15	295.70	299.81	299.91	11.3559	-1605.93	-25.27
16	280.18	284.28	284.37	11.3159	-1606.21	-25.56
17	264.73	268.79	268.89	11.2249	-1606.85	-26.20
18	249.62	253.33	253.42	10.2628	-1614.01	-33.36
19	237.31	240.69	240.77	9.3423	-1621.52	-40.87
20	225.02	228.00	228.07	8.2400	-1631.56	-50.91
21	212.75	215.27	215.33	6.9633	-1645.02	-64.36
22	200.46	202.63	202.68	5.9937	-1657.00	-76.35
23	187.89	189.94	189.99	5.6777	-1661.33	-80.68
24	175.19	177.23	177.28	5.6577	-1661.62	-80.96
25	162.39	164.43	164.48	5.6481	-1661.75	-81.10
26	149.59	151.63	151.67	5.6369	-1661.91	-81.26
27	144.23	146.26	146.31	5.6333	-1661.96	-81.31
28	136.58	138.62	138.67	5.6324	-1661.97	-81.32
29	128.87	130.90	130.95	5.6310	-1661.99	-81.34
30	121.21	123.24	123.29	5.6254	-1662.07	-81.42
31	113.52	115.55	115.60	5.6180	-1662.18	-81.53
32	105.87	107.85	107.89	5.4803	-1664.16	-83.51
33	98.60	100.27	100.31	4.6094	-1678.00	-97.35
34	93.97	95.25	95.28	3.5281	-1699.38	-118.73
35	89.49	90.24	90.26	2.0853	-1741.43	-160.78
36	85.04	85.25	85.26	.5776	-1844.12	-263.47
37	80.10	80.12	80.12	.0502	-2039.52	-458.86
38	75.87	75.88	75.88	.0314	-2077.20	-496.54
39	75.13	75.14	75.14	.0252	-2094.69	-514.03
40	74.93	74.93	74.93	.0231	-2101.70	-521.05
41	74.72	74.72	74.72	.0211	-2108.72	-528.07
42	74.44	74.45	74.45	.0194	-2115.74	-535.09
43	74.19	74.20	74.20	.0177	-2122.76	-542.10
44	73.92	73.92	73.92	.0162	-2129.77	-549.12
45	73.67	73.68	73.68	.0149	-2136.79	-556.14
46	73.39	73.40	73.40	.0136	-2143.81	-563.16
47	73.11	73.12	73.12	.0125	-2150.83	-570.17
48	72.73	72.74	72.74	.0114	-2157.84	-577.19
49	72.38	72.39	72.39	.0105	-2164.86	-584.21
50	72.00	72.00	72.00	.0096	-2171.88	-591.23

T = 80 K (cont.)

Point	N	N_o	N_{tot}	P	μ	$\mu-\mu_o$
51	71.55	71.55	71.55	.0088	-2178.90	-598.25
52	71.13	71.13	71.13	.0081	-2185.92	-605.26
53	70.54	70.54	70.54	.0074	-2192.93	-612.28
54	69.94	69.95	69.95	.0068	-2199.95	-619.30
55	69.46	69.46	69.46	.0062	-2206.97	-626.32
56	68.86	68.87	68.87	.0057	-2213.99	-633.33
57	68.10	68.10	68.10	.0052	-2221.00	-640.35
58	67.30	67.30	67.30	.0048	-2228.02	-647.37
59	66.53	66.53	66.53	.0044	-2235.04	-654.39
60	65.66	65.66	65.66	.0040	-2242.05	-661.40
61	64.79	64.79	64.79	.0037	-2249.07	-668.42
62	63.81	63.82	63.82	.0034	-2256.09	-675.44
63	62.66	62.67	62.67	.0031	-2263.11	-682.46
64	61.38	61.38	61.38	.0028	-2270.13	-689.47
65	59.84	59.84	59.84	.0026	-2277.14	-696.49
66	57.47	57.48	57.48	.0024	-2284.16	-703.51
67	54.17	54.17	54.17	.0022	-2291.18	-710.53
68	43.54	43.54	43.54	.0020	-2298.20	-717.54
69	32.39	32.40	32.40	.0018	-2305.21	-724.56
70	17.94	17.94	17.94	.0017	-2312.23	-731.58
71	13.79	13.79	13.79	.0015	-2319.25	-738.60
72	12.05	12.05	12.05	.0014	-2326.27	-745.61
73	10.80	10.80	10.80	.0013	-2333.28	-752.63
74	9.58	9.58	9.58	.0012	-2340.30	-759.65
75	8.92	8.92	8.92	.0011	-2347.32	-766.67
76	8.05	8.05	8.05	.0010	-2354.34	-773.68
77	7.49	7.49	7.49	.0009	-2361.35	-780.70
78	6.90	6.90	6.90	.0008	-2368.37	-787.72
79	6.34	6.34	6.34	.0008	-2375.39	-794.74
80	5.85	5.85	5.85	.0007	-2382.41	-801.75
81	5.50	5.50	5.50	.0006	-2389.42	-808.77
82	5.16	5.16	5.16	.0006	-2396.44	-815.79
83	4.77	4.77	4.77	.0005	-2403.46	-822.81
84	4.39	4.39	4.39	.0005	-2410.48	-829.83
85	4.15	4.15	4.15	.0004	-2417.49	-836.84
86	3.90	3.90	3.90	.0004	-2424.51	-843.86
87	3.66	3.66	3.66	.0004	-2431.53	-850.88
88	3.41	3.41	3.41	.0003	-2438.55	-857.90
89	3.17	3.17	3.17	.0003	-2445.56	-864.91
90	2.96	2.96	2.96	.0003	-2452.58	-871.93
91	2.75	2.75	2.75	.0003	-2459.60	-878.95
92	2.54	2.54	2.54	.0002	-2466.62	-885.97
93	2.37	2.37	2.37	.0002	-2473.63	-892.98
94	2.16	2.16	2.16	.0002	-2480.65	-900.00
95	.00	.00	.00	.0000	-10000.00	-10000.00

ISOTHERM: T = 81 K.

Point	N	N_o	N_{tot}	P	μ	$\mu-\mu_o$
1	526.76	532.97	533.11	17.3649	-1595.66	-5.86
2	510.98	517.28	517.43	17.2449	-1596.22	-6.42
3	495.60	501.72	501.86	17.1229	-1596.79	-6.99
4	480.27	486.31	486.45	16.8929	-1597.88	-8.09
5	463.87	469.81	469.95	16.6259	-1599.17	-9.37
6	448.42	454.32	454.46	16.5109	-1599.73	-9.94
7	432.92	438.81	438.95	16.4639	-1599.96	-10.16
8	417.43	423.28	423.42	16.3759	-1600.40	-10.60
9	401.93	407.76	407.90	16.3169	-1600.69	-10.89
10	386.51	392.23	392.37	15.9979	-1602.29	-12.49
11	371.25	376.79	376.92	15.4929	-1604.88	-15.08
12	340.57	345.85	345.98	14.7749	-1608.72	-18.92
13	325.53	330.48	330.60	13.8679	-1613.84	-24.04
14	310.19	315.04	315.16	13.5799	-1615.54	-25.74
15	294.74	299.57	299.68	13.5139	-1615.93	-26.14
16	279.22	284.03	284.15	13.4649	-1616.23	-26.43
17	263.82	268.56	268.68	13.2809	-1617.34	-27.54
18	248.77	253.11	253.22	12.1489	-1624.55	-34.75
19	236.53	240.49	240.59	11.0959	-1631.88	-42.08
20	224.30	227.82	227.90	9.8473	-1641.54	-51.74
21	212.08	215.10	215.17	8.4734	-1653.70	-63.90
22	199.88	202.48	202.55	7.2940	-1665.83	-76.03
23	187.38	189.81	189.87	6.8219	-1671.25	-81.45
24	174.68	177.11	177.16	6.7989	-1671.52	-81.72
25	161.88	164.30	164.36	6.7851	-1671.69	-81.89
26	149.08	151.50	151.56	6.7707	-1671.86	-82.06
27	143.72	146.13	146.19	6.7678	-1671.89	-82.10
28	136.08	138.49	138.55	6.7648	-1671.93	-82.13
29	128.36	130.77	130.83	6.7633	-1671.95	-82.15
30	120.70	123.12	123.18	6.7589	-1672.00	-82.20
31	113.02	115.43	115.49	6.7420	-1672.20	-82.40
32	105.41	107.73	107.79	6.4972	-1675.20	-85.40
33	98.25	100.18	100.23	5.4055	-1690.09	-100.29
34	93.71	95.18	95.22	4.1295	-1711.89	-122.09
35	89.32	90.20	90.22	2.4557	-1753.97	-164.17
36	84.98	85.24	85.24	.7258	-1852.69	-262.89
37	80.09	80.12	80.12	.0726	-2039.13	-449.33
38	75.86	75.88	75.88	.0452	-2077.50	-487.70
39	75.13	75.15	75.15	.0327	-2103.83	-514.03
40	74.93	74.94	74.94	.0300	-2110.85	-521.05
41	74.72	74.73	74.73	.0275	-2117.87	-528.07
42	74.44	74.45	74.45	.0252	-2124.89	-535.09
43	74.19	74.20	74.20	.0231	-2131.90	-542.10
44	73.92	73.92	73.92	.0212	-2138.92	-549.12
45	73.67	73.68	73.68	.0194	-2145.94	-556.14
46	73.39	73.40	73.40	.0178	-2152.96	-563.16
47	73.11	73.12	73.12	.0163	-2159.97	-570.17
48	72.73	72.74	72.74	.0150	-2166.99	-577.19
49	72.38	72.39	72.39	.0137	-2174.01	-584.21
50	72.00	72.00	72.00	.0126	-2181.03	-591.23

T = 81 K (cont.)

Point	N	N_o	N_{tot}	P	μ	$\mu-\mu_o$
51	71.55	71.55	71.55	.0115	-2188.04	-598.25
52	71.13	71.13	71.13	.0106	-2195.06	-605.26
53	70.54	70.54	70.54	.0097	-2202.08	-612.28
54	69.94	69.95	69.95	.0089	-2209.10	-619.30
55	69.46	69.46	69.46	.0082	-2216.11	-626.32
56	68.86	68.87	68.87	.0075	-2223.13	-633.33
57	68.10	68.10	68.10	.0069	-2230.15	-640.35
58	67.30	67.30	67.30	.0063	-2237.17	-647.37
59	66.53	66.53	66.53	.0058	-2244.18	-654.39
60	65.66	65.66	65.66	.0053	-2251.20	-661.40
61	64.79	64.79	64.79	.0049	-2258.22	-668.42
62	63.81	63.82	63.82	.0045	-2265.24	-675.44
63	62.66	62.67	62.67	.0041	-2272.25	-682.46
64	61.38	61.38	61.38	.0037	-2279.27	-689.47
65	59.84	59.84	59.84	.0034	-2286.29	-696.49
66	57.47	57.48	57.48	.0032	-2293.31	-703.51
67	54.17	54.17	54.17	.0029	-2300.32	-710.53
68	43.54	43.54	43.54	.0026	-2307.34	-717.54
69	32.39	32.40	32.40	.0024	-2314.36	-724.56
70	17.94	17.94	17.94	.0022	-2321.38	-731.58
71	13.79	13.79	13.79	.0020	-2328.40	-738.60
72	12.05	12.05	12.05	.0019	-2335.41	-745.61
73	10.80	10.80	10.80	.0017	-2342.43	-752.63
74	9.58	9.58	9.58	.0016	-2349.45	-759.65
75	8.92	8.92	8.92	.0014	-2356.47	-766.67
76	8.05	8.05	8.05	.0013	-2363.48	-773.68
77	7.49	7.49	7.49	.0012	-2370.50	-780.70
78	6.90	6.90	6.90	.0011	-2377.52	-787.72
79	6.34	6.34	6.34	.0010	-2384.53	-794.74
80	5.85	5.85	5.85	.0009	-2391.55	-801.75
81	5.50	5.50	5.50	.0009	-2398.57	-808.77
82	5.16	5.16	5.16	.0008	-2405.59	-815.79
83	4.77	4.77	4.77	.0007	-2412.60	-822.81
84	4.39	4.39	4.39	.0007	-2419.62	-829.83
85	4.15	4.15	4.15	.0006	-2426.64	-836.84
86	3.90	3.90	3.90	.0006	-2433.66	-843.86
87	3.66	3.66	3.66	.0005	-2440.68	-850.88
88	3.41	3.41	3.41	.0005	-2447.69	-857.90
89	3.17	3.17	3.17	.0004	-2454.71	-864.91
90	2.96	2.96	2.96	.0004	-2461.73	-871.93
91	2.75	2.75	2.75	.0004	-2468.75	-878.95
92	2.54	2.54	2.54	.0003	-2475.76	-885.97
93	2.37	2.37	2.37	.0003	-2482.78	-892.98
94	2.16	2.16	2.16	.0003	-2489.80	-900.00
95	.00	.00	.00	.0000	-10000.00	-10000.00

ISOTHERM: T = 82 K.

Point	N	N_o	N_{tot}	P	μ	$\mu-\mu_o$
1	543.49	550.90	551.08	20.9929	-1603.83	-4.84
2	525.27	532.59	532.76	20.7309	-1604.85	-5.86
3	509.63	516.91	517.09	20.6349	-1605.23	-6.24
4	494.10	501.34	501.51	20.4829	-1605.84	-6.85
5	478.83	485.94	486.11	20.1399	-1607.22	-8.23
6	462.44	469.45	469.62	19.8389	-1608.45	-9.46
7	447.05	453.97	454.14	19.6139	-1609.39	-10.40
8	431.56	438.46	438.63	19.5299	-1609.74	-10.75
9	416.04	422.93	423.09	19.5019	-1609.86	-10.87
10	400.55	407.41	407.58	19.4189	-1610.21	-11.22
11	385.16	391.89	392.05	19.0449	-1611.80	-12.81
12	369.94	376.45	376.61	18.4559	-1614.37	-15.38
13	339.31	345.53	345.68	17.6359	-1618.09	-19.10
14	324.33	330.18	330.32	16.5649	-1623.22	-24.23
15	309.11	314.76	314.90	16.0279	-1625.92	-26.93
16	293.65	299.29	299.43	15.9789	-1626.17	-27.18
17	278.13	283.76	283.89	15.9399	-1626.37	-27.38
18	262.78	268.29	268.43	15.6359	-1627.94	-28.95
19	247.81	252.87	252.99	14.3199	-1635.14	-36.15
20	235.63	240.26	240.37	13.1139	-1642.35	-43.36
21	223.46	227.60	227.71	11.7399	-1651.41	-52.42
22	211.31	214.91	214.99	10.1858	-1663.04	-64.05
23	199.20	202.31	202.39	8.8249	-1674.79	-75.80
24	186.79	189.66	189.73	8.1554	-1681.26	-82.27
25	174.10	176.96	177.03	8.1114	-1681.70	-82.71
26	161.29	164.15	164.22	8.1006	-1681.81	-82.82
27	148.50	151.35	151.42	8.0843	-1681.97	-82.98
28	143.13	145.98	146.05	8.0822	-1681.99	-83.00
29	135.50	138.34	138.41	8.0712	-1682.11	-83.12
30	127.78	130.63	130.70	8.0699	-1682.12	-83.13
31	120.13	122.97	123.04	8.0649	-1682.17	-83.18
32	112.46	115.28	115.35	8.0179	-1682.65	-83.66
33	104.91	107.60	107.67	7.6350	-1686.66	-87.67
34	97.86	100.08	100.13	6.2910	-1702.53	-103.54
35	93.42	95.11	95.15	4.7935	-1724.81	-125.82
36	89.14	90.15	90.18	2.8702	-1766.85	-167.86
37	84.90	85.22	85.22	.9031	-1861.65	-262.66
38	80.07	80.11	80.11	.1066	-2036.82	-437.83
39	75.85	75.88	75.88	.0631	-2079.86	-480.87
40	75.13	75.15	75.15	.0421	-2113.02	-514.03
41	74.93	74.94	74.94	.0386	-2120.04	-521.05
42	74.72	74.73	74.73	.0355	-2127.06	-528.07
43	74.44	74.45	74.45	.0326	-2134.08	-535.09
44	74.19	74.20	74.21	.0299	-2141.09	-542.10
45	73.92	73.93	73.93	.0275	-2148.11	-549.12
46	73.67	73.68	73.68	.0252	-2155.13	-556.14
47	73.39	73.40	73.40	.0231	-2162.15	-563.16
48	73.11	73.12	73.12	.0212	-2169.17	-570.17
49	72.73	72.74	72.74	.0195	-2176.18	-577.19
50	72.38	72.39	72.39	.0179	-2183.20	-584.21

T = 82 K (cont.)

Point	N	N_o	N_{tot}	P	μ	$\mu-\mu_o$
51	72.00	72.01	72.01	.0164	-2190.22	-591.23
52	71.55	71.55	71.55	.0151	-2197.24	-598.25
53	71.13	71.13	71.13	.0138	-2204.25	-605.26
54	70.54	70.54	70.54	.0127	-2211.27	-612.28
55	69.94	69.95	69.95	.0117	-2218.29	-619.30
56	69.46	69.46	69.46	.0107	-2225.30	-626.32
57	68.86	68.87	68.87	.0098	-2232.32	-633.33
58	68.10	68.10	68.10	.0090	-2239.34	-640.35
59	67.30	67.30	67.30	.0083	-2246.36	-647.37
60	66.53	66.53	66.53	.0076	-2253.38	-654.39
61	65.66	65.66	65.66	.0070	-2260.39	-661.40
62	64.79	64.79	64.79	.0064	-2267.41	-668.42
63	63.81	63.82	63.82	.0059	-2274.43	-675.44
64	62.66	62.67	62.67	.0054	-2281.45	-682.46
65	61.38	61.38	61.38	.0050	-2288.46	-689.47
66	59.84	59.84	59.84	.0046	-2295.48	-696.49
67	57.47	57.48	57.48	.0042	-2302.50	-703.51
68	54.17	54.17	54.17	.0038	-2309.52	-710.53
69	43.54	43.54	43.54	.0035	-2316.53	-717.54
70	32.39	32.40	32.40	.0032	-2323.55	-724.56
71	17.94	17.94	17.94	.0030	-2330.57	-731.58
72	13.79	13.79	13.79	.0027	-2337.59	-738.60
73	12.05	12.05	12.05	.0025	-2344.60	-745.61
74	10.80	10.80	10.80	.0023	-2351.62	-752.63
75	9.58	9.58	9.58	.0021	-2358.64	-759.65
76	8.92	8.92	8.92	.0019	-2365.66	-766.67
77	8.05	8.05	8.05	.0018	-2372.67	-773.68
78	7.49	7.49	7.49	.0016	-2379.69	-780.70
79	6.90	6.90	6.90	.0015	-2386.71	-787.72
80	6.34	6.34	6.34	.0014	-2393.73	-794.74
81	5.85	5.85	5.85	.0013	-2400.74	-801.75
82	5.50	5.50	5.50	.0012	-2407.76	-808.77
83	5.16	5.16	5.16	.0011	-2414.78	-815.79
84	4.77	4.77	4.77	.0010	-2421.80	-822.81
85	4.39	4.39	4.39	.0009	-2428.81	-829.83
86	4.15	4.15	4.15	.0008	-2435.83	-836.84
87	3.90	3.90	3.90	.0008	-2442.85	-843.86
88	3.66	3.66	3.66	.0007	-2449.87	-850.88
89	3.41	3.41	3.41	.0006	-2456.88	-857.90
90	3.17	3.17	3.17	.0006	-2463.90	-864.91
91	2.96	2.96	2.96	.0005	-2470.92	-871.93
92	2.75	2.75	2.75	.0005	-2477.94	-878.95
93	2.54	2.54	2.54	.0005	-2484.95	-885.97
94	2.37	2.37	2.37	.0004	-2491.97	-892.98
95	2.16	2.16	2.16	.0004	-2498.99	-900.00
96	.00	.00	.00	.0000	-10000.00	-10000.00

ISOTHERM: T = 83 K.

Point	N	N_o	N_{tot}	P	μ	$\mu-\mu_o$
1	523.45	532.12	532.33	24.8979	-1614.29	-6.04
2	507.78	516.44	516.65	24.8559	-1614.46	-6.22
3	492.29	500.87	501.08	24.6279	-1615.21	-6.96
4	477.04	485.48	485.69	24.2439	-1616.52	-8.27
5	460.64	468.98	469.19	23.9624	-1617.53	-9.28
6	445.28	453.52	453.72	23.6499	-1618.59	-10.35
7	429.82	438.01	438.21	23.5104	-1619.07	-10.82
8	414.33	422.48	422.68	23.4259	-1619.34	-11.09
9	398.86	406.97	407.17	23.2964	-1619.79	-11.54
10	383.49	391.46	391.65	22.8869	-1621.27	-13.02
11	368.31	376.03	376.22	22.1829	-1623.86	-15.61
12	337.77	345.13	345.32	21.1604	-1627.75	-19.50
13	322.89	329.81	329.98	19.8729	-1632.95	-24.70
14	307.74	314.41	314.57	19.1754	-1635.88	-27.63
15	292.31	298.94	299.11	19.0599	-1636.35	-28.10
16	276.81	283.42	283.58	18.9699	-1636.72	-28.47
17	261.51	267.97	268.12	18.5389	-1638.58	-30.33
18	246.65	252.57	252.71	17.0044	-1645.76	-37.51
19	234.54	239.98	240.11	15.6239	-1652.81	-44.56
20	222.45	227.34	227.46	14.0639	-1661.59	-53.34
21	210.38	214.66	214.77	12.3308	-1672.61	-64.36
22	198.36	202.09	202.19	10.7509	-1684.05	-75.80
23	186.02	189.47	189.55	9.9017	-1690.83	-82.58
24	173.37	176.77	176.85	9.7722	-1691.83	-83.59
25	160.58	163.96	164.05	9.7408	-1692.08	-83.83
26	147.79	151.17	151.25	9.6991	-1692.41	-84.16
27	142.44	145.80	145.89	9.6811	-1692.55	-84.30
28	134.81	138.17	138.25	9.6401	-1692.87	-84.62
29	127.10	130.45	130.53	9.6354	-1692.91	-84.66
30	119.45	122.79	122.88	9.6199	-1693.03	-84.78
31	111.80	115.11	115.19	9.5259	-1693.80	-85.55
32	104.33	107.45	107.53	8.9669	-1698.70	-90.45
33	97.42	99.96	100.03	7.3131	-1715.51	-107.26
34	93.09	95.02	95.07	5.5582	-1738.24	-130.00
35	88.93	90.10	90.13	3.3524	-1780.26	-172.01
36	84.80	85.19	85.20	1.1378	-1870.80	-262.56
37	80.05	80.11	80.11	.1608	-2036.24	-428.00
38	75.84	75.87	75.87	.0874	-2085.26	-477.01
39	75.13	75.15	75.15	.0539	-2122.26	-514.03
40	74.93	74.94	74.94	.0496	-2129.28	-521.05
41	74.72	74.73	74.73	.0455	-2136.30	-528.07
42	74.44	74.45	74.45	.0419	-2143.31	-535.09
43	74.19	74.21	74.21	.0384	-2150.33	-542.10
44	73.92	73.93	73.93	.0353	-2157.35	-549.12
45	73.67	73.68	73.68	.0325	-2164.37	-556.14
46	73.39	73.40	73.40	.0298	-2171.38	-563.16
47	73.11	73.12	73.12	.0274	-2178.40	-570.17
48	72.73	72.74	72.74	.0252	-2185.42	-577.19
49	72.38	72.39	72.39	.0232	-2192.44	-584.21
50	72.00	72.01	72.01	.0213	-2199.45	-591.23

T = 83 K (cont.)

Point	N	N_o	N_{tot}	P	μ	$\mu-\mu_o$
51	71.55	71.55	71.55	.0195	-2206.47	-598.25
52	71.13	71.14	71.14	.0180	-2213.49	-605.26
53	70.54	70.54	70.54	.0165	-2220.51	-612.28
54	69.94	69.95	69.95	.0152	-2227.52	-619.30
55	69.46	69.46	69.46	.0139	-2234.54	-626.32
56	68.86	68.87	68.87	.0128	-2241.56	-633.33
57	68.10	68.10	68.10	.0118	-2248.58	-640.35
58	67.30	67.30	67.30	.0108	-2255.59	-647.37
59	66.53	66.53	66.53	.0099	-2262.61	-654.39
60	65.66	65.66	65.66	.0091	-2269.63	-661.40
61	64.79	64.79	64.79	.0084	-2276.65	-668.42
62	63.81	63.82	63.82	.0077	-2283.66	-675.44
63	62.66	62.67	62.67	.0071	-2290.68	-682.46
64	61.38	61.38	61.38	.0065	-2297.70	-689.47
65	59.84	59.85	59.85	.0060	-2304.72	-696.49
66	57.47	57.48	57.48	.0055	-2311.73	-703.51
67	54.17	54.17	54.17	.0051	-2318.75	-710.53
68	43.54	43.54	43.54	.0046	-2325.77	-717.54
69	32.39	32.40	32.40	.0043	-2332.79	-724.56
70	17.94	17.94	17.94	.0039	-2339.80	-731.58
71	13.79	13.80	13.80	.0036	-2346.82	-738.60
72	12.05	12.05	12.05	.0033	-2353.84	-745.61
73	10.80	10.80	10.80	.0030	-2360.86	-752.63
74	9.58	9.58	9.58	.0028	-2367.88	-759.65
75	8.92	8.92	8.92	.0026	-2374.89	-766.67
76	8.05	8.05	8.05	.0024	-2381.91	-773.68
77	7.49	7.49	7.49	.0022	-2388.93	-780.70
78	6.90	6.90	6.90	.0020	-2395.95	-787.72
79	6.34	6.34	6.34	.0018	-2402.96	-794.74
80	5.85	5.85	5.85	.0017	-2409.98	-801.75
81	5.50	5.50	5.50	.0015	-2417.00	-808.77
82	5.16	5.16	5.16	.0014	-2424.01	-815.79
83	4.77	4.77	4.77	.0013	-2431.03	-822.81
84	4.39	4.39	4.39	.0012	-2438.05	-829.83
85	4.15	4.15	4.15	.0011	-2445.07	-836.84
86	3.90	3.90	3.90	.0010	-2452.08	-843.86
87	3.66	3.66	3.66	.0009	-2459.10	-850.88
88	3.41	3.41	3.41	.0009	-2466.12	-857.90
89	3.17	3.17	3.17	.0008	-2473.14	-864.91
90	2.96	2.96	2.96	.0007	-2480.16	-871.93
91	2.75	2.75	2.75	.0007	-2487.17	-878.95
92	2.54	2.54	2.54	.0006	-2494.19	-885.97
93	2.37	2.37	2.37	.0006	-2501.21	-892.98
94	2.16	2.16	2.16	.0005	-2508.23	-900.00
95	.00	.00	.00	.0000	-10000.00	-10000.00

ISOTHERM: T = 84 K.

Point	N	N_o	N_{tot}	P	μ	$\mu-\mu_o$
1	521.63	531.65	531.90	29.0649	-1623.73	-6.22
2	505.94	515.97	516.21	29.0769	-1623.69	-6.19
3	490.48	500.40	500.65	28.7729	-1624.57	-7.07
4	475.24	485.02	485.26	28.3479	-1625.82	-8.32
5	458.83	468.52	468.76	28.0859	-1626.60	-9.09
6	443.51	453.06	453.30	27.6859	-1627.80	-10.30
7	428.08	437.56	437.80	27.4909	-1628.39	-10.89
8	412.61	422.04	422.28	27.3499	-1628.82	-11.32
9	397.16	406.53	406.77	27.1739	-1629.36	-11.86
10	381.81	391.02	391.25	26.7289	-1630.75	-13.24
11	366.68	375.61	375.83	25.9099	-1633.36	-15.85
12	336.23	344.74	344.95	24.6849	-1637.42	-19.91
13	321.44	329.44	329.63	23.1809	-1642.68	-25.18
14	306.36	314.06	314.25	22.3229	-1645.85	-28.34
15	290.96	298.60	298.79	22.1409	-1646.53	-29.03
16	275.49	283.07	283.26	21.9999	-1647.07	-29.56
17	260.25	267.64	267.82	21.4419	-1649.22	-31.72
18	245.48	252.26	252.43	19.6889	-1656.37	-38.87
19	233.45	239.69	239.85	18.1339	-1663.27	-45.77
20	221.43	227.08	227.22	16.3879	-1671.76	-54.26
21	209.44	214.42	214.55	14.4759	-1682.17	-64.66
22	197.51	201.88	201.99	12.6769	-1693.30	-75.80
23	185.26	189.27	189.37	11.6479	-1700.41	-82.90
24	172.65	176.58	176.68	11.4329	-1701.97	-84.46
25	159.86	163.78	163.88	11.3809	-1702.35	-84.85
26	147.09	150.98	151.08	11.3139	-1702.85	-85.34
27	141.74	145.62	145.72	11.2799	-1703.10	-85.59
28	134.13	137.99	138.08	11.2089	-1703.63	-86.13
29	126.42	130.27	130.37	11.2009	-1703.69	-86.18
30	118.77	122.62	122.71	11.1749	-1703.89	-86.38
31	111.14	114.94	115.04	11.0339	-1704.95	-87.44
32	103.76	107.30	107.39	10.2988	-1710.73	-93.23
33	96.98	99.85	99.92	8.3352	-1728.49	-110.98
34	92.76	94.93	94.99	6.3230	-1751.68	-134.18
35	88.73	90.05	90.08	3.8346	-1793.68	-176.17
36	84.69	85.16	85.18	1.3725	-1879.96	-262.46
37	80.03	80.10	80.10	.2150	-2035.67	-418.17
38	75.83	75.87	75.87	.1117	-2090.67	-473.16
39	75.13	75.15	75.15	.0539	-2122.26	-514.03
40	74.93	74.94	74.94	.0496	-2129.28	-521.05
41	74.72	74.73	74.73	.0455	-2136.30	-528.07
42	74.44	74.45	74.45	.0419	-2143.31	-535.09
43	74.19	74.21	74.21	.0384	-2150.33	-542.10
44	73.92	73.93	73.93	.0353	-2157.35	-549.12
45	73.67	73.68	73.68	.0325	-2164.37	-556.14
46	73.39	73.40	73.40	.0298	-2171.38	-563.16
47	73.11	73.12	73.12	.0274	-2178.40	-570.17
48	72.73	72.74	72.74	.0252	-2185.42	-577.19
49	72.38	72.39	72.39	.0232	-2192.44	-584.21
50	72.00	72.01	72.01	.0213	-2199.45	-591.23

T = 84 K (cont.)

Point	N	N_o	N_{tot}	P	μ	$\mu-\mu_o$
51	71.55	71.55	71.55	.0195	-2206.47	-598.25
52	71.13	71.14	71.14	.0180	-2213.49	-605.26
53	70.54	70.54	70.54	.0165	-2220.51	-612.28
54	69.94	69.95	69.95	.0152	-2227.52	-619.30
55	69.46	69.46	69.46	.0139	-2234.54	-626.32
56	68.86	68.87	68.87	.0128	-2241.56	-633.33
57	68.10	68.10	68.10	.0118	-2248.58	-640.35
58	67.30	67.30	67.30	.0108	-2255.59	-647.37
59	66.53	66.53	66.53	.0099	-2262.61	-654.39
60	65.66	65.66	65.66	.0091	-2269.63	-661.40
61	64.79	64.79	64.79	.0084	-2276.65	-668.42
62	63.81	63.82	63.82	.0077	-2283.66	-675.44
63	62.66	62.67	62.67	.0071	-2290.68	-682.46
64	61.38	61.38	61.38	.0065	-2297.70	-689.47
65	59.84	59.85	59.85	.0060	-2304.72	-696.49
66	57.47	57.48	57.48	.0055	-2311.73	-703.51
67	54.17	54.17	54.17	.0051	-2318.75	-710.53
68	43.54	43.54	43.54	.0046	-2325.77	-717.54
69	32.39	32.40	32.40	.0043	-2332.79	-724.56
70	17.94	17.94	17.94	.0039	-2339.80	-731.58
71	13.79	13.80	13.80	.0036	-2346.82	-738.60
72	12.05	12.05	12.05	.0033	-2353.84	-745.61
73	10.80	10.80	10.80	.0030	-2360.86	-752.63
74	9.58	9.58	9.58	.0028	-2367.88	-759.65
75	8.92	8.92	8.92	.0026	-2374.89	-766.67
76	8.05	8.05	8.05	.0024	-2381.91	-773.68
77	7.49	7.49	7.49	.0022	-2388.93	-780.70
78	6.90	6.90	6.90	.0020	-2395.95	-787.72
79	6.34	6.34	6.34	.0018	-2402.96	-794.74
80	5.85	5.85	5.85	.0017	-2409.98	-801.75
81	5.50	5.50	5.50	.0015	-2417.00	-808.77
82	5.16	5.16	5.16	.0014	-2424.01	-815.79
83	4.77	4.77	4.77	.0013	-2431.03	-822.81
84	4.39	4.39	4.39	.0012	-2438.05	-829.83
85	4.15	4.15	4.15	.0011	-2445.07	-836.84
86	3.90	3.90	3.90	.0010	-2452.08	-843.86
87	3.66	3.66	3.66	.0009	-2459.10	-850.88
88	3.41	3.41	3.41	.0009	-2466.12	-857.90
89	3.17	3.17	3.17	.0008	-2473.14	-864.91
90	2.96	2.96	2.96	.0007	-2480.16	-871.93
91	2.75	2.75	2.75	.0007	-2487.17	-878.95
92	2.54	2.54	2.54	.0006	-2494.19	-885.97
93	2.37	2.37	2.37	.0006	-2501.21	-892.98
94	2.16	2.16	2.16	.0005	-2508.23	-900.00
95	.00	.00	.00	.0000	-10000.00	-10000.00

ISOTHERM: T = 85 K.

Point	N	N_o	N_{tot}	P	μ	$\mu-\mu_o$
1	519.35	531.06	531.35	34.3270	-1632.95	-6.12
2	503.78	515.40	515.69	34.0950	-1633.53	-6.70
3	488.32	499.84	500.12	33.7680	-1634.35	-7.51
4	473.12	484.47	484.75	33.2750	-1635.59	-8.76
5	456.88	468.01	468.28	32.6500	-1637.20	-10.37
6	441.49	452.53	452.81	32.3790	-1637.91	-11.07
7	426.08	437.04	437.31	32.1489	-1638.51	-11.68
8	410.61	421.52	421.79	31.9969	-1638.91	-12.08
9	395.12	406.00	406.27	31.9049	-1639.16	-12.32
10	379.80	390.50	390.77	31.3859	-1640.55	-13.72
11	364.77	375.11	375.37	30.3449	-1643.41	-16.57
12	334.41	344.26	344.51	28.9019	-1647.54	-20.70
13	319.74	328.99	329.22	27.1459	-1652.85	-26.02
14	304.76	313.64	313.86	26.0509	-1656.34	-29.51
15	289.40	298.19	298.40	25.7919	-1657.19	-30.36
16	273.95	282.67	282.89	25.5949	-1657.84	-31.01
17	258.77	267.25	267.46	24.8779	-1660.25	-33.42
18	244.09	251.90	252.09	22.9169	-1667.21	-40.38
19	232.16	239.36	239.53	21.1389	-1674.06	-47.23
20	220.22	226.76	226.92	19.2149	-1682.16	-55.33
21	208.31	214.13	214.27	17.0779	-1692.17	-65.34
22	196.47	201.61	201.73	15.0959	-1702.64	-75.81
23	184.31	189.02	189.14	13.8529	-1709.93	-83.10
24	171.78	176.36	176.47	13.4459	-1712.47	-85.64
25	159.01	163.56	163.67	13.3609	-1713.00	-86.17
26	146.25	150.76	150.88	13.2479	-1713.72	-86.89
27	140.92	145.41	145.52	13.1809	-1714.16	-87.32
28	133.33	137.78	137.89	13.0669	-1714.89	-88.06
29	125.63	130.06	130.18	13.0449	-1715.04	-88.21
30	117.99	122.41	122.52	12.9919	-1715.38	-88.55
31	110.39	114.74	114.85	12.7869	-1716.73	-89.90
32	103.10	107.13	107.23	11.8319	-1723.32	-96.49
33	96.49	99.72	99.80	9.4898	-1742.05	-115.22
34	92.39	94.84	94.90	7.1805	-1765.74	-138.91
35	88.49	89.98	90.02	4.3806	-1807.72	-180.89
36	84.56	85.13	85.14	1.6861	-1888.86	-262.03
37	79.98	80.09	80.09	.3074	-2033.53	-406.70
38	75.82	75.87	75.87	.1493	-2094.88	-468.05
39	.00	.00	.00	.0000	-10000.00	-10000.00

ISOTHERM: T = 86 K.

Point	N	N_o	N_{tot}	P	μ	$\mu-\mu_o$
1	516.81	530.39	530.73	40.2700	-1642.48	-6.28
2	501.30	514.75	515.09	39.9000	-1643.27	-7.07
3	485.86	499.19	499.52	39.5420	-1644.05	-7.84
4	470.71	483.83	484.16	38.9310	-1645.38	-9.18
5	454.49	467.38	467.70	38.2440	-1646.91	-10.70
6	439.14	451.91	452.23	37.8890	-1647.70	-11.50
7	423.71	436.41	436.73	37.6800	-1648.18	-11.98
8	408.25	420.90	421.22	37.5190	-1648.55	-12.34
9	392.80	405.39	405.70	37.3480	-1648.94	-12.73
10	377.58	389.92	390.22	36.5850	-1650.71	-14.51
11	362.60	374.54	374.84	35.4300	-1653.46	-17.25
12	332.38	343.73	344.01	33.6769	-1657.81	-21.61
13	317.82	328.48	328.75	31.6629	-1663.10	-26.90
14	302.91	313.15	313.41	30.4019	-1666.58	-30.38
15	287.58	297.71	297.96	30.0659	-1667.54	-31.33
16	272.20	282.21	282.46	29.7149	-1668.54	-32.34
17	257.09	266.80	267.05	28.8289	-1671.14	-34.94
18	242.53	251.48	251.71	26.5829	-1678.10	-41.90
19	230.68	238.96	239.17	24.6139	-1684.70	-48.50
20	218.83	226.39	226.58	22.4749	-1692.51	-56.30
21	206.95	213.77	213.94	20.2539	-1701.44	-65.24
22	195.23	201.28	201.43	17.9879	-1711.63	-75.42
23	183.23	188.74	188.88	16.3699	-1719.72	-83.52
24	170.78	176.09	176.22	15.7969	-1722.78	-86.58
25	158.04	163.30	163.43	15.6319	-1723.68	-87.48
26	145.32	150.52	150.65	15.4369	-1724.76	-88.56
27	140.01	145.17	145.30	15.3249	-1725.39	-89.18
28	132.45	137.54	137.67	15.1479	-1726.38	-90.18
29	124.75	129.83	129.96	15.1079	-1726.61	-90.41
30	117.13	122.18	122.31	15.0229	-1727.10	-90.89
31	109.57	114.53	114.65	14.7289	-1728.79	-92.59
32	102.40	106.94	107.05	13.5079	-1736.23	-100.02
33	95.97	99.58	99.67	10.7368	-1755.95	-119.75
34	92.01	94.73	94.80	8.0993	-1780.18	-143.97
35	88.24	89.92	89.96	4.9792	-1821.99	-185.79
36	84.40	85.09	85.10	2.0502	-1898.28	-262.08
37	79.93	80.07	80.08	.4335	-2031.90	-395.70
38	75.80	75.86	75.86	.1930	-2101.49	-465.28
39	.00	.00	.00	.0000	-10000.00	-10000.00

ISOTHERM: T = 87 K.

Point	N	N_o	N_{tot}	P	μ	$\mu-\mu_o$
1	529.04	544.85	545.24	47.4090	-1651.43	-5.81
2	513.96	529.64	530.03	47.0010	-1652.18	-6.56
3	498.47	514.00	514.39	46.5700	-1652.98	-7.36
4	483.05	498.44	498.83	46.1620	-1653.74	-8.12
5	467.96	483.10	483.48	45.4120	-1655.16	-9.54
6	451.79	466.66	467.04	44.6100	-1656.70	-11.09
7	436.43	451.19	451.56	44.2770	-1657.35	-11.73
8	421.06	435.71	436.08	43.9470	-1658.00	-12.38
9	405.65	420.21	420.58	43.6790	-1658.53	-12.91
10	390.27	404.71	405.08	43.3380	-1659.21	-13.59
11	375.05	389.24	389.60	42.5700	-1660.76	-15.14
12	360.22	373.91	374.25	41.0850	-1663.84	-18.22
13	330.12	343.13	343.45	39.0460	-1668.25	-22.64
14	315.68	327.91	328.22	36.7280	-1673.56	-27.94
15	300.86	312.60	312.90	35.2700	-1677.07	-31.46
16	285.61	297.18	297.47	34.7490	-1678.37	-32.75
17	270.26	281.69	281.98	34.3110	-1679.47	-33.85
18	255.20	266.30	266.58	33.3190	-1682.01	-36.39
19	240.77	251.01	251.27	30.7699	-1688.92	-43.30
20	228.95	238.50	238.74	28.6849	-1695.01	-49.39
21	217.12	225.94	226.16	26.4989	-1701.89	-56.27
22	205.46	213.37	213.57	23.7839	-1711.27	-65.65
23	193.94	200.94	201.12	21.0359	-1721.94	-76.32
24	182.04	188.42	188.58	19.1759	-1729.98	-84.36
25	169.66	175.79	175.95	18.4349	-1733.40	-87.78
26	156.98	163.01	163.17	18.1529	-1734.74	-89.12
27	144.30	150.24	150.39	17.8639	-1736.13	-90.51
28	139.01	144.90	145.05	17.7019	-1736.92	-91.31
29	131.49	137.29	137.43	17.4149	-1738.34	-92.73
30	123.80	129.58	129.72	17.3739	-1738.55	-92.93
31	116.20	121.93	122.08	17.2479	-1739.18	-93.56
32	108.68	114.29	114.43	16.8449	-1741.23	-95.62
33	101.65	106.74	106.87	15.3079	-1749.55	-103.93
34	95.42	99.43	99.53	12.0499	-1770.34	-124.73
35	91.61	94.63	94.70	9.0615	-1795.12	-149.50
36	87.97	89.84	89.89	5.6246	-1836.58	-190.97
37	84.28	85.05	85.07	2.3411	-1912.82	-267.20
38	79.85	80.06	80.06	.6096	-2029.88	-384.26
39	75.77	75.85	75.86	.2551	-2105.68	-460.06
40	.00	.00	.00	.0000	-10000.00	-10000.00

ISOTHERM: T = 88 K.

Point	N	N_o	N_{tot}	P	μ	$\mu-\mu_o$
1	525.96	544.02	544.48	54.7700	-1661.76	-6.68
2	510.79	528.79	529.24	54.5700	-1662.08	-7.00
3	495.34	513.16	513.61	54.0300	-1662.95	-7.87
4	479.98	497.62	498.06	53.4910	-1663.83	-8.75
5	464.91	482.29	482.73	52.7040	-1665.13	-10.05
6	448.79	465.86	466.29	51.7700	-1666.70	-11.62
7	433.39	450.38	450.81	51.5170	-1667.13	-12.05
8	418.14	434.93	435.35	50.9010	-1668.18	-13.10
9	402.66	419.41	419.83	50.8090	-1668.34	-13.26
10	387.38	403.94	404.36	50.2170	-1669.37	-14.28
11	372.29	388.50	388.91	49.1740	-1671.21	-16.13
12	357.54	373.19	373.59	47.4790	-1674.28	-19.20
13	327.61	342.45	342.83	45.0380	-1678.91	-23.83
14	313.26	327.27	327.62	42.5040	-1683.99	-28.91
15	298.53	311.98	312.32	40.8380	-1687.49	-32.41
16	283.34	296.57	296.91	40.1710	-1688.94	-33.86
17	268.05	281.10	281.43	39.6140	-1690.16	-35.08
18	253.01	265.71	266.03	38.5450	-1692.56	-37.48
19	238.60	250.43	250.73	35.9200	-1698.75	-43.67
20	226.96	237.97	238.25	33.4310	-1705.05	-49.97
21	215.40	225.47	225.73	30.6119	-1712.79	-57.71
22	203.92	212.96	213.19	27.4699	-1722.29	-67.21
23	192.53	200.56	200.76	24.4149	-1732.65	-77.57
24	180.72	188.07	188.25	22.3289	-1740.49	-85.41
25	168.41	175.46	175.64	21.4289	-1744.11	-89.03
26	155.76	162.69	162.86	21.0479	-1745.68	-90.60
27	143.16	149.93	150.11	20.5909	-1747.61	-92.53
28	137.91	144.60	144.77	20.3429	-1748.68	-93.60
29	130.44	137.00	137.17	19.9449	-1750.41	-95.33
30	122.76	129.30	129.46	19.8709	-1750.74	-95.66
31	115.18	121.66	121.82	19.6849	-1751.56	-96.48
32	107.73	114.03	114.19	19.1479	-1753.99	-98.91
33	100.85	106.52	106.66	17.2339	-1763.25	-108.17
34	94.85	99.27	99.38	13.4429	-1785.08	-130.00
35	91.19	94.51	94.59	10.0908	-1810.30	-155.22
36	87.69	89.76	89.82	6.3277	-1851.34	-196.26
37	84.16	85.02	85.04	2.6332	-1928.47	-273.39
38	79.75	80.03	80.04	.8447	-2028.51	-373.43
39	75.74	75.85	75.85	.3270	-2112.03	-456.95
40	.00	.00	.00	.0000	-10000.00	-10000.00

ISOTHERM: T = 89 K.

Point	N	N_o	N_{tot}	P	μ	$\mu-\mu_o$
1	522.34	543.04	543.57	63.4670	-1671.58	-7.00
2	507.24	527.83	528.35	63.1080	-1672.09	-7.50
3	491.83	512.21	512.73	62.4870	-1672.96	-8.38
4	476.51	496.68	497.19	61.8260	-1673.91	-9.32
5	461.43	481.35	481.86	61.0620	-1675.01	-10.42
6	445.36	464.93	465.43	60.0190	-1676.53	-11.95
7	430.05	449.47	449.97	59.5550	-1677.22	-12.63
8	414.76	434.01	434.50	59.0380	-1677.99	-13.41
9	399.48	418.55	419.03	58.4740	-1678.84	-14.26
10	384.21	403.08	403.56	57.8550	-1679.79	-15.20
11	369.22	387.67	388.14	56.5850	-1681.75	-17.17
12	354.50	372.37	372.83	54.7950	-1684.60	-20.01
13	324.65	341.65	342.09	52.1690	-1688.95	-24.37
14	310.44	326.50	326.91	49.2930	-1693.98	-29.39
15	295.83	311.25	311.64	47.3350	-1697.57	-32.99
16	280.83	295.89	296.28	46.2280	-1699.67	-35.09
17	265.56	280.42	280.80	45.6140	-1700.86	-36.27
18	250.63	265.06	265.43	44.2840	-1703.48	-38.90
19	236.47	249.85	250.19	41.0810	-1710.14	-45.56
20	225.02	237.44	237.75	38.1440	-1716.73	-52.14
21	213.62	224.99	225.28	34.9200	-1724.56	-59.98
22	202.31	212.52	212.78	31.3669	-1734.09	-69.50
23	191.01	200.15	200.38	28.0769	-1743.93	-79.34
24	179.27	187.67	187.89	25.8279	-1751.34	-86.76
25	167.02	175.08	175.29	24.7669	-1755.07	-90.48
26	154.46	162.33	162.53	24.2019	-1757.12	-92.53
27	141.93	149.59	149.79	23.5769	-1759.44	-94.86
28	136.72	144.27	144.47	23.2229	-1760.79	-96.20
29	129.31	136.69	136.88	22.6859	-1762.87	-98.28
30	121.65	128.99	129.18	22.5599	-1763.36	-98.77
31	114.11	121.36	121.55	22.3129	-1764.34	-99.75
32	106.72	113.75	113.93	21.6149	-1767.16	-102.58
33	100.03	106.29	106.45	19.2509	-1777.45	-112.87
34	94.28	99.11	99.23	14.8729	-1800.39	-135.80
35	90.76	94.39	94.48	11.1729	-1825.82	-161.24
36	87.39	89.68	89.74	7.0627	-1866.61	-202.03
37	84.03	84.99	85.01	2.9358	-1944.72	-280.13
38	79.62	79.99	80.00	1.1539	-2027.81	-363.23
39	75.70	75.84	75.84	.4190	-2117.96	-453.37
40	.00	.00	.00	.0000	-10000.00	-10000.00

ISOTHERM: T = 90 K.

Point	N	N_o	N_{tot}	P	μ	$\mu-\mu_o$
1	518.42	541.98	542.58	72.9800	-1681.86	-7.72
2	503.33	526.77	527.37	72.5870	-1682.34	-8.20
3	487.91	511.15	511.74	71.9940	-1683.07	-8.94
4	472.59	495.61	496.20	71.3110	-1683.93	-9.79
5	457.57	480.30	480.88	70.4210	-1685.05	-10.91
6	441.48	463.88	464.45	69.4010	-1686.36	-12.22
7	426.33	448.46	449.03	68.5610	-1687.45	-13.31
8	411.07	433.00	433.57	67.9830	-1688.21	-14.07
9	395.80	417.55	418.10	67.4040	-1688.97	-14.83
10	380.65	402.10	402.66	66.5030	-1690.18	-16.04
11	365.65	386.70	387.24	65.2370	-1691.90	-17.76
12	351.11	371.44	371.97	63.0430	-1694.96	-20.83
13	321.53	340.80	341.30	59.7590	-1699.76	-25.62
14	307.48	325.70	326.17	56.4900	-1704.80	-30.66
15	292.96	310.47	310.92	54.3180	-1708.31	-34.17
16	278.04	295.13	295.57	53.0080	-1710.50	-36.36
17	262.82	279.67	280.11	52.2900	-1711.72	-37.58
18	248.03	264.34	264.76	50.6210	-1714.63	-40.49
19	234.19	249.22	249.61	46.6580	-1721.94	-47.80
20	222.92	236.86	237.22	43.2690	-1728.70	-54.57
21	211.70	224.46	224.79	39.6210	-1736.61	-62.47
22	200.52	212.03	212.32	35.7280	-1745.89	-71.75
23	189.33	199.69	199.95	32.1910	-1755.25	-81.11
24	177.66	187.23	187.48	29.7579	-1762.30	-88.17
25	165.49	174.66	174.90	28.5029	-1766.17	-92.04
26	153.00	161.93	162.16	27.7649	-1768.53	-94.39
27	140.57	149.22	149.44	26.8839	-1771.43	-97.29
28	135.43	143.92	144.14	26.3919	-1773.08	-98.95
29	128.10	136.35	136.57	25.6669	-1775.59	-101.45
30	120.46	128.66	128.87	25.4889	-1776.21	-102.07
31	112.95	121.04	121.25	25.1499	-1777.42	-103.28
32	105.65	113.45	113.65	24.2479	-1780.70	-106.56
33	99.17	106.05	106.23	21.4069	-1791.89	-117.75
34	93.67	98.94	99.07	16.3979	-1815.85	-141.71
35	90.29	94.26	94.36	12.3529	-1841.31	-167.18
36	87.05	89.59	89.65	7.9075	-1881.43	-207.29
37	83.90	84.95	84.98	3.2722	-1960.81	-286.67
38	79.45	79.95	79.96	1.5529	-2027.88	-353.74
39	75.65	75.82	75.83	.5294	-2124.73	-450.59
40	.00	.00	.00	.0000	-10000.00	-10000.00

ISOTHERM: T = 91 K.

Point	N	N_o	N_{tot}	P	μ	$\mu-\mu_o$
1	513.93	540.74	541.43	84.0200	-1692.47	-8.30
2	499.02	525.58	526.27	83.1530	-1692.73	-8.55
3	483.59	509.96	510.64	82.5610	-1693.38	-9.20
4	468.27	494.42	495.10	81.8650	-1694.14	-9.96
5	453.37	479.15	479.81	80.7120	-1695.43	-11.25
6	437.35	462.75	463.40	79.5130	-1696.78	-12.60
7	422.17	447.32	447.96	78.7480	-1697.65	-13.48
8	407.04	431.90	432.54	77.8300	-1698.72	-14.54
9	391.92	416.48	417.11	76.9120	-1699.79	-15.61
10	376.80	401.04	401.67	75.9300	-1700.95	-16.77
11	361.98	385.69	386.30	74.2670	-1702.96	-18.78
12	347.57	370.47	371.06	71.7300	-1706.10	-21.92
13	318.23	339.89	340.45	67.8820	-1711.09	-26.92
14	304.31	324.82	325.35	64.3040	-1716.00	-31.82
15	289.81	309.60	310.11	62.0400	-1719.24	-35.07
16	274.98	294.29	294.79	60.5270	-1721.48	-37.30
17	259.86	278.86	279.35	59.5700	-1722.93	-38.75
18	245.29	263.58	264.06	57.3640	-1726.34	-42.17
19	231.80	248.56	248.99	52.5820	-1734.23	-50.06
20	220.74	236.25	236.65	48.6840	-1741.22	-57.04
21	209.68	223.90	224.26	44.6120	-1749.14	-64.96
22	198.63	211.50	211.83	40.3980	-1758.14	-73.96
23	187.51	199.18	199.49	36.6670	-1766.94	-82.76
24	175.90	186.75	187.03	34.0800	-1773.58	-89.40
25	163.80	174.19	174.46	32.6409	-1777.49	-93.32
26	151.41	161.49	161.75	31.6759	-1780.22	-96.04
27	139.12	148.82	149.07	30.4639	-1783.76	-99.58
28	134.05	143.53	143.78	29.7979	-1785.77	-101.59
29	126.82	136.00	136.23	28.8339	-1788.75	-104.57
30	119.22	128.32	128.55	28.5729	-1789.58	-105.40
31	111.76	120.71	120.94	28.1179	-1791.04	-106.86
32	104.55	113.14	113.37	26.9919	-1794.75	-110.57
33	98.29	105.80	106.00	23.6109	-1806.90	-122.73
34	93.05	98.76	98.91	17.9629	-1831.75	-147.57
35	89.81	94.12	94.23	13.5589	-1857.31	-173.13
36	86.68	89.48	89.56	8.8273	-1896.34	-212.16
37	83.76	84.91	84.94	3.6312	-1977.14	-292.96
38	79.27	79.90	79.92	1.9813	-2032.26	-348.08
39	75.60	75.81	75.81	.6644	-2131.68	-447.50
40	.00	.00	.00	.0000	-10000.00	-10000.00

ISOTHERM: T = 92 K.

Point	N	N_o	N_{tot}	P	μ	$\mu-\mu_o$
1	509.45	539.50	540.28	95.0600	-1703.09	-7.95
2	494.33	524.28	525.06	94.7440	-1703.40	-8.25
3	478.84	508.65	509.42	94.2840	-1703.84	-8.69
4	463.70	493.15	493.92	93.1590	-1704.94	-9.79
5	448.88	477.90	478.65	91.8100	-1706.27	-11.13
6	432.88	461.51	462.25	90.5700	-1707.51	-12.37
7	417.82	446.11	446.84	89.5040	-1708.60	-13.45
8	402.87	430.74	431.46	88.1800	-1709.96	-14.81
9	387.58	415.28	416.00	87.6420	-1710.52	-15.37
10	372.67	399.89	400.60	86.1470	-1712.09	-16.95
11	358.03	384.59	385.28	84.0640	-1714.33	-19.18
12	343.82	369.42	370.09	81.0680	-1717.65	-22.50
13	314.69	338.91	339.54	76.6800	-1722.74	-27.59
14	300.76	323.84	324.44	73.1070	-1727.11	-31.96
15	286.40	308.65	309.23	70.4980	-1730.43	-35.29
16	271.61	293.35	293.92	68.8770	-1732.56	-37.42
17	256.61	277.95	278.51	67.6380	-1734.22	-39.08
18	242.34	262.76	263.29	64.6940	-1738.30	-43.15
19	229.26	247.84	248.33	58.9150	-1746.87	-51.73
20	218.38	235.59	236.04	54.5650	-1753.90	-58.76
21	207.50	223.28	223.69	50.0570	-1761.80	-66.66
22	196.58	210.92	211.30	45.5110	-1770.53	-75.39
23	185.52	198.63	198.97	41.6090	-1778.76	-83.61
24	173.96	186.21	186.52	38.8850	-1784.97	-89.82
25	161.95	173.68	173.98	37.2280	-1788.96	-93.82
26	149.67	161.00	161.30	35.9970	-1792.05	-96.90
27	137.56	148.38	148.66	34.3559	-1796.33	-101.18
28	132.59	143.12	143.40	33.4630	-1798.75	-103.60
29	125.47	135.61	135.88	32.2169	-1802.23	-107.08
30	117.92	127.95	128.21	31.8629	-1803.24	-108.10
31	110.51	120.35	120.61	31.2729	-1804.96	-109.82
32	103.42	112.82	113.06	29.8649	-1809.19	-114.04
33	97.40	105.55	105.76	25.8959	-1822.28	-127.14
34	92.38	98.57	98.73	19.6779	-1847.51	-152.36
35	89.31	93.98	94.10	14.8379	-1873.45	-178.30
36	86.25	89.36	89.44	9.9090	-1910.56	-215.41
37	83.59	84.86	84.90	4.0547	-1992.73	-297.58
38	79.09	79.85	79.87	2.4143	-2040.42	-345.27
39	75.53	75.79	75.80	.8257	-2139.11	-443.97
40	.00	.00	.00	.0000	-10000.00	-10000.00

ISOTHERM: T = 93 K.

Point	N	N_o	N_{tot}	P	μ	$\mu-\mu_o$
1	504.31	538.07	538.95	107.8500	-1713.94	-7.76
2	489.45	522.92	523.79	106.9400	-1714.72	-8.54
3	473.93	507.28	508.15	106.5300	-1715.07	-8.89
4	458.66	491.74	492.61	105.7000	-1715.80	-9.61
5	443.82	476.49	477.34	104.4000	-1716.94	-10.76
6	428.06	460.16	461.00	102.6000	-1718.55	-12.36
7	412.89	444.73	445.56	101.7600	-1719.31	-13.12
8	397.85	429.34	430.16	100.6500	-1720.32	-14.14
9	383.03	414.00	414.81	99.0030	-1721.84	-15.66
10	368.30	398.66	399.46	97.0850	-1723.65	-17.47
11	353.79	383.40	384.17	94.6810	-1725.97	-19.78
12	339.78	368.29	369.04	91.1790	-1729.45	-23.27
13	310.80	337.81	338.52	86.4360	-1734.39	-28.20
14	296.98	322.78	323.45	82.5700	-1738.62	-32.44
15	282.56	307.58	308.24	80.0810	-1741.45	-35.27
16	267.98	292.33	292.97	77.9720	-1743.92	-37.73
17	253.15	276.98	277.60	76.2890	-1745.94	-39.75
18	239.25	261.88	262.47	72.4720	-1750.69	-44.50
19	226.54	247.07	247.61	65.7910	-1759.64	-53.46
20	215.94	234.89	235.39	60.7360	-1767.04	-60.86
21	205.22	222.63	223.09	55.8220	-1774.86	-68.67
22	194.41	210.31	210.73	50.9930	-1783.24	-77.06
23	183.39	198.03	198.41	46.9670	-1790.86	-84.68
24	171.87	185.62	185.98	44.1160	-1796.67	-90.49
25	159.96	173.12	173.46	42.2270	-1800.73	-94.54
26	147.81	160.48	160.81	40.6550	-1804.24	-98.06
27	135.93	147.91	148.23	38.4570	-1809.40	-103.22
28	131.07	142.69	142.99	37.3080	-1812.21	-106.03
29	124.09	135.22	135.51	35.7280	-1816.23	-110.04
30	116.58	127.56	127.85	35.2560	-1817.46	-111.28
31	109.25	119.99	120.27	34.5000	-1819.47	-113.29
32	102.28	112.49	112.76	32.7840	-1824.21	-118.02
33	96.49	105.28	105.51	28.2289	-1838.09	-131.91
34	91.73	98.38	98.55	21.3699	-1863.94	-157.75
35	88.81	93.83	93.96	16.1389	-1890.01	-183.83
36	85.95	89.27	89.36	10.6788	-1928.38	-222.20
37	83.38	84.80	84.84	4.5678	-2007.32	-301.14
38	78.91	79.80	79.82	2.8760	-2050.34	-344.15
39	75.45	75.77	75.78	1.0154	-2147.15	-440.96
40	.00	.00	.00	.0000	-10000.00	-10000.00

ISOTHERM: T = 94 K.

Point	N	N_o	N_{tot}	P	μ	$\mu-\mu_o$
1	498.72	536.50	537.49	121.9000	-1724.94	-7.65
2	483.80	521.33	522.32	121.1100	-1725.54	-8.25
3	468.41	505.72	506.70	120.4100	-1726.08	-8.79
4	453.30	490.23	491.20	119.1800	-1727.04	-9.75
5	438.65	475.03	475.99	117.4500	-1728.40	-11.11
6	422.73	458.66	459.60	115.9800	-1729.58	-12.29
7	407.73	443.27	444.21	114.7500	-1730.57	-13.28
8	392.69	427.88	428.80	113.6200	-1731.50	-14.21
9	378.02	412.59	413.50	111.6300	-1733.15	-15.86
10	363.33	397.26	398.15	109.5800	-1734.88	-17.59
11	349.21	382.10	382.97	106.2500	-1737.76	-20.47
12	335.41	367.05	367.88	102.2300	-1741.35	-24.07
13	306.85	336.69	337.48	96.4670	-1746.77	-29.49
14	292.76	321.59	322.34	93.1940	-1750.00	-32.71
15	278.47	306.43	307.16	90.4000	-1752.84	-35.55
16	263.90	291.18	291.90	88.2410	-1755.10	-37.81
17	249.47	275.94	276.63	85.6240	-1757.91	-40.63
18	235.97	260.94	261.60	80.8000	-1763.33	-46.05
19	223.69	246.26	246.85	73.0510	-1772.76	-55.47
20	212.98	234.05	234.60	68.2390	-1779.14	-61.85
21	202.52	221.86	222.37	62.6750	-1787.10	-69.81
22	191.90	209.59	210.06	57.3350	-1795.44	-78.15
23	181.01	197.36	197.79	52.9840	-1802.83	-85.54
24	169.57	184.97	185.37	49.9080	-1808.43	-91.14
25	157.78	172.50	172.89	47.7230	-1812.63	-95.34
26	145.81	159.91	160.28	45.7290	-1816.63	-99.34
27	134.18	147.41	147.76	42.9170	-1822.57	-105.29
28	129.47	142.23	142.57	41.3780	-1826.00	-108.71
29	122.66	134.80	135.13	39.4100	-1830.57	-113.28
30	115.22	127.17	127.48	38.7730	-1832.09	-114.81
31	107.96	119.62	119.93	37.8320	-1834.40	-117.11
32	101.13	112.15	112.44	35.7850	-1839.61	-122.32
33	95.58	105.01	105.26	30.6149	-1854.25	-136.96
34	91.06	98.18	98.37	23.1229	-1880.58	-163.30
35	88.25	93.67	93.81	17.5859	-1906.28	-188.99
36	85.67	89.19	89.28	11.4429	-1946.64	-229.35
37	83.05	84.71	84.75	5.4079	-2017.05	-299.77
38	78.70	79.74	79.77	3.3788	-2061.25	-343.96
39	75.36	75.74	75.75	1.2392	-2155.53	-438.24
40	.00	.00	.00	.0000	-10000.00	-10000.00

ISOTHERM: T = 95 K.

Point	N	N_o	N_{tot}	P	μ	$\mu-\mu_o$
1	492.75	534.80	535.91	137.0500	-1736.23	-7.77
2	477.83	519.64	520.74	136.2500	-1736.79	-8.32
3	462.55	504.06	505.15	135.2700	-1737.46	-9.00
4	447.39	488.54	489.63	134.1500	-1738.25	-9.79
5	432.91	473.40	474.47	132.0000	-1739.77	-11.31
6	417.05	457.05	458.10	130.3800	-1740.93	-12.47
7	402.00	441.64	442.69	129.2600	-1741.75	-13.28
8	387.07	426.28	427.32	127.8600	-1742.77	-14.31
9	372.48	411.02	412.03	125.6700	-1744.40	-15.94
10	358.30	395.82	396.81	122.4000	-1746.88	-18.42
11	344.33	380.71	381.67	118.6900	-1749.79	-21.33
12	330.75	365.72	366.64	114.1300	-1753.48	-25.02
13	301.93	335.30	336.18	108.9400	-1757.87	-29.41
14	288.23	320.30	321.15	104.7100	-1761.61	-33.15
15	273.76	305.09	305.92	102.3400	-1763.77	-35.31
16	259.93	290.05	290.84	98.3940	-1767.48	-39.02
17	245.68	274.85	275.62	95.3220	-1770.47	-42.01
18	232.65	259.98	260.71	89.3520	-1776.58	-48.12
19	220.25	245.27	245.93	81.8290	-1784.89	-56.43
20	210.11	233.22	233.83	75.6020	-1792.37	-63.91
21	199.79	221.08	221.64	69.6580	-1800.11	-71.65
22	189.30	208.85	209.36	64.0040	-1808.12	-79.66
23	178.49	196.63	197.11	59.4280	-1815.14	-86.68
24	167.13	184.27	184.72	56.1330	-1820.54	-92.08
25	155.46	171.83	172.27	53.6350	-1824.85	-96.39
26	143.69	159.30	159.71	51.1560	-1829.33	-100.87
27	132.36	146.88	147.27	47.6040	-1836.14	-107.68
28	127.81	141.74	142.12	45.6830	-1840.05	-111.58
29	121.01	134.32	134.68	43.6570	-1844.34	-115.88
30	113.44	126.66	127.01	43.3260	-1845.06	-116.60
31	106.26	119.13	119.47	42.1880	-1847.58	-119.12
32	99.39	111.65	111.98	40.2170	-1852.12	-123.66
33	94.57	104.71	104.98	33.2850	-1870.05	-141.59
34	90.40	97.98	98.19	24.8819	-1897.64	-169.18
35	87.69	93.50	93.65	19.0819	-1922.82	-194.35
36	85.39	89.10	89.20	12.2019	-1965.25	-236.79
37	82.45	84.54	84.60	6.8779	-2019.68	-291.22
38	78.49	79.68	79.71	3.9214	-2073.04	-344.58
39	75.26	75.71	75.73	1.4985	-2164.42	-435.95
40	.00	.00	.00	.0000	-10000.00	-10000.00

ISOTHERM: T = 96 K.

Point	N	N_o	N_{tot}	P	μ	$\mu-\mu_o$
1	471.26	517.76	518.99	153.0300	-1748.01	-8.30
2	456.17	502.23	503.45	151.5900	-1748.91	-9.20
3	441.24	486.78	487.99	149.8800	-1749.99	-10.28
4	426.64	471.61	472.80	148.0300	-1751.17	-11.46
5	410.94	455.29	456.47	146.0200	-1752.47	-12.76
6	396.02	439.93	441.09	144.5600	-1753.42	-13.72
7	381.16	424.58	425.74	142.9900	-1754.46	-14.76
8	366.67	409.35	410.48	140.5700	-1756.09	-16.38
9	352.94	394.27	395.37	136.1700	-1759.11	-19.41
10	339.12	379.21	380.27	132.0800	-1762.02	-22.31
11	325.74	364.28	365.30	127.0200	-1765.74	-26.03
12	296.99	333.88	334.86	121.6300	-1769.87	-30.16
13	283.18	318.85	319.80	117.6400	-1773.04	-33.34
14	269.27	303.80	304.72	113.8900	-1776.13	-36.43
15	255.42	288.75	289.64	109.9800	-1779.46	-39.76
16	241.59	273.67	274.52	105.8700	-1783.09	-43.39
17	228.93	258.90	259.70	98.9560	-1789.54	-49.83
18	216.99	244.32	245.05	90.2870	-1798.29	-58.58
19	206.75	232.25	232.93	84.2520	-1804.89	-65.18
20	196.68	220.17	220.80	77.6830	-1812.64	-72.94
21	186.35	207.99	208.57	71.5900	-1820.45	-80.74
22	175.66	195.82	196.36	66.7020	-1827.21	-87.50
23	164.43	183.49	184.00	63.0630	-1832.57	-92.87
24	152.92	171.10	171.58	60.1780	-1837.05	-97.35
25	141.35	158.62	159.08	57.1610	-1841.97	-102.26
26	130.30	146.28	146.71	52.9230	-1849.34	-109.63
27	125.63	141.11	141.53	51.2860	-1852.35	-112.64
28	118.28	133.55	133.96	50.5560	-1853.72	-114.01
29	110.88	125.93	126.33	49.8210	-1855.12	-115.41
30	103.97	118.47	118.86	48.0300	-1858.62	-118.92
31	98.19	111.29	111.65	43.4100	-1868.31	-128.60
32	93.67	104.44	104.73	35.6980	-1887.04	-147.33
33	89.67	97.76	97.98	26.8539	-1914.31	-174.61
34	87.24	93.36	93.52	20.3219	-1941.03	-201.32
35	85.09	89.01	89.12	13.0279	-1983.67	-243.96
36	81.60	84.31	84.38	8.9992	-2019.16	-279.45
37	78.26	79.62	79.65	4.5006	-2085.65	-345.95
38	75.14	75.68	75.70	1.7951	-2173.88	-434.17
39	.00	.00	.00	.0000	-10000.00	-10000.00

Isotherms: Ω and its Proper Derivatives

The entire purpose of the thermodynamic technique, as stated in Chap. 2, is to obtain a free energy function in terms of its proper thermodynamic variables. This has been done for the multilayer methane/graphite system, and the following isotherm tables give $\Omega(T,\mu)$ along with its proper derivatives N and S. However, since it is usually more convenient to work in the N-T plane instead of the μ-T plane, the tables also give $(\partial\mu/\partial T)_N$ and $(\partial\mu/\partial N)_T$ in order to convert from one scheme to the other.

Note that $(\partial\mu/\partial T)_N$ has little meaning for N=0. Hence, for temperatures greater than 84 K, it is arbitrarily listed as -10.0000. Recall that the units for these tables are given on p. 85.

ISOTHERM: T = 78 K.

Point	N	μ	$(\partial\mu/\partial T)_N$	$(\partial\mu/\partial N)_T$	Ω	S
1	522.48	-1566.61	-10.1648	.0982	-73235.77	4920.01
2	507.53	-1568.08	-9.6036	.0804	-72571.47	4765.04
3	492.47	-1569.02	-9.5756	.0614	-72065.16	4611.93
4	477.33	-1569.93	-9.5129	.0599	-71654.96	4457.04
5	462.22	-1570.83	-9.3782	.0553	-71288.66	4301.43
6	447.11	-1571.60	-9.1938	.0312	-71044.24	4144.95
7	431.91	-1571.78	-9.4193	.0143	-70961.95	3982.29
8	416.76	-1572.04	-9.5459	.0122	-70807.86	3858.30
9	401.61	-1572.15	-9.9789	.0213	-70620.83	3735.57
10	386.47	-1572.68	-10.4187	.0612	-70293.32	3606.29
11	371.38	-1574.00	-10.8423	.0980	-69756.86	3470.94
12	356.31	-1575.64	-11.4353	.1348	-69037.30	3328.08
13	341.27	-1578.05	-11.8235	.1884	-68109.58	3178.17
14	326.26	-1581.30	-11.9086	.2388	-66959.88	3025.06
15	311.16	-1585.25	-10.4657	.1698	-65889.12	2881.20
16	296.02	-1586.43	-9.6005	.0426	-65310.09	2754.46
17	280.81	-1586.53	-9.5992	.0065	-65116.28	2633.72
18	265.63	-1586.62	-10.7374	.0534	-64910.89	2504.58
19	250.52	-1588.14	-14.1875	.3044	-64144.04	2341.36
20	235.69	-1595.63	-15.8264	.7118	-62251.86	2143.36
21	221.23	-1608.84	-15.9399	1.2443	-59385.71	1905.11
22	211.00	-1623.97	-13.1442	1.4783	-56410.83	1743.54
23	201.34	-1638.25	-7.5426	.9289	-54024.75	1633.43
24	192.75	-1642.03	-9.0349	.2354	-53045.28	1554.39
25	183.84	-1642.23	-9.1254	.0230	-52841.23	1466.33
26	175.16	-1642.44	-9.1969	.0173	-52824.30	1380.63
27	165.87	-1642.54	-9.1794	.0077	-52818.18	1289.32
28	157.07	-1642.58	-9.2169	.0094	-52817.85	1203.40
29	148.37	-1642.70	-9.1713	.0114	-52814.61	1118.92
30	123.69	-1642.80	-9.1259	.0040	-52812.70	882.44
31	115.89	-1642.83	-9.3645	.0040	-52815.69	807.42
32	108.25	-1642.86	-9.6788	.4504	-52633.87	732.09
33	100.66	-1649.64	-10.9113	2.6146	-51456.02	651.55
34	93.55	-1679.71	-11.2454	8.3985	-47731.27	570.63
35	90.08	-1715.89	-11.0555	20.2964	-43200.22	530.96
36	89.44	-1730.03	-5.9482	19.5895	-42056.50	525.35
37	87.62	-1752.63	-11.4575	17.8289	-39031.94	508.95
38	86.60	-1773.86	-10.5417	24.4891	-37158.93	497.48
39	86.13	-1786.02	-12.2360	27.3312	-36118.59	492.05
40	84.74	-1829.24	-14.0725	33.5056	-32487.05	473.27
41	83.22	-1884.21	-18.2167	49.1343	-27245.76	448.43
42	81.75	-1974.94	1.0682	47.3907	-21382.57	435.41
43	80.11	-2026.71	-4.5673	23.3653	-16671.31	432.12
44	77.90	-2053.93	3.2922	6.4288	-14054.60	430.14
45	76.38	-2057.52	-5.5994	11.6502	-13000.17	428.00
46	74.76	-2092.66	-17.6814	21.2470	-10985.29	408.66
47	71.71	-2171.52	4.2659	20.4129	-6337.15	387.47
48	70.54	-2174.77	-9.0341	13.5008	-4918.63	386.75
49	69.94	-2181.79	-9.0341	12.5529	-4644.46	383.51
50	69.46	-2188.81	-9.0341	11.8683	-4372.78	380.83

T = 78 K (cont.)

Point	N	μ	$(\partial\mu/\partial T)_N$	$(\partial\mu/\partial N)_T$	Ω	S
51	68.86	-2195.83	-9.0341	11.0486	-4102.78	377.59
52	68.10	-2202.84	-9.0341	9.9073	-3834.74	373.38
53	67.30	-2209.86	-9.0341	8.8243	-3569.60	368.99
54	66.53	-2216.88	-9.0341	8.6429	-3307.63	364.79
55	65.66	-2223.90	-9.0341	8.0585	-3048.42	360.02
56	64.79	-2230.92	-9.0341	7.6512	-2792.58	355.24
57	63.81	-2237.93	-9.0341	6.6947	-2539.91	349.89
58	62.66	-2244.95	-9.0341	5.7938	-2290.67	343.59
59	61.38	-2251.97	-9.0341	5.0493	-2045.62	336.52
60	59.84	-2258.99	-9.0341	3.9438	-1805.08	328.12
61	57.47	-2266.00	-9.0341	2.6114	-1568.87	315.13
62	54.17	-2273.02	-9.0341	1.7739	-1339.99	296.99
63	43.54	-2280.04	-9.0341	.6454	-1109.77	238.74
64	32.39	-2287.05	-9.0341	.5668	-919.66	177.62
65	17.94	-2294.07	-9.0341	1.4239	-766.29	98.36
66	13.79	-2301.09	-9.0341	3.3380	-688.83	75.63
67	12.05	-2308.11	-9.0341	4.9687	-632.07	66.08
68	10.80	-2315.13	-9.0341	6.3740	-582.99	59.21
69	9.58	-2322.14	-9.0341	8.0495	-538.84	52.52
70	8.92	-2329.16	-9.0341	9.1378	-500.48	48.89
71	8.05	-2336.18	-9.0341	10.8099	-464.27	44.12
72	7.49	-2343.20	-9.0341	12.0449	-432.05	41.06
73	6.90	-2350.21	-9.0341	13.5162	-401.92	37.82
74	6.34	-2357.23	-9.0341	15.0650	-374.14	34.76
75	5.85	-2364.25	-9.0341	16.5615	-348.66	32.09
76	5.50	-2371.26	-9.0341	17.7397	-325.34	30.18
77	5.16	-2378.28	-9.0341	19.1319	-303.35	28.27
78	4.77	-2385.30	-9.0341	21.3526	-282.66	26.17
79	4.39	-2392.32	-9.0341	24.4127	-263.45	24.06
80	4.15	-2399.33	-9.0341	26.2162	-245.98	22.73
81	3.90	-2406.35	-9.0341	27.8845	-229.47	21.39
82	3.66	-2413.37	-9.0341	29.3976	-213.90	20.05
83	3.41	-2420.39	-9.0341	30.7358	-199.27	18.72
84	3.17	-2427.41	-9.0341	31.8792	-185.58	17.38
85	2.96	-2434.42	-9.0341	32.6894	-172.91	16.23
86	2.75	-2441.44	-9.0341	33.5553	-161.04	15.09
87	2.54	-2448.46	-9.0341	35.5937	-149.99	13.94
88	2.37	-2455.48	-9.0341	39.1570	-139.81	12.99
89	2.16	-2462.49	-9.0341	47.3723	-121.87	11.84
90	.00	-10000.00	-9.0341	9999.9990	.00	.00

ISOTHERM: T = 79 K.

Point	N	μ	$(\partial\mu/\partial T)_N$	$(\partial\mu/\partial N)_T$	Ω	S
1	501.77	-1578.03	-9.6150	.0086	-71169.52	4718.88
2	485.88	-1579.00	-9.5511	.0159	-71092.73	4560.85
3	470.41	-1579.81	-9.5132	.0114	-71013.98	4406.49
4	454.75	-1580.58	-9.3376	.0077	-70973.09	4250.22
5	438.23	-1581.06	-9.3464	.0132	-70935.44	4083.89
6	422.90	-1581.39	-9.4097	.0210	-70822.37	3939.69
7	407.44	-1581.88	-9.4929	.0368	-70588.51	3808.68
8	392.10	-1582.52	-9.7267	.0724	-70206.66	3676.20
9	376.77	-1584.10	-10.2941	.1199	-69594.10	3537.77
10	361.48	-1586.19	-10.8582	.1537	-68775.16	3391.00
11	346.22	-1588.80	-11.0706	.1945	-67789.06	3238.65
12	331.10	-1592.09	-11.0059	.2241	-66670.63	3086.51
13	315.96	-1595.58	-11.0198	.1296	-65750.85	2934.61
14	300.70	-1596.01	-10.0829	.0161	-65352.76	2788.49
15	285.22	-1596.07	-9.7778	.0096	-65244.70	2649.87
16	269.96	-1596.30	-9.8853	.1310	-64905.49	2514.83
17	254.92	-1599.99	-10.8962	.3901	-63843.40	2373.21
18	240.05	-1607.91	-12.9351	.6725	-61857.05	2210.62
19	225.30	-1619.88	-13.6151	1.0077	-58900.49	2016.39
20	210.50	-1637.71	-11.2893	1.0449	-55635.63	1821.01
21	195.45	-1650.98	-9.3029	.4671	-53326.80	1657.23
22	175.60	-1651.63	-9.5830	.0256	-52409.47	1460.70
23	160.24	-1651.77	-9.5972	.0089	-52384.62	1307.81
24	144.87	-1651.90	-9.6063	.0055	-52384.76	1155.59
25	123.40	-1651.93	-9.6582	.0263	-52361.16	943.45
26	115.59	-1652.20	-9.7013	.0408	-52336.31	866.23
27	107.96	-1652.55	-11.3896	.5748	-52087.16	784.22
28	100.44	-1660.80	-15.2430	2.7944	-50803.52	682.66
29	93.43	-1691.48	-11.8975	8.5623	-47020.85	586.32
30	90.03	-1727.48	-10.5144	13.6289	-43578.14	547.66
31	89.62	-1733.22	-12.6490	14.2106	-43065.50	542.84
32	87.36	-1767.97	-16.0161	19.8609	-39671.21	510.12
33	86.61	-1784.08	-16.9131	24.1643	-38227.74	497.58
34	85.10	-1829.03	-21.9810	33.3897	-34505.14	467.99
35	82.72	-1921.89	-15.2681	47.7710	-26432.65	423.35
36	81.21	-2002.82	3.5288	39.6200	-20993.14	414.20
37	79.69	-2042.12	-6.0762	15.3695	-17628.78	412.04
38	78.13	-2049.14	-4.7605	5.4844	-16341.30	403.36
39	76.50	-2059.77	-9.9568	11.3458	-15283.89	391.10
40	73.38	-2150.43	-11.2661	23.0113	-11293.03	357.50
41	72.38	-2155.76	-9.0791	18.5707	-9785.63	349.50
42	72.00	-2162.78	-9.0791	17.1420	-9330.00	347.65
43	71.55	-2169.80	-9.0791	15.7454	-8876.56	345.46
44	71.13	-2176.81	-9.0791	14.6918	-8426.08	343.45
45	70.54	-2183.83	-9.0791	13.5008	-7977.66	340.59
46	69.94	-2190.85	-9.0791	12.5529	-7532.97	337.73
47	69.46	-2197.87	-9.0791	11.8683	-7092.33	335.37
48	68.86	-2204.88	-9.0791	11.0486	-6654.41	332.51
49	68.10	-2211.90	-9.0791	9.9073	-6219.67	328.81
50	67.30	-2218.92	-9.0791	8.8243	-5789.63	324.95

T = 79 K (cont.)

Point	N	μ	$(\partial\mu/\partial T)_N$	$(\partial\mu/\partial N)_T$	Ω	S
51	66.53	-2225.94	-9.0791	8.6429	-5364.73	321.25
52	65.66	-2232.95	-9.0791	8.0585	-4944.31	317.04
53	64.79	-2239.97	-9.0791	7.6512	-4529.36	312.84
54	63.81	-2246.99	-9.0791	6.6947	-4119.54	308.13
55	62.66	-2254.01	-9.0791	5.7938	-3715.30	302.58
56	61.38	-2261.02	-9.0791	5.0493	-3317.85	296.35
57	59.84	-2268.04	-9.0791	3.9438	-2927.71	288.95
58	57.47	-2275.06	-9.0791	2.6114	-2544.58	277.52
59	54.17	-2282.08	-9.0791	1.7739	-2173.37	261.54
60	43.54	-2289.09	-9.0791	.6454	-1799.96	210.24
61	32.39	-2296.11	-9.0791	.5668	-1491.63	156.42
62	17.94	-2303.13	-9.0791	1.4239	-1242.87	86.62
63	13.79	-2310.15	-9.0791	3.3380	-1117.23	66.60
64	12.05	-2317.16	-9.0791	4.9687	-1025.17	58.19
65	10.80	-2324.18	-9.0791	6.3740	-945.57	52.14
66	9.58	-2331.20	-9.0791	8.0495	-873.95	46.25
67	8.92	-2338.22	-9.0791	9.1378	-811.74	43.06
68	8.05	-2345.23	-9.0791	10.8099	-753.02	38.85
69	7.49	-2352.25	-9.0791	12.0449	-700.76	36.16
70	6.90	-2359.27	-9.0791	13.5162	-651.88	33.30
71	6.34	-2366.29	-9.0791	15.0650	-606.83	30.61
72	5.85	-2373.30	-9.0791	16.5615	-565.50	28.26
73	5.50	-2380.32	-9.0791	17.7397	-527.67	26.57
74	5.16	-2387.34	-9.0791	19.1319	-492.02	24.89
75	4.77	-2394.36	-9.0791	21.3526	-458.45	23.04
76	4.39	-2401.38	-9.0791	24.4127	-427.29	21.19
77	4.15	-2408.39	-9.0791	26.2162	-398.97	20.01
78	3.90	-2415.41	-9.0791	27.8845	-372.19	18.84
79	3.66	-2422.43	-9.0791	29.3976	-346.93	17.66
80	3.41	-2429.45	-9.0791	30.7358	-323.20	16.48
81	3.17	-2436.46	-9.0791	31.8792	-301.00	15.31
82	2.96	-2443.48	-9.0791	32.6894	-280.45	14.30
83	2.75	-2450.50	-9.0791	33.5553	-261.20	13.29
84	2.54	-2457.51	-9.0791	35.5937	-243.27	12.28
85	2.37	-2464.53	-9.0791	39.1570	-226.76	11.44
86	2.16	-2471.55	-9.0791	47.3723	-197.67	10.43
87	.00	-10000.00	-9.0791	9999.9990	.00	.00

ISOTHERM: T = 80 K.

Point	N	μ	$(\partial\mu/\partial T)_N$	$(\partial\mu/\partial N)_T$	Ω	S
1	528.05	-1586.49	-9.1909	.0386	-72887.70	4928.54
2	512.42	-1587.09	-8.3092	.0425	-72558.21	4791.77
3	496.89	-1587.81	-8.8600	.0589	-72161.80	4658.44
4	481.54	-1588.91	-8.8861	.0506	-71750.33	4522.29
5	465.06	-1589.38	-9.7037	.0422	-71387.67	4369.04
6	449.62	-1590.22	-9.4652	.0360	-71111.34	4221.13
7	434.13	-1590.49	-9.4602	.0221	-70911.56	4074.47
8	418.62	-1590.91	-9.4535	.0237	-70760.28	3927.85
9	403.12	-1591.22	-9.4465	.0530	-70517.82	3781.39
10	387.66	-1592.55	-9.6189	.1411	-69929.91	3634.03
11	372.40	-1595.54	-9.1493	.1737	-69018.48	3490.75
12	341.68	-1599.51	-9.0656	.2457	-66735.76	3211.00
13	326.53	-1604.10	-9.3955	.2060	-65590.57	3071.20
14	311.17	-1605.76	-9.6731	.0595	-64931.72	2924.74
15	295.70	-1605.93	-9.9824	.0145	-64755.36	2772.71
16	280.18	-1606.21	-10.0018	.0300	-64656.87	2617.65
17	264.73	-1606.85	-10.4207	.2600	-64060.20	2459.88
18	249.62	-1614.01	-10.1307	.5490	-62503.98	2304.52
19	237.31	-1621.52	-9.8899	.7135	-60619.12	2181.35
20	225.02	-1631.56	-9.4147	.9570	-58255.55	2062.73
21	212.75	-1645.02	-8.0095	1.0362	-55582.52	1955.86
22	200.46	-1657.00	-8.2489	.6634	-53410.54	1855.95
23	187.89	-1661.33	-9.6940	.1841	-52357.01	1743.15
24	175.19	-1661.62	-9.8960	.0164	-52119.11	1618.74
25	162.39	-1661.75	-9.9294	.0115	-52088.76	1491.82
26	149.59	-1661.91	-9.9412	.0104	-52066.86	1364.67
27	144.23	-1661.96	-9.9287	.0062	-52060.29	1311.39
28	136.58	-1661.97	-9.9536	.0021	-52055.77	1235.43
29	128.87	-1661.99	-9.9528	.0065	-52051.43	1158.62
30	121.21	-1662.07	-9.9235	.0120	-52042.66	1082.54
31	113.52	-1662.18	-10.0109	.1366	-51977.46	1005.92
32	105.87	-1664.16	-10.8546	1.1039	-51470.60	926.02
33	98.60	-1678.00	-11.3527	3.5626	-49770.47	845.37
34	93.97	-1699.38	-11.2292	7.0346	-47427.67	793.12
35	89.49	-1741.43	-10.9569	16.2726	-42679.10	743.36
36	85.04	-1844.12	-7.0514	30.8707	-33609.14	703.34
37	80.10	-2039.52	.7828	23.0175	-22558.66	687.84
38	75.87	-2077.20	-.2507	8.9042	-17228.33	688.97
39	75.13	-2094.69	-9.1240	30.4380	-16142.58	685.53
40	74.93	-2101.70	-9.1240	29.8418	-15614.59	683.62
41	74.72	-2108.72	-9.1240	29.2027	-15088.05	681.72
42	74.44	-2115.74	-9.1240	28.2844	-14562.76	679.17
43	74.19	-2122.76	-9.1240	27.4190	-14039.52	676.95
44	73.92	-2129.77	-9.1240	26.3600	-13517.89	674.41
45	73.67	-2136.79	-9.1240	25.3723	-12998.32	672.18
46	73.39	-2143.81	-9.1240	24.1744	-12480.34	669.64
47	73.11	-2150.83	-9.1240	22.0526	-11964.33	667.10
48	72.73	-2157.84	-9.1240	20.0958	-11449.90	663.60
49	72.38	-2164.86	-9.1240	18.5707	-10938.28	660.42
50	72.00	-2171.88	-9.1240	17.1420	-10428.99	656.93

T = 80 K (cont.)

Point	N	μ	$(\partial\mu/\partial T)_N$	$(\partial\mu/\partial N)_T$	Ω	S
51	71.55	-2178.90	-9.1240	15.7454	-9922.14	652.80
52	71.13	-2185.92	-9.1240	14.6918	-9418.59	648.98
53	70.54	-2192.93	-9.1240	13.5008	-8917.36	643.58
54	69.94	-2199.95	-9.1240	12.5529	-8420.28	638.18
55	69.46	-2206.97	-9.1240	11.8683	-7927.73	633.73
56	68.86	-2213.99	-9.1240	11.0486	-7438.24	628.32
57	68.10	-2221.00	-9.1240	9.9073	-6952.28	621.33
58	67.30	-2228.02	-9.1240	8.8243	-6471.59	614.02
59	66.53	-2235.04	-9.1240	8.6429	-5996.64	607.03
60	65.66	-2242.05	-9.1240	8.0585	-5526.70	599.08
61	64.79	-2249.07	-9.1240	7.6512	-5062.87	591.14
62	63.81	-2256.09	-9.1240	6.6947	-4604.79	582.24
63	62.66	-2263.11	-9.1240	5.7938	-4152.93	571.75
64	61.38	-2270.13	-9.1240	5.0493	-3708.66	559.99
65	59.84	-2277.14	-9.1240	3.9438	-3272.57	546.01
66	57.47	-2284.16	-9.1240	2.6114	-2844.31	524.40
67	54.17	-2291.18	-9.1240	1.7739	-2429.37	494.20
68	43.54	-2298.20	-9.1240	.6454	-2011.98	397.27
69	32.39	-2305.21	-9.1240	.5668	-1667.33	295.57
70	17.94	-2312.23	-9.1240	1.4239	-1389.27	163.68
71	13.79	-2319.25	-9.1240	3.3380	-1248.83	125.86
72	12.05	-2326.27	-9.1240	4.9687	-1145.93	109.96
73	10.80	-2333.28	-9.1240	6.3740	-1056.95	98.52
74	9.58	-2340.30	-9.1240	8.0495	-976.89	87.40
75	8.92	-2347.32	-9.1240	9.1378	-907.36	81.36
76	8.05	-2354.34	-9.1240	10.8099	-841.72	73.42
77	7.49	-2361.35	-9.1240	12.0449	-783.30	68.33
78	6.90	-2368.37	-9.1240	13.5162	-728.66	62.93
79	6.34	-2375.39	-9.1240	15.0650	-678.31	57.84
80	5.85	-2382.41	-9.1240	16.5615	-632.11	53.39
81	5.50	-2389.42	-9.1240	17.7397	-589.82	50.22
82	5.16	-2396.44	-9.1240	19.1319	-549.97	47.04
83	4.77	-2403.46	-9.1240	21.3526	-512.45	43.54
84	4.39	-2410.48	-9.1240	24.4127	-477.62	40.04
85	4.15	-2417.49	-9.1240	26.2162	-445.96	37.82
86	3.90	-2424.51	-9.1240	27.8845	-416.03	35.60
87	3.66	-2431.53	-9.1240	29.3976	-387.79	33.37
88	3.41	-2438.55	-9.1240	30.7358	-361.27	31.15
89	3.17	-2445.56	-9.1240	31.8792	-336.45	28.92
90	2.96	-2452.58	-9.1240	32.6894	-313.48	27.01
91	2.75	-2459.60	-9.1240	33.5553	-291.97	25.11
92	2.54	-2466.62	-9.1240	35.5937	-271.93	23.20
93	2.37	-2473.63	-9.1240	39.1570	-253.47	21.61
94	2.16	-2480.65	-9.1240	47.3723	-220.96	19.70
95	.00	-10000.00	-9.1240	9999.9990	.00	.00

ISOTHERM: T = 81 K.

Point	N	μ	$(\partial\mu/\partial T)_N$	$(\partial\mu/\partial N)_T$	Ω	S
1	526.76	-1595.66	-9.0365	.0356	-73318.84	4957.61
2	510.98	-1596.22	-8.9803	.0585	-72937.58	4815.78
3	495.60	-1596.79	-8.9396	.0814	-72400.01	4678.22
4	480.27	-1597.88	-9.0653	.0748	-71818.92	4540.62
5	463.87	-1599.17	-9.4575	.0568	-71312.73	4389.23
6	448.42	-1599.73	-9.5387	.0256	-71025.88	4243.09
7	432.92	-1599.96	-9.5970	.0214	-70872.11	4095.60
8	417.43	-1600.40	-9.4497	.0234	-70721.33	3946.75
9	401.93	-1600.69	-9.4222	.0613	-70446.04	3799.61
10	386.51	-1602.29	-9.4495	.1369	-69839.70	3653.27
11	371.25	-1604.88	-9.2323	.1550	-68988.07	3509.79
12	340.57	-1608.72	-9.0313	.2697	-66679.43	3227.87
13	325.53	-1613.84	-9.2979	.2267	-65424.82	3089.11
14	310.19	-1615.54	-9.9922	.0683	-64687.75	2940.27
15	294.74	-1615.93	-10.0997	.0222	-64464.89	2784.17
16	279.22	-1616.23	-10.0433	.0457	-64306.44	2627.00
17	263.82	-1617.34	-10.2805	.2781	-63634.25	2469.53
18	248.77	-1624.55	-10.0792	.5452	-62053.91	2315.52
19	236.53	-1631.88	-9.8311	.6946	-60210.51	2192.89
20	224.30	-1641.54	-9.2283	.8923	-58020.06	2075.78
21	212.08	-1653.70	-8.3070	.9946	-55510.50	1969.17
22	199.88	-1665.83	-8.4467	.7175	-53352.71	1867.49
23	187.38	-1671.25	-9.8149	.2290	-52190.45	1753.75
24	174.68	-1671.52	-10.0309	.0172	-51900.99	1628.08
25	161.88	-1671.69	-10.0221	.0131	-51869.96	1500.01
26	149.08	-1671.86	-10.0256	.0086	-51849.72	1372.00
27	143.72	-1671.89	-10.0142	.0058	-51844.63	1318.35
28	136.08	-1671.93	-10.0631	.0035	-51840.39	1241.78
29	128.36	-1671.95	-10.0602	.0046	-51836.99	1164.26
30	120.70	-1672.00	-10.0415	.0166	-51827.72	1087.42
31	113.02	-1672.20	-10.1409	.2107	-51729.16	1009.99
32	105.41	-1675.20	-10.6808	1.2616	-51133.23	930.88
33	98.25	-1690.09	-11.0089	3.7443	-49339.84	853.28
34	93.71	-1711.89	-10.7345	7.2429	-46963.59	803.95
35	89.32	-1753.97	-9.9333	16.1849	-42307.67	758.70
36	84.98	-1852.69	-6.5681	29.9715	-33631.16	722.89
37	80.09	-2039.13	1.6813	22.5532	-22990.74	710.99
38	75.86	-2077.50	-1.2629	9.0778	-17716.96	711.91
39	75.13	-2103.83	-9.1688	30.4380	-16635.92	708.03
40	74.93	-2110.85	-9.1688	29.8418	-16091.80	706.06
41	74.72	-2117.87	-9.1688	29.2027	-15549.17	704.09
42	74.44	-2124.89	-9.1688	28.2844	-15007.82	701.47
43	74.19	-2131.90	-9.1688	27.4190	-14468.59	699.17
44	73.92	-2138.92	-9.1688	26.3600	-13931.01	696.54
45	73.67	-2145.94	-9.1688	25.3723	-13395.57	694.25
46	73.39	-2152.96	-9.1688	24.1744	-12861.76	691.62
47	73.11	-2159.97	-9.1688	22.0526	-12329.98	688.99
48	72.73	-2166.99	-9.1688	20.0958	-11799.83	685.38
49	72.38	-2174.01	-9.1688	18.5707	-11272.57	682.10
50	72.00	-2181.03	-9.1688	17.1420	-10747.71	678.49

T = 81 K (cont.)

Point	N	μ	$(\partial\mu/\partial T)_N$	$(\partial\mu/\partial N)_T$	Ω	S
51	71.55	-2188.04	-9.1688	15.7454	-10225.38	674.22
52	71.13	-2195.06	-9.1688	14.6918	-9706.44	670.28
53	70.54	-2202.08	-9.1688	13.5008	-9189.88	664.70
54	69.94	-2209.10	-9.1688	12.5529	-8677.62	659.12
55	69.46	-2216.11	-9.1688	11.8683	-8170.02	654.53
56	68.86	-2223.13	-9.1688	11.0486	-7665.56	648.95
57	68.10	-2230.15	-9.1688	9.9073	-7164.76	641.73
58	67.30	-2237.17	-9.1688	8.8243	-6669.37	634.18
59	66.53	-2244.18	-9.1688	8.6429	-6179.91	626.96
60	65.66	-2251.20	-9.1688	8.0585	-5695.61	618.75
61	64.79	-2258.22	-9.1688	7.6512	-5217.60	610.54
62	63.81	-2265.24	-9.1688	6.6947	-4745.52	601.35
63	62.66	-2272.25	-9.1688	5.7938	-4279.85	590.52
64	61.38	-2279.27	-9.1688	5.0493	-3822.00	578.38
65	59.84	-2286.29	-9.1688	3.9438	-3372.58	563.93
66	57.47	-2293.31	-9.1688	2.6114	-2931.24	541.61
67	54.17	-2300.32	-9.1688	1.7739	-2503.62	510.43
68	43.54	-2307.34	-9.1688	.6454	-2073.47	410.31
69	32.39	-2314.36	-9.1688	.5668	-1718.28	305.27
70	17.94	-2321.38	-9.1688	1.4239	-1431.73	169.05
71	13.79	-2328.40	-9.1688	3.3380	-1287.00	129.99
72	12.05	-2335.41	-9.1688	4.9687	-1180.95	113.57
73	10.80	-2342.43	-9.1688	6.3740	-1089.25	101.76
74	9.58	-2349.45	-9.1688	8.0495	-1006.75	90.27
75	8.92	-2356.47	-9.1688	9.1378	-935.09	84.03
76	8.05	-2363.48	-9.1688	10.8099	-867.44	75.83
77	7.49	-2370.50	-9.1688	12.0449	-807.24	70.57
78	6.90	-2377.52	-9.1688	13.5162	-750.93	64.99
79	6.34	-2384.53	-9.1688	15.0650	-699.04	59.74
80	5.85	-2391.55	-9.1688	16.5615	-651.43	55.15
81	5.50	-2398.57	-9.1688	17.7397	-607.85	51.86
82	5.16	-2405.59	-9.1688	19.1319	-566.78	48.58
83	4.77	-2412.60	-9.1688	21.3526	-528.11	44.97
84	4.39	-2419.62	-9.1688	24.4127	-492.22	41.36
85	4.15	-2426.64	-9.1688	26.2162	-459.59	39.06
86	3.90	-2433.66	-9.1688	27.8845	-428.74	36.76
87	3.66	-2440.68	-9.1688	29.3976	-399.64	34.47
88	3.41	-2447.69	-9.1688	30.7358	-372.31	32.17
89	3.17	-2454.71	-9.1688	31.8792	-346.74	29.87
90	2.96	-2461.73	-9.1688	32.6894	-323.06	27.90
91	2.75	-2468.75	-9.1688	33.5553	-300.89	25.93
92	2.54	-2475.76	-9.1688	35.5937	-280.24	23.96
93	2.37	-2482.78	-9.1688	39.1570	-261.21	22.32
94	2.16	-2489.80	-9.1688	47.3723	-227.71	20.35
95	.00	-10000.00	-9.1688	9999.9990	.00	.00

ISOTHERM: T = 82 K.

Point	N	μ	$(\partial\mu/\partial T)_N$	$(\partial\mu/\partial N)_T$	Ω	S
1	543.49	-1603.83	-9.1477	.0564	-73624.91	5133.19
2	525.27	-1604.85	-9.0721	.0391	-73161.84	4967.60
3	509.63	-1605.23	-9.0812	.0317	-72878.26	4826.06
4	494.10	-1605.84	-9.1086	.0649	-72507.87	4685.34
5	478.83	-1607.22	-9.1846	.0831	-71963.77	4546.20
6	462.44	-1608.45	-9.0807	.0677	-71387.45	4397.29
7	447.05	-1609.39	-9.3596	.0417	-71010.30	4256.20
8	431.56	-1609.74	-9.5157	.0152	-70824.99	4111.27
9	416.04	-1609.86	-9.4468	.0151	-70714.30	3962.57
10	400.55	-1610.21	-9.4556	.0631	-70458.45	3814.83
11	385.16	-1611.80	-9.2952	.1363	-69848.63	3669.20
12	369.94	-1614.37	-9.2722	.1531	-69006.38	3526.49
13	339.31	-1618.09	-9.2046	.2700	-66713.13	3240.81
14	324.33	-1623.22	-9.2189	.2606	-65383.39	3101.57
15	309.11	-1625.92	-10.0319	.0973	-64499.80	2953.69
16	293.65	-1626.17	-10.1832	.0146	-64222.74	2796.09
17	278.13	-1626.37	-10.1851	.0580	-64052.79	2636.67
18	262.78	-1627.94	-10.2997	.2944	-63323.63	2478.05
19	247.81	-1635.14	-10.0380	.5420	-61729.12	2324.60
20	235.63	-1642.35	-9.7998	.6682	-59943.20	2202.72
21	223.46	-1651.41	-9.2404	.8512	-57890.74	2086.02
22	211.31	-1663.04	-8.6390	.9636	-55502.36	1978.29
23	199.20	-1674.79	-8.5394	.7480	-53369.55	1874.94
24	186.79	-1681.26	-9.5781	.2806	-52122.29	1763.11
25	174.10	-1681.70	-10.1316	.0218	-51768.00	1638.57
26	161.29	-1681.81	-10.1877	.0107	-51734.66	1508.93
27	148.50	-1681.97	-10.2675	.0066	-51719.07	1378.44
28	143.13	-1681.99	-10.3186	.0084	-51713.87	1323.38
29	135.50	-1682.11	-10.4590	.0082	-51705.91	1244.23
30	127.78	-1682.12	-10.4755	.0042	-51700.36	1163.65
31	120.13	-1682.17	-10.4968	.0345	-51683.19	1083.54
32	112.46	-1682.65	-10.6412	.2989	-51539.10	1002.63
33	104.91	-1686.66	-11.0370	1.4200	-50850.94	920.99
34	97.86	-1702.53	-11.2400	3.9456	-48965.20	842.59
35	93.42	-1724.81	-10.9187	7.4713	-46556.86	793.43
36	89.14	-1766.85	-10.0526	16.1099	-41996.23	748.67
37	84.90	-1861.65	-6.4338	28.8760	-33747.81	713.76
38	80.07	-2036.82	1.9449	22.3804	-23511.05	703.00
39	75.85	-2079.86	-3.7805	10.1974	-18097.29	699.19
40	75.13	-2113.02	-9.2137	30.4380	-16997.82	694.51
41	74.93	-2120.04	-9.2137	29.8418	-16441.85	692.58
42	74.72	-2127.06	-9.2137	29.2027	-15887.42	690.65
43	74.44	-2134.08	-9.2137	28.2844	-15334.29	688.07
44	74.19	-2141.09	-9.2137	27.4190	-14783.33	685.82
45	73.92	-2148.11	-9.2137	26.3600	-14234.07	683.24
46	73.67	-2155.13	-9.2137	25.3723	-13686.98	680.98
47	73.39	-2162.15	-9.2137	24.1744	-13141.55	678.41
48	73.11	-2169.17	-9.2137	22.0526	-12598.20	675.83
49	72.73	-2176.18	-9.2137	20.0958	-12056.52	672.29
50	72.38	-2183.20	-9.2137	18.5707	-11517.79	669.07

T = 82 K (cont.)

Point	N	μ	$(\partial\mu/\partial T)_N$	$(\partial\mu/\partial N)_T$	Ω	S
51	72.00	-2190.22	-9.2137	17.1420	-10981.52	665.53
52	71.55	-2197.24	-9.2137	15.7454	-10447.82	661.35
53	71.13	-2204.25	-9.2137	14.6918	-9917.59	657.48
54	70.54	-2211.27	-9.2137	13.5008	-9389.80	652.01
55	69.94	-2218.29	-9.2137	12.5529	-8866.39	646.53
56	69.46	-2225.30	-9.2137	11.8683	-8347.75	642.03
57	68.86	-2232.32	-9.2137	11.0486	-7832.32	636.55
58	68.10	-2239.34	-9.2137	9.9073	-7320.62	629.47
59	67.30	-2246.36	-9.2137	8.8243	-6814.46	622.06
60	66.53	-2253.38	-9.2137	8.6429	-6314.34	614.98
61	65.66	-2260.39	-9.2137	8.0585	-5819.51	606.93
62	64.79	-2267.41	-9.2137	7.6512	-5331.10	598.88
63	63.81	-2274.43	-9.2137	6.6947	-4848.75	589.87
64	62.66	-2281.45	-9.2137	5.7938	-4372.95	579.24
65	61.38	-2288.46	-9.2137	5.0493	-3905.15	567.33
66	59.84	-2295.48	-9.2137	3.9438	-3445.95	553.16
67	57.47	-2302.50	-9.2137	2.6114	-2995.00	531.27
68	54.17	-2309.52	-9.2137	1.7739	-2558.08	500.68
69	43.54	-2316.53	-9.2137	.6454	-2118.58	402.47
70	32.39	-2323.55	-9.2137	.5668	-1755.66	299.44
71	17.94	-2330.57	-9.2137	1.4239	-1462.87	165.82
72	13.79	-2337.59	-9.2137	3.3380	-1315.00	127.50
73	12.05	-2344.60	-9.2137	4.9687	-1206.64	111.40
74	10.80	-2351.62	-9.2137	6.3740	-1112.95	99.81
75	9.58	-2358.64	-9.2137	8.0495	-1028.65	88.54
76	8.92	-2365.66	-9.2137	9.1378	-955.43	82.43
77	8.05	-2372.67	-9.2137	10.8099	-886.31	74.38
78	7.49	-2379.69	-9.2137	12.0449	-824.80	69.23
79	6.90	-2386.71	-9.2137	13.5162	-767.27	63.75
80	6.34	-2393.73	-9.2137	15.0650	-714.24	58.60
81	5.85	-2400.74	-9.2137	16.5615	-665.60	54.09
82	5.50	-2407.76	-9.2137	17.7397	-621.07	50.87
83	5.16	-2414.78	-9.2137	19.1319	-579.11	47.65
84	4.77	-2421.80	-9.2137	21.3526	-539.60	44.11
85	4.39	-2428.81	-9.2137	24.4127	-502.93	40.57
86	4.15	-2435.83	-9.2137	26.2162	-469.59	38.32
87	3.90	-2442.85	-9.2137	27.8845	-438.07	36.06
88	3.66	-2449.87	-9.2137	29.3976	-408.34	33.81
89	3.41	-2456.88	-9.2137	30.7358	-380.41	31.55
90	3.17	-2463.90	-9.2137	31.8792	-354.28	29.30
91	2.96	-2470.92	-9.2137	32.6894	-330.09	27.37
92	2.75	-2477.94	-9.2137	33.5553	-307.44	25.44
93	2.54	-2484.95	-9.2137	35.5937	-286.33	23.50
94	2.37	-2491.97	-9.2137	39.1570	-266.90	21.89
95	2.16	-2498.99	-9.2137	47.3723	-232.66	19.96
96	.00	-10000.00	-9.2137	9999.9990	.00	.00

ISOTHERM: T = 83 K.

Point	N	μ	$(\partial\mu/\partial T)_N$	$(\partial\mu/\partial N)_T$	Ω	S
1	523.45	-1614.29	-9.4165	.0110	-73039.77	4973.66
2	507.78	-1614.46	-9.1848	.0296	-72878.95	4828.73
3	492.29	-1615.21	-9.2391	.0672	-72508.62	4686.89
4	477.04	-1616.52	-9.1628	.0742	-71989.12	4547.58
5	460.64	-1617.53	-8.9646	.0655	-71455.28	4400.36
6	445.28	-1618.59	-9.1176	.0501	-71056.69	4263.15
7	429.82	-1619.07	-9.2859	.0241	-70900.16	4121.80
8	414.33	-1619.34	-9.4419	.0233	-70731.23	3974.24
9	398.86	-1619.79	-9.4675	.0629	-70448.70	3825.56
10	383.49	-1621.27	-9.2543	.1339	-69847.42	3679.23
11	368.31	-1623.86	-9.2524	.1563	-69007.34	3536.40
12	337.77	-1627.75	-9.2964	.2767	-66673.73	3248.33
13	322.89	-1632.95	-9.3442	.2721	-65311.57	3107.31
14	307.74	-1635.88	-9.8107	.1126	-64369.85	2959.80
15	292.31	-1636.35	-10.1450	.0271	-64027.66	2803.43
16	276.81	-1636.72	-10.2571	.0731	-63795.63	2642.91
17	261.51	-1638.58	-10.2511	.3049	-63017.21	2483.61
18	246.65	-1645.76	-9.9897	.5377	-61425.55	2330.83
19	234.54	-1652.81	-9.7438	.6543	-59683.14	2209.48
20	222.45	-1661.59	-9.3376	.8193	-57741.21	2093.75
21	210.38	-1672.61	-8.6941	.9323	-55461.23	1986.40
22	198.36	-1684.05	-8.6316	.7536	-53387.58	1883.49
23	186.02	-1690.83	-9.3368	.3177	-52104.26	1773.72
24	173.37	-1691.83	-10.0925	.0494	-51678.74	1651.72
25	160.58	-1692.08	-10.2556	.0226	-51602.89	1522.31
26	147.79	-1692.41	-10.4199	.0255	-51557.45	1390.81
27	142.44	-1692.55	-10.5299	.0323	-51535.73	1334.96
28	134.81	-1692.87	-10.7412	.0236	-51507.00	1254.21
29	127.10	-1692.91	-10.7789	.0104	-51490.49	1171.52
30	119.45	-1693.03	-10.8221	.0585	-51459.51	1089.17
31	111.80	-1693.80	-10.9154	.3819	-51270.26	1006.31
32	104.33	-1698.70	-11.1544	1.5777	-50497.11	924.17
33	97.42	-1715.51	-11.2943	4.1632	-48526.51	846.78
34	93.09	-1738.24	-10.9102	7.7335	-46088.99	798.80
35	88.93	-1780.26	-10.0421	16.0071	-41638.09	755.41
36	84.80	-1870.80	-6.1993	27.9266	-33792.23	721.91
37	80.05	-2036.24	1.1198	22.5588	-23889.03	709.99
38	75.84	-2085.26	-5.2786	11.6508	-18231.93	701.34
39	75.13	-2122.26	-9.2585	30.4380	-17110.02	696.20
40	74.93	-2129.28	-9.2585	29.8418	-16550.39	694.26
41	74.72	-2136.30	-9.2585	29.2027	-15992.30	692.33
42	74.44	-2143.31	-9.2585	28.2844	-15435.52	689.74
43	74.19	-2150.33	-9.2585	27.4190	-14880.92	687.48
44	73.92	-2157.35	-9.2585	26.3600	-14328.03	684.90
45	73.67	-2164.37	-9.2585	25.3723	-13777.33	682.64
46	73.39	-2171.38	-9.2585	24.1744	-13228.30	680.06
47	73.11	-2178.40	-9.2585	22.0526	-12681.36	677.48
48	72.73	-2185.42	-9.2585	20.0958	-12136.11	673.93
49	72.38	-2192.44	-9.2585	18.5707	-11593.82	670.70
50	72.00	-2199.45	-9.2585	17.1420	-11054.01	667.15

T = 83 K (cont.)

Point	N	μ	$(\partial\mu/\partial T)_N$	$(\partial\mu/\partial N)_T$	Ω	S
51	71.55	-2206.47	-9.2585	15.7454	-10516.78	662.95
52	71.13	-2213.49	-9.2585	14.6918	-9983.05	659.08
53	70.54	-2220.51	-9.2585	13.5008	-9451.78	653.59
54	69.94	-2227.52	-9.2585	12.5529	-8924.92	648.11
55	69.46	-2234.54	-9.2585	11.8683	-8402.85	643.59
56	68.86	-2241.56	-9.2585	11.0486	-7884.02	638.10
57	68.10	-2248.58	-9.2585	9.9073	-7368.94	631.00
58	67.30	-2255.59	-9.2585	8.8243	-6859.44	623.58
59	66.53	-2262.61	-9.2585	8.6429	-6356.02	616.48
60	65.66	-2269.63	-9.2585	8.0585	-5857.92	608.41
61	64.79	-2276.65	-9.2585	7.6512	-5366.30	600.34
62	63.81	-2283.66	-9.2585	6.6947	-4880.76	591.30
63	62.66	-2290.68	-9.2585	5.7938	-4401.82	580.65
64	61.38	-2297.70	-9.2585	5.0493	-3930.92	568.71
65	59.84	-2304.72	-9.2585	3.9438	-3468.70	554.51
66	57.47	-2311.73	-9.2585	2.6114	-3014.77	532.56
67	54.17	-2318.75	-9.2585	1.7739	-2574.97	501.90
68	43.54	-2325.77	-9.2585	.6454	-2132.56	403.45
69	32.39	-2332.79	-9.2585	.5668	-1767.25	300.17
70	17.94	-2339.80	-9.2585	1.4239	-1472.53	166.22
71	13.79	-2346.82	-9.2585	3.3380	-1323.68	127.81
72	12.05	-2353.84	-9.2585	4.9687	-1214.61	111.68
73	10.80	-2360.86	-9.2585	6.3740	-1120.29	100.06
74	9.58	-2367.88	-9.2585	8.0495	-1035.44	88.76
75	8.92	-2374.89	-9.2585	9.1378	-961.73	82.63
76	8.05	-2381.91	-9.2585	10.8099	-892.16	74.56
77	7.49	-2388.93	-9.2585	12.0449	-830.24	69.39
78	6.90	-2395.95	-9.2585	13.5162	-772.33	63.91
79	6.34	-2402.96	-9.2585	15.0650	-718.96	58.74
80	5.85	-2409.98	-9.2585	16.5615	-669.99	54.22
81	5.50	-2417.00	-9.2585	17.7397	-625.17	51.00
82	5.16	-2424.01	-9.2585	19.1319	-582.93	47.77
83	4.77	-2431.03	-9.2585	21.3526	-543.16	44.22
84	4.39	-2438.05	-9.2585	24.4127	-506.25	40.67
85	4.15	-2445.07	-9.2585	26.2162	-472.69	38.41
86	3.90	-2452.08	-9.2585	27.8845	-440.96	36.15
87	3.66	-2459.10	-9.2585	29.3976	-411.03	33.89
88	3.41	-2466.12	-9.2585	30.7358	-382.92	31.63
89	3.17	-2473.14	-9.2585	31.8792	-356.62	29.37
90	2.96	-2480.16	-9.2585	32.6894	-332.27	27.43
91	2.75	-2487.17	-9.2585	33.5553	-309.47	25.50
92	2.54	-2494.19	-9.2585	35.5937	-288.22	23.56
93	2.37	-2501.21	-9.2585	39.1570	-268.66	21.95
94	2.16	-2508.23	-9.2585	47.3723	-234.20	20.01
95	.00	-10000.00	-9.2585	9999.9990	.00	.00

ISOTHERM: T = 84 K.

Point	N	μ	$(\partial\mu/\partial T)_N$	$(\partial\mu/\partial N)_T$	Ω	S
1	521.63	-1623.73	-9.3074	.0000	-73090.05	5020.83
2	505.94	-1623.69	-9.4655	.0276	-72983.64	4873.69
3	490.48	-1624.57	-9.4341	.0695	-72615.90	4727.73
4	475.24	-1625.82	-9.3993	.0653	-72124.24	4584.43
5	458.83	-1626.60	-9.6981	.0635	-71636.53	4427.97
6	443.51	-1627.80	-9.5626	.0585	-71221.62	4280.67
7	428.08	-1628.39	-9.6633	.0331	-70986.81	4132.01
8	412.61	-1628.82	-9.7313	.0314	-70761.16	3981.65
9	397.16	-1629.36	-9.5800	.0626	-70453.24	3832.15
10	381.81	-1630.75	-9.4019	.1315	-69861.12	3686.06
11	366.68	-1633.36	-9.4918	.1594	-69023.82	3542.83
12	336.23	-1637.42	-9.4983	.2835	-66651.39	3253.03
13	321.44	-1642.68	-9.4982	.2838	-65257.36	3112.29
14	306.36	-1645.85	-10.0276	.1280	-64258.33	2964.72
15	290.96	-1646.53	-10.3612	.0396	-63851.96	2807.42
16	275.49	-1647.07	-10.4446	.0883	-63558.78	2646.11
17	260.25	-1649.22	-10.4178	.3154	-62732.14	2486.76
18	245.48	-1656.37	-10.0581	.5334	-61143.89	2335.23
19	233.45	-1663.27	-9.8651	.6402	-59444.91	2215.12
20	221.43	-1671.76	-9.4142	.7872	-57605.28	2097.67
21	209.44	-1682.17	-8.8591	.9006	-55432.71	1988.33
22	197.51	-1693.30	-8.5830	.7591	-53417.97	1884.57
23	185.26	-1700.41	-9.2314	.3551	-52099.43	1775.62
24	172.65	-1701.97	-10.2366	.0773	-51603.14	1653.02
25	159.86	-1702.35	-10.4346	.0344	-51485.03	1521.01
26	147.09	-1702.85	-10.6244	.0448	-51409.86	1386.64
27	141.74	-1703.10	-10.7589	.0565	-51371.59	1329.51
28	134.13	-1703.63	-10.9766	.0389	-51322.29	1246.86
29	126.42	-1703.69	-11.0532	.0167	-51294.98	1161.97
30	118.77	-1703.89	-11.1226	.0826	-51250.29	1077.25
31	111.14	-1704.95	-11.1704	.4666	-51015.93	992.29
32	103.76	-1710.73	-11.3085	1.7408	-50158.07	909.31
33	96.98	-1728.49	-11.4215	4.3918	-48103.15	832.32
34	92.76	-1751.68	-11.0341	8.0107	-45636.72	784.96
35	88.73	-1793.68	-10.2505	15.9018	-41294.39	742.06
36	84.69	-1879.96	-5.8309	26.9446	-33846.74	709.65
37	80.03	-2035.67	2.1725	22.7011	-24284.34	701.14
38	75.83	-2090.67	-4.6260	13.1140	-18390.17	696.01
39	75.13	-2131.54	-9.3034	30.4380	-17246.76	691.20
40	74.93	-2138.56	-9.3034	29.8418	-16682.65	689.27
41	74.72	-2145.58	-9.3034	29.2027	-16120.10	687.35
42	74.44	-2152.59	-9.3034	28.2844	-15558.87	684.79
43	74.19	-2159.61	-9.3034	27.4190	-14999.84	682.54
44	73.92	-2166.63	-9.3034	26.3600	-14442.53	679.98
45	73.67	-2173.65	-9.3034	25.3723	-13887.43	677.74
46	73.39	-2180.66	-9.3034	24.1744	-13334.02	675.17
47	73.11	-2187.68	-9.3034	22.0526	-12782.71	672.61
48	72.73	-2194.70	-9.3034	20.0958	-12233.09	669.08
49	72.38	-2201.72	-9.3034	18.5707	-11686.48	665.88
50	72.00	-2208.73	-9.3034	17.1420	-11142.35	662.36

T = 84 K (cont.)

Point	N	μ	$(\partial\mu/\partial T)_N$	$(\partial\mu/\partial N)_T$	Ω	S
51	71.55	-2215.75	-9.3034	15.7454	-10600.83	658.19
52	71.13	-2222.77	-9.3034	14.6918	-10062.84	654.34
53	70.54	-2229.79	-9.3034	13.5008	-9527.32	648.90
54	69.94	-2236.80	-9.3034	12.5529	-8996.24	643.45
55	69.46	-2243.82	-9.3034	11.8683	-8470.00	638.96
56	68.86	-2250.84	-9.3034	11.0486	-7947.02	633.52
57	68.10	-2257.86	-9.3034	9.9073	-7427.83	626.47
58	67.30	-2264.88	-9.3034	8.8243	-6914.26	619.10
59	66.53	-2271.89	-9.3034	8.6429	-6406.82	612.05
60	65.66	-2278.91	-9.3034	8.0585	-5904.74	604.03
61	64.79	-2285.93	-9.3034	7.6512	-5409.18	596.02
62	63.81	-2292.95	-9.3034	6.6947	-4919.76	587.05
63	62.66	-2299.96	-9.3034	5.7938	-4437.00	576.48
64	61.38	-2306.98	-9.3034	5.0493	-3962.34	564.62
65	59.84	-2314.00	-9.3034	3.9438	-3496.42	550.52
66	57.47	-2321.01	-9.3034	2.6114	-3038.87	528.73
67	54.17	-2328.03	-9.3034	1.7739	-2595.55	498.29
68	43.54	-2335.05	-9.3034	.6454	-2149.60	400.55
69	32.39	-2342.07	-9.3034	.5668	-1781.37	298.01
70	17.94	-2349.08	-9.3034	1.4239	-1484.30	165.03
71	13.79	-2356.10	-9.3034	3.3380	-1334.25	126.90
72	12.05	-2363.12	-9.3034	4.9687	-1224.31	110.87
73	10.80	-2370.14	-9.3034	6.3740	-1129.25	99.34
74	9.58	-2377.16	-9.3034	8.0495	-1043.72	88.12
75	8.92	-2384.17	-9.3034	9.1378	-969.42	82.03
76	8.05	-2391.19	-9.3034	10.8099	-899.29	74.02
77	7.49	-2398.21	-9.3034	12.0449	-836.88	68.90
78	6.90	-2405.23	-9.3034	13.5162	-778.51	63.45
79	6.34	-2412.24	-9.3034	15.0650	-724.71	58.32
80	5.85	-2419.26	-9.3034	16.5615	-675.35	53.83
81	5.50	-2426.28	-9.3034	17.7397	-630.17	50.63
82	5.16	-2433.30	-9.3034	19.1319	-587.59	47.43
83	4.77	-2440.31	-9.3034	21.3526	-547.50	43.90
84	4.39	-2447.33	-9.3034	24.4127	-510.29	40.38
85	4.15	-2454.35	-9.3034	26.2162	-476.47	38.13
86	3.90	-2461.37	-9.3034	27.8845	-444.48	35.89
87	3.66	-2468.38	-9.3034	29.3976	-414.32	33.65
88	3.41	-2475.40	-9.3034	30.7358	-385.98	31.40
89	3.17	-2482.42	-9.3034	31.8792	-359.47	29.16
90	2.96	-2489.44	-9.3034	32.6894	-334.92	27.24
91	2.75	-2496.45	-9.3034	33.5553	-311.94	25.32
92	2.54	-2503.47	-9.3034	35.5937	-290.53	23.39
93	2.37	-2510.49	-9.3034	39.1570	-270.80	21.79
94	2.16	-2517.51	-9.3034	47.3723	-236.07	19.87
95	.00	-10000.00	-9.3034	9999.9990	.00	.00

ISOTHERM: T = 85 K.

Point	N	μ	$(\partial\mu/\partial T)_N$	$(\partial\mu/\partial N)_T$	Ω	S
1	519.35	-1632.95	-9.3009	.0369	-73373.84	5047.18
2	503.78	-1633.53	-9.6757	.0449	-73051.25	4899.09
3	488.32	-1634.35	-9.5837	.0675	-72625.24	4749.96
4	473.12	-1635.59	-9.5992	.0902	-72054.34	4603.74
5	456.88	-1637.20	-9.9773	.0717	-71447.09	4444.20
6	441.49	-1637.91	-9.8551	.0426	-71057.09	4291.00
7	426.08	-1638.51	-9.8247	.0326	-70827.25	4139.05
8	410.61	-1638.91	-9.8064	.0209	-70642.59	3988.17
9	395.12	-1639.16	-9.6704	.0534	-70401.81	3838.25
10	379.80	-1640.55	-9.6836	.1410	-69819.07	3690.88
11	364.77	-1643.41	-9.7198	.1723	-68933.77	3545.97
12	334.41	-1647.54	-9.7289	.2885	-66494.00	3252.57
13	319.74	-1652.85	-9.6694	.2983	-65075.91	3111.11
14	304.76	-1656.34	-10.1128	.1452	-64019.73	2963.86
15	289.40	-1657.19	-10.4192	.0486	-63560.93	2807.05
16	273.95	-1657.84	-10.5752	.1010	-63227.66	2645.80
17	258.77	-1660.25	-10.4678	.3192	-62380.24	2487.02
18	244.09	-1667.21	-10.0947	.5293	-60815.13	2336.95
19	232.16	-1674.06	-9.8505	.6261	-59168.16	2218.62
20	220.22	-1682.16	-9.3876	.7596	-57421.82	2100.80
21	208.31	-1692.17	-8.5830	.8623	-55358.19	1993.45
22	196.47	-1702.64	-8.3110	.7437	-53429.39	1893.05
23	184.31	-1709.93	-9.2371	.4039	-52088.89	1786.06
24	171.78	-1712.47	-10.2781	.1229	-51490.96	1663.59
25	159.01	-1713.00	-10.6179	.0493	-51306.57	1529.94
26	146.25	-1713.72	-10.8975	.0737	-51188.27	1392.55
27	140.92	-1714.16	-11.0636	.0875	-51126.80	1333.93
28	133.33	-1714.89	-11.3212	.0581	-51050.80	1248.87
29	125.63	-1715.04	-11.4358	.0320	-51005.66	1161.11
30	117.99	-1715.38	-11.5203	.1116	-50940.24	1073.41
31	110.39	-1716.73	-11.5225	.5485	-50660.32	985.78
32	103.10	-1723.32	-11.5134	1.9148	-49720.22	901.75
33	96.49	-1742.05	-11.5792	4.6566	-47581.48	825.33
34	92.39	-1765.74	-11.1824	8.3338	-45085.81	778.70
35	88.49	-1807.72	-10.3514	15.6583	-40881.05	736.67
36	84.56	-1888.86	-5.3541	25.7159	-33870.61	705.71
37	79.98	-2033.53	3.0220	22.7938	-24734.84	700.35
38	75.82	-2094.88	-5.1450	14.7139	-18608.63	695.89
39	.00	-10000.00	-10.0000	9999.9990	.00	.00

ISOTHERM: T = 86 K.

Point	N	μ	$(\partial\mu/\partial T)_N$	$(\partial\mu/\partial N)_T$	Ω	S
1	516.81	-1642.48	-9.4893	.0510	-73479.38	5034.82
2	501.30	-1643.27	-9.5878	.0505	-73081.63	4886.79
3	485.86	-1644.05	-9.5217	.0693	-72630.00	4739.23
4	470.71	-1645.38	-9.5420	.0910	-72055.02	4594.80
5	454.49	-1646.91	-9.5658	.0725	-71446.48	4439.80
6	439.14	-1647.70	-9.6185	.0414	-71061.51	4292.54
7	423.71	-1648.18	-9.6676	.0272	-70843.62	4143.71
8	408.25	-1648.55	-9.7478	.0246	-70665.96	3993.70
9	392.80	-1648.94	-9.8630	.0712	-70361.27	3842.22
10	377.58	-1650.71	-9.7623	.1502	-69706.37	3693.00
11	362.60	-1653.46	-9.8324	.1704	-68808.10	3546.29
12	332.38	-1657.81	-9.8257	.2918	-66387.39	3249.36
13	317.82	-1663.10	-9.7405	.2992	-64978.21	3106.93
14	302.91	-1666.58	-10.0703	.1492	-63922.09	2959.34
15	287.58	-1667.54	-10.4672	.0638	-63424.18	2801.99
16	272.20	-1668.54	-10.6023	.1192	-63022.67	2640.02
17	257.09	-1671.14	-10.3196	.3278	-62130.42	2482.08
18	242.53	-1678.10	-9.9889	.5215	-60585.84	2334.30
19	230.68	-1684.70	-9.5151	.6078	-58929.11	2221.04
20	218.83	-1692.51	-8.7794	.7054	-57194.90	2112.48
21	206.95	-1701.44	-8.3737	.8110	-55291.09	2010.52
22	195.23	-1711.63	-8.6753	.7729	-53429.70	1910.45
23	183.23	-1719.72	-9.4996	.4641	-52020.56	1801.32
24	170.78	-1722.78	-10.2927	.1592	-51327.22	1677.99
25	158.04	-1723.68	-10.7859	.0778	-51080.58	1543.69
26	145.32	-1724.76	-11.1075	.1080	-50906.71	1404.41
27	140.01	-1725.39	-11.2649	.1236	-50820.62	1344.96
28	132.45	-1726.38	-11.6385	.0812	-50716.57	1258.31
29	124.75	-1726.61	-11.7192	.0467	-50654.72	1168.40
30	117.13	-1727.10	-11.7786	.1444	-50569.89	1078.85
31	109.57	-1728.79	-11.7424	.6411	-50242.09	989.92
32	102.40	-1736.23	-11.6556	2.1072	-49217.71	905.97
33	95.97	-1755.95	-11.7195	4.9605	-46994.55	830.79
34	92.01	-1780.18	-11.3380	8.6710	-44476.15	785.18
35	88.24	-1821.99	-10.3811	15.4285	-40408.33	744.25
36	84.40	-1898.28	-8.3369	24.4941	-33819.35	708.27
37	79.93	-2031.90	3.3424	23.1119	-25072.57	697.09
38	75.80	-2101.49	-5.0125	16.8370	-18618.54	693.63
39	.00	-10000.00	-10.0000	9999.9990	.00	.00

ISOTHERM: T = 87 K.

Point	N	μ	$(\partial\mu/\partial T)_N$	$(\partial\mu/\partial N)_T$	Ω	S
1	529.04	-1651.43	-9.8932	.0497	-73919.22	5190.27
2	513.96	-1652.18	-9.6709	.0506	-73528.22	5043.02
3	498.47	-1652.98	-9.6857	.0505	-73135.62	4893.32
4	483.05	-1653.74	-9.6833	.0720	-72677.88	4744.24
5	467.96	-1655.16	-9.6071	.0948	-72086.36	4599.05
6	451.79	-1656.70	-9.6874	.0682	-71485.92	4443.49
7	436.43	-1657.35	-9.6080	.0422	-71116.94	4295.85
8	421.06	-1658.00	-9.8813	.0383	-70846.43	4146.25
9	405.65	-1658.53	-9.8180	.0393	-70587.66	3993.71
10	390.27	-1659.21	-9.9956	.0732	-70233.70	3840.57
11	375.05	-1660.76	-9.8470	.1554	-69561.61	3688.92
12	360.22	-1663.84	-9.9601	.1874	-68617.16	3541.25
13	330.12	-1668.25	-9.9475	.2960	-66107.80	3240.18
14	315.68	-1673.56	-9.7572	.3032	-64700.61	3097.25
15	300.86	-1677.07	-10.1030	.1619	-63619.01	2949.34
16	285.61	-1678.37	-10.5309	.0782	-63065.81	2791.28
17	270.26	-1679.47	-10.5603	.1208	-62632.39	2628.73
18	255.20	-1682.01	-10.0782	.3271	-61746.38	2472.56
19	240.77	-1688.92	-9.3613	.4989	-60266.36	2331.59
20	228.95	-1695.01	-9.1144	.5484	-58791.80	2222.92
21	217.12	-1701.89	-8.9376	.6939	-57165.68	2116.54
22	205.46	-1711.27	-9.1277	.8657	-55257.22	2011.57
23	193.94	-1721.94	-9.4272	.8028	-53341.96	1905.01
24	182.04	-1729.98	-9.7883	.4801	-51900.78	1790.96
25	169.66	-1733.40	-10.4353	.1920	-51162.38	1665.98
26	156.98	-1734.74	-10.8785	.1078	-50852.22	1531.00
27	144.30	-1736.13	-11.2817	.1380	-50622.01	1390.70
28	139.01	-1736.92	-11.4679	.1659	-50509.59	1330.60
29	131.49	-1738.34	-11.8896	.1087	-50370.86	1242.91
30	123.80	-1738.55	-12.0107	.0551	-50291.17	1151.03
31	116.20	-1739.18	-12.0697	.1788	-50187.71	1059.58
32	108.68	-1741.23	-11.9669	.7422	-49807.98	969.36
33	101.65	-1749.55	-11.8097	2.3275	-48692.90	885.76
34	95.42	-1770.34	-11.8588	5.3038	-46382.56	812.15
35	91.61	-1795.12	-11.4244	9.0048	-43848.25	767.84
36	87.97	-1836.58	-10.2960	15.9698	-39791.14	728.34
37	84.28	-1912.82	-12.1091	23.2771	-33567.89	686.95
38	79.85	-2029.88	3.6211	22.3525	-25280.38	668.21
39	75.77	-2105.68	-4.7317	18.5637	-18765.21	665.97
40	.00	-10000.00	-10.0000	9999.9990	.00	.00

ISOTHERM: T = 88 K.

Point	N	μ	$(\partial\mu/\partial T)_N$	$(\partial\mu/\partial N)_T$	Ω	S
1	525.96	-1661.76	-9.9744	.0211	-73666.36	5197.80
2	510.79	-1662.08	-9.8206	.0386	-73439.96	5048.43
3	495.34	-1662.95	-9.8101	.0568	-73079.21	4897.71
4	479.98	-1663.83	-9.8414	.0718	-72608.73	4747.77
5	464.91	-1665.13	-9.6378	.0915	-72041.23	4602.29
6	448.79	-1666.70	-9.6974	.0618	-71492.12	4448.22
7	433.39	-1667.13	-9.7881	.0486	-71137.84	4300.36
8	418.14	-1668.18	-9.8621	.0399	-70818.02	4149.37
9	402.66	-1668.34	-10.0201	.0389	-70542.45	3992.69
10	387.38	-1669.37	-10.0238	.0948	-70117.61	3836.93
11	372.29	-1671.21	-10.0142	.1657	-69350.64	3683.10
12	357.54	-1674.28	-9.8738	.1907	-68368.96	3533.85
13	327.61	-1678.91	-9.6755	.2893	-65881.83	3236.06
14	313.26	-1683.99	-9.4232	.2967	-64511.71	3096.52
15	298.53	-1687.49	-9.8187	.1676	-63434.37	2952.16
16	283.34	-1688.94	-10.4207	.0876	-62841.39	2795.82
17	268.05	-1690.16	-10.4164	.1202	-62380.50	2633.82
18	253.01	-1692.56	-10.0397	.2975	-61548.03	2477.40
19	238.60	-1698.75	-9.5619	.4913	-60138.15	2333.69
20	226.96	-1705.05	-9.6942	.6052	-58626.22	2221.01
21	215.40	-1712.79	-10.0328	.7487	-56916.24	2108.62
22	203.92	-1722.29	-10.0302	.8688	-54987.05	1994.81
23	192.53	-1732.65	-9.8489	.7890	-53124.16	1882.71
24	180.72	-1740.49	-10.0253	.4829	-51722.26	1766.39
25	168.41	-1744.11	-10.5559	.2102	-50975.68	1640.54
26	155.76	-1745.68	-11.0171	.1388	-50622.90	1504.94
27	143.16	-1747.61	-11.4513	.1881	-50323.54	1364.00
28	137.91	-1748.68	-11.6792	.2150	-50177.48	1303.52
29	130.44	-1750.41	-12.0981	.1388	-50002.49	1215.06
30	122.76	-1750.74	-12.3265	.0760	-49900.31	1121.59
31	115.18	-1751.56	-12.3632	.2184	-49772.60	1028.36
32	107.73	-1753.99	-12.1825	.8565	-49337.54	937.13
33	100.85	-1763.25	-11.9795	2.5703	-48131.45	854.30
34	94.85	-1785.08	-12.0173	5.6593	-45744.97	782.49
35	91.19	-1810.30	-11.3872	9.3453	-43204.78	739.78
36	87.69	-1851.34	-10.1730	16.7650	-39132.09	702.06
37	84.16	-1928.47	-13.0905	22.2362	-33238.57	661.13
38	79.75	-2028.51	3.4011	21.7165	-25302.20	639.90
39	75.74	-2112.03	-5.4124	20.8158	-18665.81	635.98
40	.00	-10000.00	-10.0000	9999.9990	.00	.00

ISOTHERM: T = 89 K.

Point	N	μ	$(\partial\mu/\partial T)_N$	$(\partial\mu/\partial N)_T$	Ω	S
1	522.34	-1671.58	-9.9342	.0333	-73706.17	5211.79
2	507.24	-1672.09	-9.9652	.0449	-73410.29	5062.72
3	491.83	-1672.96	-9.8540	.0592	-73019.34	4911.37
4	476.51	-1673.91	-9.7952	.0673	-72561.39	4762.52
5	461.43	-1675.01	-9.6511	.0837	-72041.44	4617.92
6	445.36	-1676.53	-9.5975	.0693	-71500.70	4465.96
7	430.05	-1677.22	-9.9526	.0477	-71129.59	4319.74
8	414.76	-1677.99	-9.8662	.0531	-70789.59	4163.67
9	399.48	-1678.84	-10.1168	.0587	-70415.80	4007.11
10	384.21	-1679.79	-10.0789	.0968	-69926.48	3849.05
11	369.22	-1681.75	-9.8180	.1627	-69171.50	3696.08
12	354.50	-1684.60	-9.7698	.1778	-68240.42	3548.23
13	324.65	-1688.95	-9.6587	.2867	-65858.45	3250.59
14	310.44	-1693.98	-9.5369	.3006	-64509.72	3110.60
15	295.83	-1697.57	-9.9000	.1936	-63384.13	2964.85
16	280.83	-1699.67	-10.4821	.1091	-62699.04	2808.20
17	265.56	-1700.86	-10.4626	.1273	-62180.63	2644.40
18	250.63	-1703.48	-10.2562	.3269	-61290.93	2485.94
19	236.47	-1710.14	-10.4303	.5280	-59802.39	2335.87
20	225.02	-1716.73	-10.5509	.6313	-58288.08	2216.16
21	213.62	-1724.56	-10.4995	.7652	-56562.36	2098.52
22	202.31	-1734.09	-10.3357	.8566	-54670.10	1982.56
23	191.01	-1743.93	-10.0891	.7536	-52888.54	1868.77
24	179.27	-1751.34	-10.1893	.4713	-51556.51	1751.11
25	167.02	-1755.07	-10.6946	.2346	-50807.24	1624.45
26	154.46	-1757.12	-11.1842	.1743	-50399.10	1488.10
27	141.93	-1759.44	-11.6237	.2369	-50025.84	1346.11
28	136.72	-1760.79	-11.8645	.2674	-49845.52	1285.34
29	129.31	-1762.87	-12.3685	.1743	-49629.68	1196.04
30	121.65	-1763.36	-12.6273	.0973	-49501.06	1100.80
31	114.11	-1764.34	-12.6506	.2573	-49348.29	1005.80
32	106.72	-1767.16	-12.4004	.9898	-48852.18	913.65
33	100.03	-1777.45	-12.0525	2.8526	-47547.39	832.24
34	94.28	-1800.39	-12.0797	5.9969	-45100.20	763.04
35	90.76	-1825.82	-11.1711	9.7184	-42554.62	722.28
36	87.39	-1866.61	-9.5930	17.7145	-38460.72	687.44
37	84.03	-1944.72	-13.2588	21.3643	-32857.17	649.27
38	79.62	-2027.81	3.1908	21.0348	-25197.55	627.22
39	75.70	-2117.96	-5.3623	23.0003	-18504.60	623.12
40	.00	-10000.00	-10.0000	9999.9990	.00	.00

ISOTHERM: T = 90 K.

Point	N	μ	$(\partial\mu/\partial T)_N$	$(\partial\mu/\partial N)_T$	Ω	S
1	518.42	-1681.86	-10.3252	.0321	-73598.59	5269.63
2	503.33	-1682.34	-10.1663	.0397	-73328.19	5116.51
3	487.91	-1683.07	-9.9950	.0517	-72986.56	4962.72
4	472.59	-1683.93	-9.8595	.0654	-72565.27	4812.77
5	457.57	-1685.05	-9.8705	.0779	-72075.79	4667.12
6	441.48	-1686.36	-9.8389	.0764	-71532.05	4512.08
7	426.33	-1687.45	-9.9886	.0646	-71100.26	4363.38
8	411.07	-1688.21	-10.1460	.0672	-70657.90	4204.98
9	395.80	-1688.97	-10.2263	.0697	-70215.19	4044.76
10	380.65	-1690.18	-10.2134	.0973	-69704.65	3885.29
11	365.65	-1691.90	-10.0116	.1635	-68957.94	3729.06
12	351.11	-1694.96	-10.1102	.1946	-68006.20	3578.29
13	321.53	-1699.76	-10.2406	.2955	-65549.63	3268.27
14	307.48	-1704.80	-10.0834	.3014	-64211.96	3121.23
15	292.96	-1708.31	-10.2633	.1949	-63103.93	2968.99
16	278.04	-1710.50	-10.5663	.1139	-62421.39	2809.12
17	262.82	-1711.72	-10.6479	.1393	-61880.43	2642.95
18	248.03	-1714.63	-10.4863	.3679	-60914.43	2482.14
19	234.19	-1721.94	-10.7102	.5679	-59343.66	2331.24
20	222.92	-1728.70	-10.8445	.6523	-57817.62	2211.87
21	211.70	-1736.61	-10.7694	.7676	-56100.23	2093.20
22	200.52	-1745.89	-10.4872	.8332	-54267.24	1976.58
23	189.33	-1755.25	-10.2440	.7226	-52572.90	1862.32
24	177.66	-1762.30	-10.3480	.4643	-51299.66	1743.78
25	165.49	-1766.17	-10.8068	.2542	-50547.62	1616.51
26	153.00	-1768.53	-11.2336	.2109	-50088.40	1480.13
27	140.57	-1771.43	-11.7721	.2963	-49633.51	1338.31
28	135.43	-1773.08	-12.0410	.3302	-49412.95	1277.45
29	128.10	-1775.59	-12.6586	.2143	-49150.64	1187.49
30	120.46	-1776.21	-12.9631	.1213	-48992.21	1090.23
31	112.95	-1777.42	-13.0032	.3068	-48809.15	993.21
32	105.65	-1780.70	-12.6578	1.1255	-48250.31	899.98
33	99.17	-1791.89	-12.1174	3.1499	-46853.18	820.01
34	93.67	-1815.85	-12.0336	6.3215	-44367.63	753.91
35	90.29	-1841.31	-11.0258	10.0090	-41838.96	715.09
36	87.05	-1881.43	-8.4434	18.8979	-37711.43	683.72
37	83.90	-1960.81	-13.1808	21.0205	-32348.99	649.86
38	79.45	-2027.88	1.0503	20.7049	-24767.39	623.09
39	75.65	-2124.73	-5.5615	25.5091	-17981.94	614.70
40	.00	-10000.00	-10.0000	9999.9990	.00	.00

ISOTHERM: T = 91 K.

Point	N	μ	$(\partial\mu/\partial T)_N$	$(\partial\mu/\partial N)_T$	Ω	S
1	513.93	-1692.47	-10.5204	.0379	-73544.79	5318.47
2	499.02	-1692.73	-10.3877	.0419	-73256.02	5163.81
3	483.59	-1693.38	-10.1852	.0460	-72938.41	5006.63
4	468.27	-1694.14	-10.1914	.0683	-72541.77	4852.45
5	453.37	-1695.43	-10.2378	.0853	-72037.79	4702.46
6	437.35	-1696.78	-10.2628	.0707	-71511.91	4541.47
7	422.17	-1697.65	-10.3077	.0620	-71075.05	4385.03
8	407.04	-1698.72	-10.5844	.0684	-70627.38	4223.11
9	391.92	-1699.79	-10.5051	.0748	-70155.95	4059.69
10	376.80	-1700.95	-10.5284	.1063	-69592.26	3896.71
11	361.98	-1702.96	-10.5369	.1774	-68780.99	3736.71
12	347.57	-1706.10	-10.6250	.2025	-67774.43	3580.57
13	318.23	-1711.09	-10.6006	.2936	-65294.87	3261.50
14	304.31	-1716.00	-10.1940	.2894	-63995.20	3113.09
15	289.81	-1719.24	-10.4384	.1879	-62924.70	2959.78
16	274.98	-1721.48	-10.6492	.1234	-62230.88	2799.56
17	259.86	-1722.93	-10.7649	.1664	-61607.99	2633.66
18	245.29	-1726.34	-10.6908	.4164	-60511.36	2473.58
19	231.80	-1734.23	-10.9446	.6103	-58832.59	2324.07
20	220.74	-1741.22	-11.0702	.6741	-57289.86	2205.49
21	209.68	-1749.14	-10.9835	.7657	-55600.03	2085.73
22	198.63	-1758.14	-10.7269	.8026	-53848.54	1967.54
23	187.51	-1766.94	-10.4579	.6835	-52262.70	1851.19
24	175.90	-1773.58	-10.5120	.4504	-51070.81	1730.75
25	163.80	-1777.49	-10.9193	.2725	-50332.92	1602.35
26	151.41	-1780.22	-11.3478	.2542	-49827.45	1465.39
27	139.12	-1783.76	-11.9414	.3644	-49287.99	1323.23
28	134.05	-1785.77	-12.2490	.4029	-49025.67	1262.23
29	126.82	-1788.75	-12.9565	.2647	-48713.34	1171.57
30	119.22	-1789.58	-13.3269	.1524	-48520.94	1072.18
31	111.76	-1791.04	-13.3518	.3580	-48307.68	973.06
32	104.55	-1794.75	-12.9257	1.2781	-47685.30	878.72
33	98.29	-1806.90	-12.2891	3.4650	-46203.23	800.07
34	93.05	-1831.75	-11.8169	6.6850	-43683.04	737.14
35	89.81	-1857.31	-11.0752	10.2132	-41189.71	700.19
36	86.68	-1896.34	-7.0554	20.3223	-36996.07	671.93
37	83.76	-1977.14	-12.5258	21.5946	-31781.89	643.45
38	79.27	-2032.26	-2.9012	20.4098	-24099.45	609.04
39	75.60	-2131.68	-5.5442	27.0623	-17370.49	593.67
40	.00	-10000.00	-10.0000	9999.9990	.00	.00

ISOTHERM: T = 92 K.

Point	N	μ	$(\partial\mu/\partial T)_N$	$(\partial\mu/\partial N)_T$	Ω	S
1	509.45	-1703.09	-10.5969	.0202	-73321.04	5343.37
2	494.33	-1703.40	-10.8241	.0244	-73164.92	5182.88
3	478.84	-1703.84	-10.6410	.0508	-72898.99	5018.41
4	463.70	-1704.94	-10.4755	.0813	-72448.65	4860.72
5	448.88	-1706.27	-10.3643	.0841	-71913.00	4708.91
6	432.88	-1707.51	-10.5225	.0747	-71385.23	4545.50
7	417.82	-1708.60	-10.4999	.0815	-70868.80	4384.44
8	402.87	-1709.96	-10.4874	.0642	-70382.63	4223.35
9	387.58	-1710.52	-10.6715	.0715	-69933.93	4057.30
10	372.67	-1712.09	-10.8024	.1294	-69329.73	3893.04
11	358.03	-1714.33	-10.7277	.1938	-68431.01	3731.25
12	343.82	-1717.65	-10.8634	.2143	-67378.00	3573.83
13	314.69	-1722.74	-10.7218	.2685	-65000.15	3251.31
14	300.76	-1727.11	-10.3201	.2731	-63803.25	3100.75
15	286.40	-1730.43	-10.4397	.1885	-62789.54	2947.71
16	271.61	-1732.56	-10.7592	.1275	-62096.41	2786.80
17	256.61	-1734.22	-10.8694	.2005	-61412.01	2620.27
18	242.34	-1738.30	-10.7727	.4785	-60181.74	2461.93
19	229.26	-1746.87	-10.9669	.6502	-58286.83	2316.59
20	218.38	-1753.90	-11.2428	.6863	-56691.11	2198.43
21	207.50	-1761.80	-11.1483	.7630	-55040.15	2078.86
22	196.58	-1770.53	-10.9067	.7715	-53368.81	1960.29
23	185.52	-1778.76	-10.6477	.6425	-51888.98	1842.67
24	173.96	-1784.97	-10.6843	.4369	-50776.66	1720.75
25	161.95	-1788.96	-11.0630	.2925	-50050.71	1591.49
26	149.67	-1792.05	-11.4838	.3028	-49494.27	1454.12
27	137.56	-1796.33	-12.1566	.4473	-48858.55	1311.97
28	132.59	-1798.75	-12.4896	.4874	-48548.93	1251.03
29	125.47	-1802.23	-13.2880	.3174	-48183.11	1159.85
30	117.92	-1803.24	-13.7030	.1834	-47956.48	1058.35
31	110.51	-1804.96	-13.7112	.4179	-47710.51	957.29
32	103.42	-1809.19	-13.1997	1.4497	-47019.72	862.27
33	97.40	-1822.28	-12.3778	3.7313	-45477.68	785.57
34	92.38	-1847.51	-11.6584	7.1513	-42912.15	725.54
35	89.31	-1873.45	-11.1062	10.2828	-40490.25	690.75
36	86.25	-1910.56	-7.8584	22.1771	-36154.60	661.84
37	83.59	-1992.73	-10.9938	23.3657	-31017.60	636.90
38	79.09	-2040.42	-5.6575	20.1454	-23049.62	599.68
39	75.53	-2139.11	-5.7446	27.7031	-16485.89	579.53
40	.00	-10000.00	-10.0000	9999.9990	.00	.00

ISOTHERM: T = 93 K.

Point	N	μ	$(\partial\mu/\partial T)_N$	$(\partial\mu/\partial N)_T$	Ω	S
1	504.31	-1713.94	-10.6990	.0527	-73090.26	5341.23
2	489.45	-1714.72	-10.8784	.0381	-72767.17	5182.40
3	473.93	-1715.07	-10.8949	.0351	-72510.02	5015.47
4	458.66	-1715.80	-10.6930	.0624	-72184.64	4853.02
5	443.82	-1716.94	-10.6198	.0891	-71703.71	4697.83
6	428.06	-1718.55	-10.6519	.0755	-71204.84	4532.91
7	412.89	-1719.31	-10.6434	.0587	-70735.49	4367.05
8	397.85	-1720.32	-10.4296	.0852	-70257.91	4204.15
9	383.03	-1721.84	-10.7844	.1128	-69647.23	4042.72
10	368.30	-1723.65	-10.7518	.1413	-68906.04	3879.76
11	353.79	-1725.97	-10.7861	.2049	-67963.67	3719.27
12	339.78	-1729.45	-10.9484	.2232	-66887.54	3563.00
13	310.80	-1734.39	-11.0586	.2623	-64529.46	3235.64
14	296.98	-1738.62	-10.4781	.2524	-63410.91	3082.76
15	282.56	-1741.45	-10.4995	.1829	-62459.73	2927.39
16	267.98	-1743.92	-10.7140	.1528	-61745.16	2768.44
17	253.15	-1745.94	-10.9991	.2422	-60947.59	2603.20
18	239.25	-1750.69	-10.8578	.5310	-59601.03	2447.21
19	226.54	-1759.64	-10.9834	.7012	-57731.46	2307.43
20	215.94	-1767.04	-10.7729	.7138	-56098.58	2194.71
21	205.22	-1774.86	-10.7413	.7521	-54466.47	2081.53
22	194.41	-1783.24	-10.6934	.7339	-52878.48	1967.44
23	183.39	-1790.86	-10.6666	.6000	-51501.80	1851.33
24	171.87	-1796.67	-10.8104	.4237	-50462.59	1729.03
25	159.96	-1800.73	-11.1832	.3154	-49740.91	1599.29
26	147.81	-1804.24	-11.6115	.3626	-49120.17	1461.98
27	135.93	-1809.40	-12.2761	.5362	-48378.54	1321.07
28	131.07	-1812.21	-12.7030	.5770	-48020.63	1260.63
29	124.09	-1816.23	-13.6189	.3775	-47598.32	1169.31
30	116.58	-1817.46	-14.1299	.2199	-47331.11	1065.64
31	109.25	-1819.47	-14.1257	.4821	-47048.29	962.44
32	102.28	-1824.21	-13.4965	1.6190	-46292.05	866.63
33	96.49	-1838.09	-12.4828	4.0579	-44683.23	791.78
34	91.73	-1863.94	-11.8419	7.5979	-42092.20	734.07
35	88.81	-1890.01	-10.7163	11.2089	-39622.73	701.28
36	85.95	-1928.38	-11.4690	22.5356	-35437.11	669.74
37	83.38	-2007.32	-6.2745	23.0234	-30483.26	647.06
38	78.91	-2050.34	-6.8081	20.0136	-22649.86	617.97
39	75.45	-2147.15	-5.8582	28.0384	-16272.91	596.26
40	.00	-10000.00	-10.0000	9999.9990	.00	.00

ISOTHERM: T = 94 K.

Point	N	μ	$(\partial\mu/\partial T)_N$	$(\partial\mu/\partial N)_T$	Ω	S
1	498.72	-1724.94	-10.9020	.0406	-72921.20	5322.82
2	483.80	-1725.54	-10.8345	.0379	-72658.70	5162.37
3	468.41	-1726.08	-10.9258	.0494	-72371.38	4997.05
4	453.30	-1727.04	-10.8278	.0784	-71967.18	4835.33
5	438.65	-1728.40	-10.9038	.0838	-71485.80	4679.34
6	422.73	-1729.58	-10.8300	.0699	-70966.35	4506.65
7	407.73	-1730.57	-10.8821	.0638	-70482.65	4339.31
8	392.69	-1731.50	-10.7667	.0872	-69962.45	4172.02
9	378.02	-1733.15	-10.6676	.1151	-69326.76	4010.43
10	363.33	-1734.88	-10.7988	.1617	-68510.14	3848.38
11	349.21	-1737.76	-10.8245	.2328	-67458.35	3691.49
12	335.41	-1741.35	-11.0010	.2378	-66285.91	3536.83
13	306.85	-1746.77	-10.7928	.2159	-64073.07	3217.03
14	292.76	-1750.00	-10.5101	.2140	-63102.37	3062.78
15	278.47	-1752.84	-10.4167	.1772	-62238.33	2908.98
16	263.90	-1755.10	-11.0262	.1751	-61477.14	2748.40
17	249.47	-1757.91	-11.1997	.3018	-60535.97	2583.69
18	235.97	-1763.33	-11.0186	.5934	-59023.11	2429.76
19	223.69	-1772.76	-10.4679	.6755	-57266.00	2297.77
20	212.98	-1779.14	-10.6083	.6790	-55718.14	2187.39
21	202.52	-1787.10	-10.5441	.7732	-54172.67	2078.83
22	191.90	-1795.44	-10.5729	.7328	-52621.12	1968.55
23	181.01	-1802.83	-10.7097	.5866	-51299.48	1854.20
24	169.57	-1808.43	-10.9464	.4239	-50301.71	1731.79
25	157.78	-1812.63	-11.3011	.3449	-49575.06	1601.86
26	145.81	-1816.63	-11.6897	.4241	-48895.17	1465.34
27	134.18	-1822.57	-12.2941	.6652	-48030.54	1326.86
28	129.47	-1826.00	-12.7614	.7040	-47611.15	1268.26
29	122.66	-1830.57	-13.3878	.4478	-47120.21	1179.61
30	115.22	-1832.09	-13.4656	.2620	-46810.80	1080.24
31	107.96	-1834.40	-13.3076	.5472	-46493.24	983.49
32	101.13	-1839.61	-11.8838	1.8001	-45675.31	897.83
33	95.58	-1854.25	-11.8250	4.3945	-44011.45	832.45
34	91.06	-1880.58	-11.7933	7.8761	-41444.04	779.29
35	88.25	-1906.28	-9.7792	12.5099	-38888.76	749.15
36	85.67	-1946.64	-11.9609	21.1926	-35115.15	721.16
37	83.05	-2017.05	2.1758	20.5785	-30496.72	708.47
38	78.70	-2061.25	-7.2505	20.3694	-23308.07	697.66
39	75.36	-2155.53	-5.8987	28.2120	-17079.23	675.84
40	.00	-10000.00	-10.0000	9999.9990	.00	.00

ISOTHERM: T = 95 K.

Point	N	μ	$(\partial\mu/\partial T)_N$	$(\partial\mu/\partial N)_T$	Ω	S
1	492.75	-1736.23	-10.9010	.0369	-72701.07	5298.96
2	477.83	-1736.79	-11.0403	.0407	-72439.45	5136.89
3	462.55	-1737.46	-11.0778	.0481	-72144.94	4969.92
4	447.39	-1738.25	-10.9900	.0790	-71738.27	4805.09
5	432.91	-1739.77	-10.8789	.0900	-71237.41	4649.86
6	417.05	-1740.93	-11.0347	.0634	-70629.80	4474.26
7	402.00	-1741.75	-11.0621	.0614	-70203.11	4303.99
8	387.07	-1742.77	-10.9630	.0904	-69716.16	4135.69
9	372.48	-1744.40	-10.7412	.1438	-69029.77	3973.59
10	358.30	-1746.88	-11.0719	.1916	-68123.45	3815.17
11	344.33	-1749.79	-10.9365	.2404	-67027.16	3657.84
12	330.75	-1753.48	-11.1033	.2337	-65902.58	3504.66
13	301.93	-1757.87	-10.5640	.2340	-63690.32	3184.89
14	288.23	-1761.61	-10.4939	.2128	-62748.56	3037.15
15	273.76	-1763.77	-10.7349	.2102	-61847.75	2879.70
16	259.93	-1767.48	-11.2048	.2397	-60980.68	2724.40
17	245.68	-1770.47	-11.2847	.3452	-59892.88	2560.45
18	232.65	-1776.58	-10.9978	.5720	-58436.96	2411.87
19	220.25	-1784.89	-10.4746	.7075	-56782.84	2278.59
20	210.11	-1792.37	-10.6318	.7442	-55216.82	2173.66
21	199.79	-1800.11	-10.5343	.7566	-53644.42	2066.23
22	189.30	-1808.12	-10.5206	.7069	-52160.86	1957.24
23	178.49	-1815.14	-10.6743	.5646	-50903.88	1844.05
24	167.13	-1820.54	-10.9846	.4231	-49940.08	1722.32
25	155.46	-1824.85	-11.3158	.3748	-49196.16	1593.28
26	143.69	-1829.33	-11.6125	.4932	-48443.48	1459.23
27	132.36	-1836.14	-12.0093	.7841	-47460.95	1326.27
28	127.81	-1840.05	-11.8154	.7670	-47004.27	1272.38
29	121.01	-1844.34	-10.9066	.3779	-46518.92	1195.55
30	113.44	-1845.06	-11.0347	.2266	-46252.23	1112.99
31	106.26	-1847.58	-11.0195	.5089	-45968.92	1034.20
32	99.39	-1852.12	-10.9447	2.4579	-44946.71	959.10
33	94.57	-1870.05	-11.4860	5.2783	-43156.67	905.27
34	90.40	-1897.64	-11.3529	8.2259	-40570.39	857.91
35	87.69	-1922.82	-10.2897	14.2481	-37864.75	828.64
36	85.39	-1965.25	-12.4828	18.4899	-34614.95	802.57
37	82.45	-2019.68	8.4304	16.3720	-30313.83	796.75
38	78.49	-2073.04	-7.2947	21.6296	-24277.17	799.17
39	75.26	-2164.42	-6.0483	28.2851	-18097.70	777.75
40	.00	-10000.00	-10.0000	9999.9990	.00	.00

ISOTHERM: T = 96 K.

Point	N	μ	$(\partial\mu/\partial T)_N$	$(\partial\mu/\partial N)_T$	Ω	S
1	471.26	-1748.01	-10.9305	.0596	-72291.73	5097.37
2	456.17	-1748.91	-11.1123	.0660	-71880.09	4933.31
3	441.24	-1749.99	-11.0919	.0766	-71437.63	4770.41
4	426.64	-1751.17	-10.9371	.0818	-70953.40	4611.96
5	410.94	-1752.47	-11.2040	.0732	-70392.68	4433.94
6	396.02	-1753.42	-11.2662	.0670	-69922.20	4262.30
7	381.16	-1754.46	-11.0303	.0913	-69418.48	4092.62
8	366.67	-1756.09	-10.6676	.1677	-68673.98	3931.50
9	352.94	-1759.11	-11.1157	.2153	-67686.04	3778.29
10	339.12	-1762.02	-10.8140	.2446	-66543.69	3623.11
11	325.74	-1765.74	-11.4932	.2353	-65432.58	3470.24
12	296.99	-1769.87	-10.6488	.2021	-63374.96	3144.19
13	283.18	-1773.04	-10.6843	.2261	-62474.11	2993.21
14	269.27	-1776.13	-11.1626	.2312	-61551.01	2837.55
15	255.42	-1779.46	-11.0364	.2515	-60630.00	2680.03
16	241.59	-1783.09	-10.7067	.3911	-59488.10	2526.00
17	228.93	-1789.54	-10.4652	.6241	-57783.70	2390.87
18	216.99	-1798.29	-10.9910	.6857	-56084.39	2265.46
19	206.75	-1804.89	-9.9995	.7079	-54603.12	2159.90
20	196.68	-1812.64	-10.1534	.7626	-53134.95	2059.96
21	186.35	-1820.45	-10.4126	.6950	-51712.91	1955.11
22	175.66	-1827.21	-10.7234	.5571	-50517.11	1843.38
23	164.43	-1832.57	-11.0377	.4339	-49585.27	1722.40
24	152.92	-1837.05	-11.2343	.4071	-48831.66	1595.14
25	141.35	-1841.97	-11.2384	.5488	-48037.28	1466.12
26	130.30	-1849.34	-11.4312	.6505	-47151.88	1341.58
27	125.63	-1852.35	-10.9241	.4660	-46821.72	1289.65
28	118.28	-1853.72	-9.1171	.1881	-46531.81	1216.47
29	110.88	-1855.12	-9.1588	.3535	-46310.98	1149.29
30	103.97	-1858.62	-9.5283	1.1437	-45770.07	1085.05
31	98.19	-1868.31	-11.7384	3.0617	-44562.57	1023.90
32	93.67	-1887.04	-11.0657	5.5549	-42711.13	972.59
33	89.67	-1914.31	-9.8367	9.4108	-39980.08	930.89
34	87.24	-1941.03	-9.8623	15.6873	-37292.91	907.05
35	85.09	-1983.67	-12.8046	16.1535	-34346.82	882.79
36	81.60	-2019.16	12.0487	15.1693	-29789.55	881.62
37	78.26	-2085.65	-6.1899	24.2422	-24566.33	891.52
38	75.14	-2173.88	-6.1242	28.2642	-18292.88	872.43
39	.00	-10000.00	-10.0000	9999.9990	.00	.00

Heat Capacities and Specific Heats

The data for thirteen runs plotted in Fig. 6 are listed in the following tables. Each run is identified by N_{TOT} (not to be confused with the N_{tot} of the first isotherm tables) which was the total charge of methane in the entire system. However, at any given time only a certain fraction of N_{TOT} was on the surface, and this coverage is listed as N. (Recall that one nominal monolayer is 90.9 STPCC.) Although N changes from point to point, corrections have been applied (see Chap. 2) to make each point locally isosteric. That is, at each listed N and T, the heat capacity is $C = T(\partial S / \partial T)_N$.

Heat capacities are listed in both J/K and STPCC-k_B. (They differ only by the conversion factor 1 J/K = 2695.8 STPCC-k_B.) Should heat capacities at intermediate temperatures and coverages be desired, they can be obtained either by (a) differentiating the entropy from the preceding isotherm tables, or (b) using the tables beginning on p. 154.

HEAT CAPACITIES AND SPECIFIC HEATS

N_{TOT} = 45.05 STPCC

Point	T (K)	N (STPCC)	C (STPCC-k_B)	C (J/K)	C/Nk_B
1	67.5578	45.05	434.56	.1612	9.6462
2	68.7057	45.05	370.94	.1376	8.2340
3	69.8619	45.05	335.63	.1245	7.4501
4	71.0027	45.05	319.18	.1184	7.0850
5	72.1556	45.05	313.52	.1163	6.9594
6	73.2973	45.05	358.00	.1328	7.9467
7	74.4319	45.05	266.08	.0987	5.9062
8	75.5746	45.05	309.21	.1147	6.8620
9	76.7108	45.05	274.43	.1018	6.0918
10	77.8244	45.05	253.94	.0942	5.6371
11	78.9252	45.05	164.71	.0611	3.6564
12	80.0326	45.05	260.95	.0968	5.7950
13	81.1581	45.05	230.22	.0854	5.1091
14	82.2865	45.05	208.39	.0773	4.6263
15	83.4203	45.05	193.83	.0719	4.3006
16	84.5552	45.05	210.81	.0782	4.6787
17	85.6805	45.05	242.62	.0900	5.3868
18	86.8203	45.05	205.69	.0763	4.5660
19	87.9783	45.04	198.14	.0735	4.3981
20	89.1380	45.04	127.51	.0473	2.8317
21	90.2797	45.04	307.59	.1141	6.8268
22	91.4526	45.04	85.19	.0316	1.8919
23	92.6167	45.03	219.98	.0816	4.8877
24	93.7716	45.03	217.01	.0805	4.8208
25	94.9128	45.02	235.88	.0875	5.2389
26	96.0486	45.02	250.98	.0931	5.5732
27	97.1881	45.01	268.23	.0995	5.9575

HEAT CAPACITIES (cont.)

N_{TOT} = 83.56 STPCC

Point	T (K)	N (STPCC)	C (STPCC-k_B)	C (J/K)	C/Nk_B
1	67.4798	83.56	330.24	.1225	3.9527
2	68.6162	83.56	204.88	.0760	2.4527
3	69.7507	83.56	282.52	.1048	3.3799
4	70.8943	83.55	265.27	.0984	3.1750
5	72.0257	83.55	325.92	.1209	3.8997
6	73.1664	83.54	317.30	.1177	3.7973
7	74.2968	83.54	340.48	.1263	4.0743
8	75.4154	83.53	363.39	.1348	4.3505
9	76.5406	83.51	268.23	.0995	3.2121
10	77.6519	83.47	405.72	.1505	4.8608
11	78.7221	83.43	272.55	.1011	3.2667
12	79.8421	83.40	427.28	.1585	5.1233
13	80.9602	83.38	283.33	.1051	3.3979
14	82.0877	83.37	301.93	.1120	3.6214
15	83.2179	83.26	307.59	.1141	3.6945
16	84.3579	83.23	313.79	.1164	3.7700
17	85.5040	83.16	365.01	.1354	4.3891
18	86.6458	83.08	329.16	.1221	3.9620
19	87.7706	82.98	371.75	.1379	4.4801
20	88.8810	82.88	405.99	.1506	4.8984
21	89.9799	82.75	478.50	.1775	5.7824
22	91.0800	82.54	491.44	.1823	5.9542
23	92.1702	82.24	381.19	.1414	4.6353
24	93.2479	81.78	221.33	.0821	2.7065
25	94.3322	81.22	136.41	.0506	1.6794
26	95.4420	80.66	686.62	.2547	8.5120
27	96.6067	80.23	614.64	.2280	7.6612

HEAT CAPACITIES (cont.)

N_{TOT} = 99.44 STPCC

Point	T (K)	N (STPCC)	C (STPCC-k_B)	C (J/K)	C/Nk_B
1	67.7552	99.28	459.63	.1705	4.6297
2	68.9160	99.19	571.51	.2120	5.7615
3	70.0771	99.15	486.05	.1803	4.9024
4	71.1629	99.03	553.72	.2054	5.5913
5	72.2263	98.92	549.94	.2040	5.5592
6	73.3029	98.81	472.84	.1754	4.7856
7	74.3953	98.66	582.02	.2159	5.8995
8	75.5214	98.45	738.38	.2739	7.5002
9	76.6760	98.22	556.95	.2066	5.6707
10	78.1623	97.89	491.98	.1825	5.0258
11	79.2951	97.59	498.99	.1851	5.1134
12	80.4441	97.18	478.50	.1775	4.9239
13	81.5542	96.80	612.22	.2271	6.3248
14	82.7904	96.31	473.92	.1758	4.9209
15	84.0075	95.79	567.47	.2105	5.9240
16	85.1071	95.29	569.89	.2114	5.9809
17	86.2398	94.70	500.34	.1856	5.2832
18	87.3845	94.12	474.19	.1759	5.0383
19	88.5072	93.52	584.72	.2169	6.2523
20	89.6375	92.89	402.75	.1494	4.3357
21	90.7768	92.17	575.55	.2135	6.2446
22	91.9163	91.45	580.68	.2154	6.3496
23	93.0539	90.73	620.84	.2303	6.8431
24	94.2024	89.98	566.93	.2103	6.3004
25	95.3516	89.21	796.34	.2954	8.9261
26	96.4796	88.44	820.33	.3043	9.2759

HEAT CAPACITIES (cont.)

N_{TOT} = 121.94 STPCC

Point	T (K)	N (STPCC)	C (STPCC-k_B)	C (J/K)	C/Nk_B
1	67.6822	121.76	636.48	.2361	5.2275
2	68.8355	121.67	598.20	.2219	4.9166
3	69.9927	121.59	655.62	.2432	5.3921
4	71.1400	121.53	577.71	.2143	4.7538
5	72.2641	121.40	616.80	.2288	5.0806
6	73.3779	121.25	627.04	.2326	5.1715
7	74.4695	121.03	693.36	.2572	5.7289
8	75.5585	120.81	744.04	.2760	6.1588
9	76.6587	120.53	780.70	.2896	6.4770
10	77.7732	120.18	884.22	.3280	7.3572
11	78.9312	119.77	753.21	.2794	6.2887
12	80.0339	119.30	830.31	.3080	6.9601
13	81.1312	118.76	823.03	.3053	6.9303
14	82.2515	118.11	613.56	.2276	5.1947
15	83.3608	117.33	523.79	.1943	4.4641
16	84.4600	116.54	621.38	.2305	5.3321
17	85.5820	115.57	617.07	.2289	5.3394
18	86.7068	114.52	602.78	.2236	5.2634
19	87.8451	113.33	576.09	.2137	5.0832
20	88.9783	112.05	633.51	.2350	5.6536
21	90.0907	110.68	632.97	.2348	5.7191
22	91.2052	109.21	618.15	.2293	5.6604
23	92.4218	107.50	582.02	.2159	5.4144
24	93.5423	105.88	641.33	.2379	6.0573
25	94.6575	104.25	660.74	.2451	6.3381
26	95.7755	102.59	723.01	.2682	7.0475

HEAT CAPACITIES (cont.)

N_{TOT} = 160.57 STPCC

Point	T (K)	N (STPCC)	C (STPCC-k_B)	C (J/K)	C/Nk_B
1	67.2741	160.40	863.46	.3203	5.3833
2	68.4309	160.33	837.05	.3105	5.2208
3	69.5836	160.24	824.11	.3057	5.1428
4	70.7123	160.16	822.22	.3050	5.1337
5	71.8420	160.07	857.53	.3181	5.3572
6	72.9722	159.90	842.44	.3125	5.2685
7	74.0924	159.75	942.99	.3498	5.9030
8	75.1920	159.50	1036.27	.3844	6.4969
9	76.2999	159.26	1143.02	.4240	7.1772
10	77.4232	158.93	1158.65	.4298	7.2904
11	78.5826	158.51	1188.04	.4407	7.4950
12	79.6961	158.07	1239.26	.4597	7.8398
13	80.8072	157.53	1296.41	.4809	8.2294
14	81.9211	156.90	1240.34	.4601	7.9054
15	83.0347	156.11	1141.67	.4235	7.3131
16	84.1563	155.21	1060.26	.3933	6.8312
17	85.2707	154.21	950.27	.3525	6.1621
18	86.3800	153.02	986.66	.3660	6.4480
19	87.5211	151.64	910.91	.3379	6.0070
20	88.6553	150.10	971.30	.3603	6.4709
21	89.7857	148.38	816.02	.3027	5.4995
22	90.7986	146.66	844.05	.3131	5.7551
23	91.9340	144.59	839.74	.3115	5.8076
24	93.0646	142.28	812.51	.3014	5.7106
25	94.1988	139.79	756.44	.2806	5.4113
26	95.3177	137.05	756.44	.2806	5.5193

HEAT CAPACITIES (cont.)

N_{TOT} = 177.55 STPCC

Point	T (K)	N (STPCC)	C (STPCC-k_B)	C (J/K)	C/Nk_B
1	68.6102	177.28	698.21	.2590	3.9384
2	69.8132	177.17	806.31	.2991	4.5511
3	70.8397	177.06	974.53	.3615	5.5040
4	71.8655	176.95	910.91	.3379	5.1479
5	72.9851	176.80	1013.35	.3759	5.7315
6	74.1579	176.54	1012.81	.3757	5.7371
7	75.3881	176.27	1141.13	.4233	6.4737
8	76.5728	175.94	1023.60	.3797	5.8180
9	78.0961	175.35	1053.25	.3907	6.0067
10	79.3137	174.74	1122.26	.4163	6.4224
11	80.4294	174.11	1114.17	.4133	6.3992
12	81.5237	173.36	1148.95	.4262	6.6277
13	82.5899	172.50	1272.15	.4719	7.3748
14	83.6640	171.55	1080.75	.4009	6.2999
15	84.7703	170.41	1180.76	.4380	6.9289
16	85.8759	169.11	1004.45	.3726	5.9396
17	86.9916	167.65	1109.32	.4115	6.6167
18	88.1194	166.05	1255.16	.4656	7.5590
19	89.2448	164.28	1112.56	.4127	6.7723
20	90.3627	162.39	1083.98	.4021	6.6750
21	91.4857	160.27	1013.89	.3761	6.3263
22	92.5826	158.04	1083.17	.4018	6.8537
23	93.6718	155.65	1036.54	.3845	6.6592
24	94.7489	153.09	946.76	.3512	6.1845
25	95.8104	150.36	984.78	.3653	6.5494

HEAT CAPACITIES (cont.)

N_{TOT} = 198.96 STPCC

Point	T (K)	N (STPCC)	C (STPCC-k_B)	C (J/K)	C/Nk_B
1	67.5727	198.61	996.10	.3695	5.0153
2	68.7634	198.46	988.01	.3665	4.9783
3	69.9100	198.35	993.40	.3685	5.0084
4	71.0603	198.13	1058.10	.3925	5.3405
5	72.2178	197.89	1079.40	.4004	5.4544
6	73.3762	197.59	1169.17	.4337	5.9170
7	74.5340	197.23	1173.48	.4353	5.9497
8	75.6793	196.79	1193.43	.4427	6.0645
9	76.8064	196.31	1278.62	.4743	6.5131
10	77.9477	195.69	1191.27	.4419	6.0875
11	79.1187	194.97	1209.07	.4485	6.2014
12	80.2406	194.15	1270.80	.4714	6.5453
13	81.3354	193.22	1421.50	.5273	7.3569
14	82.4123	192.20	1455.73	.5400	7.5740
15	83.4899	191.00	1497.79	.5556	7.8418
16	84.6008	189.62	1444.68	.5359	7.6187
17	85.6916	188.11	1532.83	.5686	8.1486
18	86.7592	186.43	1544.15	.5728	8.2829
19	87.8313	184.58	1583.78	.5875	8.5803
20	88.9188	182.56	1562.49	.5796	8.5588
21	90.0407	180.32	1452.50	.5388	8.0549
22	91.0959	178.11	1475.95	.5475	8.2869
23	92.1473	175.74	1352.21	.5016	7.6942
24	93.2513	173.14	1357.07	.5034	7.8380
25	94.3595	170.42	1470.83	.5456	8.6308
26	95.4745	167.54	1437.94	.5334	8.5829
27	96.5850	164.53	1481.61	.5496	9.0050

HEAT CAPACITIES (cont.)

N_{TOT} = 237.39 STPCC

Point	T (K)	N (STPCC)	C (STPCC-k_B)	C (J/K)	C/Nk_B
1	67.3977	236.97	1220.12	.4526	5.1489
2	68.5652	236.84	1317.98	.4889	5.5649
3	69.7107	236.68	1277.27	.4738	5.3965
4	70.8394	236.47	1260.83	.4677	5.3318
5	71.9726	236.27	1278.62	.4743	5.4117
6	73.0920	235.92	1344.93	.4989	5.7007
7	74.2089	235.54	1380.79	.5122	5.8622
8	75.3359	235.09	1582.97	.5872	6.7334
9	76.4439	234.57	1675.98	.6217	7.1449
10	77.5184	233.93	1762.24	.6537	7.5331
11	78.1802	233.49	1714.53	.6360	7.3431
12	79.3134	232.62	1546.58	.5737	6.6486
13	80.4384	231.68	1568.15	.5817	6.7687
14	81.5737	230.53	1477.84	.5482	6.4106
15	82.7084	229.20	1339.27	.4968	5.8433
16	83.8478	227.68	1304.50	.4839	5.7296
17	84.9840	225.91	1330.38	.4935	5.8889
18	86.0953	223.93	1411.79	.5237	6.3047
19	87.1971	221.76	1400.20	.5194	6.3141
20	88.2815	219.33	1575.16	.5843	7.1817
21	89.3635	216.63	1542.27	.5721	7.1194
22	90.4425	213.61	1427.43	.5295	6.6825
23	91.5095	210.33	1511.53	.5607	7.1865
24	92.5721	206.75	1464.63	.5433	7.0841
25	93.6352	202.93	1471.37	.5458	7.2507
26	94.7073	198.83	1221.47	.4531	6.1434
27	95.7944	194.56	1339.00	.4967	6.8822

HEAT CAPACITIES (cont.)

N_{TOT} = 276.38 STPCC

Point	T (K)	N (STPCC)	C (STPCC-k_B)	C (J/K)	C/Nk_B
1	66.8133	275.96	1299.38	.4820	4.7085
2	68.0746	275.85	1336.58	.4958	4.8453
3	69.2842	275.66	1303.15	.4834	4.7273
4	70.4526	275.46	1397.77	.5185	5.0743
5	71.5752	275.26	1426.35	.5291	5.1819
6	72.6886	274.97	1542.81	.5723	5.6109
7	73.7888	274.59	1570.57	.5826	5.7198
8	74.8636	274.18	2035.33	.7550	7.4234
9	75.9156	273.70	2116.47	.7851	7.7329
10	76.9572	273.11	2025.35	.7513	7.4158
11	78.1572	272.32	1860.91	.6903	6.8335
12	79.2206	271.45	1799.99	.6677	6.6310
13	80.2556	270.48	1678.14	.6225	6.2043
14	81.2917	269.34	1704.28	.6322	6.3276
15	82.3519	268.00	1599.96	.5935	5.9699
16	83.3931	266.52	1772.76	.6576	6.6516
17	84.4281	264.85	1762.51	.6538	6.6548
18	85.4919	262.88	1660.61	.6160	6.3170
19	86.6242	260.57	1755.24	.6511	6.7361
20	87.7231	258.07	1818.86	.6747	7.0480
21	88.6538	255.68	1880.86	.6977	7.3562
22	89.7126	252.74	1941.25	.7201	7.6807
23	90.7763	249.50	2057.16	.7631	8.2453
24	91.8427	245.89	1982.76	.7355	8.0637
25	92.8933	241.99	2044.22	.7583	8.4477
26	93.9404	237.71	1955.26	.7253	8.2255
27	94.9703	233.10	1772.49	.6575	7.6040
28	95.9969	228.09	1608.04	.5965	7.0499

HEAT CAPACITIES (cont.)

N_{TOT} = 437.36 STPCC

Point	T (K)	N (STPCC)	C (STPCC-k_B)	C (J/K)	C/Nk_B
1	64.1236	437.14	2066.60	.7666	4.7275
2	65.2884	437.07	2131.30	.7906	4.8763
3	66.3974	437.01	2327.01	.8632	5.3248
4	67.5249	436.86	2157.99	.8005	4.9398
5	68.6351	436.72	2122.40	.7873	4.8599
6	69.7350	436.50	2233.20	.8284	5.1161
7	70.8724	436.25	2192.49	.8133	5.0258
8	71.9973	435.99	2305.99	.8554	5.2891
9	73.1194	435.59	2359.09	.8751	5.4158
10	74.2438	435.10	2403.04	.8914	5.5230
11	75.3495	434.57	2661.29	.9872	6.1239
12	76.4313	433.89	2892.32	1.0729	6.6661
13	77.4972	433.14	2934.11	1.0884	6.7741
14	78.5521	432.26	3075.64	1.1409	7.1152
15	79.6028	431.23	2873.18	1.0658	6.6627
16	80.6743	430.00	2547.53	.9450	5.9245
17	81.7643	428.55	2196.00	.8146	5.1242
18	82.8579	426.88	2207.86	.8190	5.1721
19	83.9326	424.90	2272.29	.8429	5.3478
20	85.0130	422.68	2188.45	.8118	5.1776
21	86.0356	420.22	2267.44	.8411	5.3958
22	87.0437	417.57	2557.24	.9486	6.1241
23	88.0390	414.55	3093.97	1.1477	7.4634
24	89.0046	411.25	5005.83	1.8569	12.1723
25	89.9322	407.73	7797.87	2.8926	19.1252
26	90.9206	403.71	3856.88	1.4307	9.5536
27	91.9247	399.29	3119.85	1.1573	7.8135
28	92.9292	394.50	2821.15	1.0465	7.1513
29	93.9334	389.26	2615.47	.9702	6.7190
30	94.9397	383.61	2449.40	.9086	6.3851
31	95.9567	377.49	2694.45	.9995	7.1379
32	96.9229	371.16	2427.84	.9006	6.5412
33	97.8904	364.42	2380.39	.8830	6.5320
34	98.8645	357.17	2548.88	.9455	7.1363
35	99.8454	349.59	2692.03	.9986	7.7005
36	100.8383	341.43	2683.40	.9954	7.8593
37	101.8418	332.76	2567.48	.9524	7.7156
38	102.8416	323.74	2505.75	.9295	7.7401
39	103.8254	314.53	2451.83	.9095	7.7952
40	104.8108	304.98	2471.24	.9167	8.1030

HEAT CAPACITIES (cont.)

N_{TOT} = 477.18 STPCC

Point	T (K)	N (STPCC)	C (STPCC-k_B)	C (J/K)	C/Nk_B
1	63.9640	476.99	2420.83	.8980	5.0752
2	65.0900	476.92	2315.42	.8589	4.8549
3	66.2301	476.82	2400.07	.8903	5.0335
4	67.4077	476.68	2382.55	.8838	4.9982
5	68.5913	476.49	2282.80	.8468	4.7909
6	69.7511	476.29	2343.73	.8694	4.9208
7	70.8807	476.07	2411.12	.8944	5.0646
8	72.0082	475.76	2563.44	.9509	5.3881
9	73.1416	475.33	2549.15	.9456	5.3629
10	74.2141	474.93	2728.15	1.0120	5.7443
11	75.2808	474.39	3010.40	1.1167	6.3459
12	76.3581	473.72	3188.59	1.1828	6.7309
13	77.5722	472.83	3158.40	1.1716	6.6798
14	78.6360	471.91	2855.93	1.0594	6.0519
15	79.7120	470.74	2898.79	1.0753	6.1579
16	80.7965	469.43	2538.63	.9417	5.4079
17	81.8766	467.89	2467.74	.9154	5.2742
18	82.9474	466.14	2386.86	.8854	5.1205
19	83.9848	464.11	2494.42	.9253	5.3746
20	85.0331	461.85	2409.24	.8937	5.2165
21	86.7490	457.46	2813.07	1.0435	6.1493
22	87.7431	454.44	3235.50	1.2002	7.1198
23	88.7195	451.20	4088.45	1.5166	9.0613
24	89.6355	447.74	9354.69	3.4701	20.8930
25	90.5558	443.99	6167.72	2.2879	13.8916
26	91.5358	439.69	4221.08	1.5658	9.6001
27	92.5413	434.99	3502.11	1.2991	8.0511
28	93.5404	429.83	3193.44	1.1846	7.4296
29	94.5351	424.30	2557.24	.9486	6.0269
30	95.4733	418.70	3240.89	1.2022	7.7403
31	96.4284	412.48	2722.22	1.0098	6.5997
32	97.4245	405.53	3051.65	1.1320	7.5250
33	98.4318	397.93	2494.96	.9255	6.2698
34	99.4446	389.79	2410.04	.8940	6.1829
35	100.4446	381.23	2397.91	.8895	6.2900
36	101.4546	372.04	2480.94	.9203	6.6684
37	102.4603	362.34	2294.13	.8510	6.3315
38	103.4446	352.39	2338.34	.8674	6.6356
39	104.4648	341.63	2124.83	.7882	6.2197

HEAT CAPACITIES (cont.)

N_{TOT} = 517.03 STPCC

Point	T (K)	N (STPCC)	C (STPCC-k_B)	C (J/K)	C/Nk_B
1	64.0190	516.81	2397.37	.8893	4.6388
2	65.7570	516.66	2604.68	.9662	5.0414
3	67.4024	516.49	2710.90	1.0056	5.2487
4	68.5509	516.32	2481.48	.9205	4.8061
5	69.6900	516.13	2594.71	.9625	5.0272
6	70.7594	515.89	2645.12	.9812	5.1273
7	71.8317	515.56	2705.77	1.0037	5.2482
8	72.9261	515.19	2796.08	1.0372	5.4273
9	73.9848	514.75	2907.42	1.0785	5.6482
10	75.0158	514.23	3037.63	1.1268	5.9071
11	76.0517	513.63	3294.81	1.2222	6.4147
12	77.1308	512.85	3270.27	1.2131	6.3767
13	78.1675	511.97	3364.90	1.2482	6.5725
14	79.2044	510.95	3040.86	1.1280	5.9514
15	80.2304	509.77	2798.24	1.0380	5.4892
16	81.2598	508.38	2815.76	1.0445	5.5387
17	82.2876	506.77	2810.10	1.0424	5.5451
18	83.3070	504.96	2804.17	1.0402	5.5532
19	84.3226	502.88	2864.56	1.0626	5.6963
20	85.3226	500.54	2663.72	.9881	5.3217
21	86.8506	496.43	3238.73	1.2014	6.5241
22	87.7668	493.58	3499.42	1.2981	7.0898
23	88.7039	490.37	4515.73	1.6751	9.2089
24	89.6153	486.95	9811.36	3.6395	20.1486
25	90.5242	483.18	8405.77	3.1181	17.3968
26	91.5323	478.68	5017.42	1.8612	10.4818
27	92.6829	473.10	3708.61	1.3757	7.8389
28	93.6729	467.85	3468.42	1.2866	7.4135
29	94.6693	462.06	3192.64	1.1843	6.9095
30	95.6861	455.68	3031.16	1.1244	6.6519
31	96.7008	448.82	2907.96	1.0787	6.4791
32	97.7344	441.24	2748.37	1.0195	6.2288
33	98.7610	433.13	2874.53	1.0663	6.6366
34	99.7977	424.27	2532.43	.9394	5.9689
35	100.8374	414.83	2721.14	1.0094	6.5596
36	101.8865	404.67	2623.82	.9733	6.4838
37	102.9211	393.88	2901.49	1.0763	7.3664
38	103.9505	382.66	2569.10	.9530	6.7137
39	104.9522	371.11	2808.75	1.0419	7.5685

HEAT CAPACITIES (cont.)

N_{TOT} = 555.86 STPCC

Point	T (K)	N (STPCC)	C (STPCC-k_B)	C (J/K)	C/Nk_B
1	64.1182	555.52	2592.01	.9615	4.6659
2	65.1356	555.42	2456.95	.9114	4.4236
3	66.2062	555.34	2550.77	.9462	4.5932
4	67.3321	555.20	2556.70	.9484	4.6050
5	68.3543	555.04	2706.04	1.0038	4.8754
6	69.3542	554.82	2782.07	1.0320	5.0144
7	70.3709	554.61	2654.82	.9848	4.7868
8	71.3064	554.35	2783.68	1.0326	5.0215
9	72.2126	554.05	2927.64	1.0860	5.2841
10	73.1597	553.70	3081.57	1.1431	5.5654
11	74.1430	553.26	3162.17	1.1730	5.7155
12	75.1240	552.78	3459.52	1.2833	6.2584
13	76.1068	552.15	3597.54	1.3345	6.5155
14	77.1601	551.38	3364.90	1.2482	6.1027
15	79.0739	549.54	3014.71	1.1183	5.4859
16	82.1719	545.39	3027.92	1.1232	5.5518
17	83.2263	543.51	3074.83	1.1406	5.6574
18	85.3769	538.81	3209.08	1.1904	5.9559
19	86.4402	535.99	3469.49	1.2870	6.4730
20	87.4721	532.87	3868.47	1.4350	7.2597
21	88.4706	529.50	4565.34	1.6935	8.6219
22	89.4332	525.92	8125.14	3.0140	15.4494
23	90.3206	522.29	12759.76	4.7332	24.4306
24	91.2142	518.36	5707.28	2.1171	11.0103
25	92.1467	513.92	4992.08	1.8518	9.7138
26	93.1064	508.89	4076.86	1.5123	8.0112
27	94.0922	503.34	3836.39	1.4231	7.6219
28	95.1314	496.99	3405.87	1.2634	6.8530
29	96.2307	489.68	3188.86	1.1829	6.5121
30	97.2781	482.10	2835.44	1.0518	5.8815
31	98.3019	474.06	2765.08	1.0257	5.8328
32	99.3175	465.53	2850.27	1.0573	6.1226
33	100.3382	456.20	2837.33	1.0525	6.2195
34	101.3696	446.18	2829.24	1.0495	6.3410
35	102.3760	435.75	2722.76	1.0100	6.2484
36	103.3845	424.67	2527.58	.9376	5.9519
37	104.3879	412.92	2629.21	.9753	6.3673

Interpolated Heat Capacities and Specific Heats

While the preceding heat capacity tables cover a wide range of coverage and temperature, the points are distributed more or less randomly over the N-T plane. Thus, anyone using them for numerical work would likely find the task cumbersome. For this reason, these same data have been interpolated to integral values of temperature, and re-listed in the following tables.

INTERPOLATED HEAT CAPACITIES AND SPECIFIC HEATS

T (K)	N (STPCC)	C (STPCC-k_B)	C (J/K)	C/Nk_B
64	476.97	2417.46	.8967	5.0682
65	555.44	2474.95	.9181	4.4559
	516.72	2514.39	.9327	4.8660
	476.91	2323.85	.8620	4.8725
	437.10	2115.28	.7847	4.8395
66	555.34	2532.70	.9395	4.5605
	516.63	2620.37	.9720	5.0720
	476.83	2382.99	.8840	4.9975
	437.02	2256.88	.8372	5.1641
67	555.22	2554.95	.9478	4.6015
	516.53	2684.92	.9960	5.1980
	476.73	2388.61	.8861	5.0104
	436.93	2236.68	.8297	5.1190
	275.96	1304.88	.4840	4.7287
68	555.08	2654.28	.9846	4.7817
	516.40	2591.53	.9613	5.0184
	476.61	2332.63	.8653	4.8945
	436.80	2142.76	.7949	4.9056
	275.85	1334.38	.4950	4.8372
	236.93	1270.60	.4713	5.3635
	198.56	993.20	.3684	5.0020
	160.37	846.89	.3142	5.2813
	121.74	625.93	.2322	5.1418
	99.25	483.23	.1793	4.8684
	83.56	272.85	.1012	3.2661
	45.05	410.05	.1521	9.1022
69	554.91	2755.14	1.0220	4.9652
	516.24	2526.12	.9371	4.8933
	476.45	2304.27	.8548	4.8367
	436.65	2159.16	.8009	4.9449
	275.72	1311.00	.4863	4.7550
	236.80	1302.53	.4832	5.5010
	198.45	989.12	.3669	4.9845
	177.25	733.24	.2720	4.1369
	160.31	830.66	.3081	5.1823
	121.68	606.36	.2249	4.9842
	99.20	565.33	.2097	5.6993
	83.56	231.15	.0857	2.7664
	45.05	361.95	.1343	8.0345
70	554.70	2701.24	1.0020	4.8698
	516.04	2609.32	.9679	5.0562
	476.26	2358.58	.8749	4.9525
	436.46	2223.72	.8249	5.0951
	275.56	1361.12	.5049	4.9399

I.TERPOLATED HEAT CAPACITIES (cont.)

T (K)	N (STPCC)	C (STPCC-k_B)	C (J/K)	C/Nk_B
70	236.65	1273.06	.4722	5.3799
	198.32	998.46	.3704	5.0344
	177.17	836.93	.3105	4.7245
	160.24	823.41	.3054	5.1394
	121.61	655.12	.2430	5.3880
	99.14	491.73	.1824	4.9594
	83.55	278.76	.1034	3.3352
	45.05	333.64	.1238	7.4059
71	554.44	2741.48	1.0169	4.9446
	515.81	2658.73	.9862	5.1544
	476.03	2427.24	.9004	5.0988
	436.23	2205.37	.8181	5.0557
	275.37	1411.71	.5237	5.1268
	236.46	1263.35	.4686	5.3431
	198.15	1054.71	.3912	5.3231
	177.06	964.59	.3578	5.4484
	160.15	831.21	.3083	5.1906
	121.52	587.22	.2178	4.8317
	99.06	543.57	.2016	5.4879
	83.55	270.93	.1005	3.2427
	45.05	319.22	.1184	7.0859
72	554.14	2893.87	1.0735	5.2225
	515.52	2719.66	1.0089	5.2757
	475.75	2562.33	.9505	5.3857
	435.96	2306.12	.8554	5.2894
	275.14	1470.78	.5456	5.3456
	236.24	1280.24	.4749	5.4188
	197.95	1075.39	.3989	5.4330
	176.93	923.22	.3425	5.2180
	160.04	855.42	.3173	5.3448
	121.41	607.62	.2254	5.0038
	98.96	550.75	.2043	5.5660
	83.55	324.54	.1204	3.8832
	45.05	314.29	.1166	6.9764
73	553.78	3055.61	1.1335	5.5180
	515.17	2803.85	1.0401	5.4427
	475.41	2550.93	.9463	5.3660
	435.62	2353.44	.8730	5.4023
	274.85	1550.67	.5752	5.6417
	235.96	1339.48	.4969	5.6769
	197.71	1140.02	.4229	5.7668
	176.78	1013.34	.3759	5.7316
	159.91	844.93	.3134	5.2842
	121.28	623.57	.2313	5.1407
	98.85	494.54	.1834	5.0033
	83.54	318.55	.1182	3.8122
	45.05	346.42	.1285	7.6896

INTERPOLATED HEAT CAPACITIES (cont.)

T (K)	N (STPCC)	C (STPCC-k_B)	C (J/K)	C/Nk_B
74	553.35	3150.45	1.1687	5.6937
	514.75	2909.34	1.0792	5.6520
	475.00	2692.42	.9987	5.6682
	435.22	2393.51	.8879	5.4998
	274.52	1661.90	.6165	6.0546
	235.64	1374.08	.5097	5.8320
	197.43	1171.49	.4346	5.9346
	176.59	1012.88	.3757	5.7363
	159.75	934.70	.3467	5.8507
	121.13	664.84	.2466	5.4892
	98.72	542.51	.2012	5.4964
	83.54	334.39	.1240	4.0016
	45.05	301.07	.1117	6.6829
75	552.84	3421.93	1.2694	6.1898
	514.26	3035.63	1.1261	5.9031
	474.52	2936.10	1.0891	6.1875
	434.74	2579.66	.9569	5.9340
	274.12	2045.85	.7589	7.4635
	235.25	1522.71	.5648	6.4737
	197.08	1181.60	.4383	5.9964
	176.37	1100.65	.4083	6.2413
	159.56	1019.98	.3784	6.3932
	120.94	718.05	.2664	5.9383
	98.56	665.98	.2470	6.7591
	83.53	354.88	.1316	4.2479
	45.05	287.52	.1067	6.3814
76	552.23	3582.55	1.3289	6.4876
	513.66	3281.97	1.2174	6.3894
	473.95	3129.36	1.1608	6.6029
	434.18	2800.22	1.0387	6.4499
	273.65	2109.09	.7824	7.7072
	234.79	1638.72	.6079	6.9800
	196.68	1217.67	.4517	6.1921
	176.10	1080.42	.4008	6.1350
	159.33	1114.12	.4133	6.9930
	120.71	758.75	.2815	6.2865
	98.37	663.18	.2460	6.7418
	83.52	313.95	.1165	3.7590
	45.05	296.19	.1099	6.5736
77	551.49	3400.26	1.2613	6.1654
	512.95	3273.25	1.2142	6.3813
	473.28	3172.63	1.1769	6.7039
	433.51	2914.62	1.0812	6.7237
	273.09	2019.49	.7491	7.3950
	234.25	1720.62	.6383	7.3458
	196.20	1263.80	.4688	6.4409
	175.77	1031.91	.3828	5.8709

INTERPOLATED HEAT CAPACITIES (cont.)

T (K)	N (STPCC)	C (STPCC-k_B)	C (J/K)	C/Nk_B
77	159.06	1152.76	.4276	7.2478
	120.43	812.40	.3014	6.7465
	98.16	542.79	.2013	5.5301
	83.50	325.07	.1206	3.8937
	45.05	269.11	.0998	5.9737
78	550.60	3211.21	1.1912	5.8320
	512.13	3349.61	1.2425	6.5409
	472.48	3036.76	1.1265	6.4273
	432.75	3001.57	1.1134	6.9367
	272.43	1882.45	.6983	6.9098
	233.60	1727.52	.6408	7.3948
	195.66	1192.07	.4422	6.0926
	175.38	1051.38	.3900	5.9948
	158.74	1173.27	.4352	7.3922
	120.11	858.56	.3185	7.1479
	97.92	499.08	.1851	5.0962
	83.48	362.40	.1344	4.3423
	45.05	239.71	.0889	5.3211
79	549.63	3028.23	1.1233	5.5097
	511.17	3104.74	1.1517	6.0738
	471.53	2870.43	1.0648	6.0878
	431.86	2989.33	1.1089	6.9223
	271.65	1812.62	.6724	6.6730
	232.88	1593.03	.5909	6.8407
	195.04	1207.26	.4478	6.1899
	174.93	1104.48	.4097	6.3153
	158.36	1207.24	.4478	7.6242
	119.74	758.02	.2812	6.3306
	97.65	497.17	.1844	5.0906
	83.45	310.94	.1153	3.7274
	45.05	171.21	.0635	3.8009
80	548.49	3018.66	1.1198	5.5056
	510.05	2852.72	1.0582	5.5930
	470.43	2803.15	1.0398	5.9587
	430.82	2752.47	1.0210	6.3891
	270.74	1708.23	.6337	6.3097
	232.07	1559.74	.5786	6.7219
	194.33	1257.56	.4665	6.4715
	174.38	1117.29	.4145	6.4081
	157.93	1254.89	.4655	7.9464
	119.31	827.94	.3071	6.9395
	97.35	486.42	.1804	4.9971
	83.42	406.95	.1510	4.8796
	45.05	258.12	.0957	5.7320
81	547.18	3022.93	1.1213	5.5269
	508.75	2811.34	1.0429	5.5262

INTERPOLATED HEAT CAPACITIES (cont.)

T (K)	N (STPCC)	C (STPCC-k_B)	C (J/K)	C/Nk_B
81	469.15	2525.28	.9367	5.3827
	429.61	2442.49	.9060	5.6854
	269.69	1696.92	.6295	6.2929
	231.13	1523.47	.5651	6.5916
	193.52	1375.33	.5102	7.1083
	173.74	1132.31	.4200	6.5183
	157.43	1286.70	.4773	8.1733
	118.81	823.90	.3056	6.9339
	97.01	545.46	.2023	5.6254
	83.38	283.99	.1053	3.4058
	45.05	234.54	.0870	5.2054
82	545.67	3027.19	1.1229	5.5481
	507.25	2811.69	1.0430	5.5433
	467.69	2458.42	.9119	5.2565
	428.21	2198.55	.8155	5.1345
	268.49	1634.59	.6063	6.0886
	230.05	1425.78	.5289	6.1975
	192.61	1442.62	.5351	7.4909
	173.00	1203.99	.4466	6.9615
	156.84	1233.35	.4575	7.8634
	118.24	660.59	.2450	5.5843
	96.64	562.34	.2086	5.8185
	83.34	300.48	.1115	3.6040
	45.05	213.93	.0794	4.7489
83	543.95	3064.76	1.1369	5.6347
	505.54	2805.96	1.0409	5.5508
	466.01	2392.31	.8874	5.1334
	426.61	2216.38	.8222	5.1953
	267.12	1707.52	.6334	6.3942
	228.82	1330.37	.4935	5.8142
	191.58	1478.67	.5485	7.7201
	172.16	1199.07	.4448	6.9644
	156.15	1144.75	.4246	7.3316
	117.60	552.99	.2051	4.7017
	96.24	490.03	.1818	5.0936
	83.30	306.50	.1137	3.6804
	45.05	199.22	.0739	4.4213
84	541.97	3123.13	1.1585	5.7648
	503.58	2845.38	1.0555	5.6508
	464.09	2493.19	.9248	5.3723
	424.76	2267.06	.8410	5.3372
	265.58	1766.75	.6554	6.6535
	227.43	1307.96	.4852	5.7509
	190.41	1473.40	.5466	7.7394
	171.21	1111.12	.4122	6.4909
	155.35	1071.60	.3975	6.8984
	116.88	580.54	.2154	4.9689

INTERPOLATED HEAT CAPACITIES (cont.)

T (K)	N (STPCC)	C (STPCC-k_B)	C (J/K)	C/Nk_B
84	95.80	566.89	.2103	5.9178
	83.25	311.84	.1157	3.7463
	45.05	202.50	.0751	4.4937
85	539.73	3185.55	1.1817	5.9036
	501.33	2728.51	1.0121	5.4425
	461.86	2411.93	.8947	5.2215
	422.68	2189.46	.8122	5.1796
	263.85	1707.73	.6335	6.4732
	225.87	1331.55	.4939	5.8949
	189.10	1476.94	.5479	7.8126
	170.14	1144.13	.4244	6.7234
	154.46	976.99	.3624	6.3246
	116.09	619.31	.2297	5.3356
	95.34	569.66	.2113	5.9754
	83.20	342.49	.1270	4.1168
	45.05	223.39	.0829	4.9586
86	537.21	3361.68	1.2470	6.2589
	498.77	2918.64	1.0827	5.8548
	459.45	2636.79	.9781	5.7421
	420.32	2264.69	.8401	5.3882
	261.91	1703.07	.6318	6.5051
	224.11	1404.81	.5211	6.2690
	187.65	1536.10	.5698	8.1874
	168.96	1016.12	.3769	6.0149
	153.44	974.20	.3614	6.3501
	115.20	611.76	.2269	5.3112
	94.85	515.06	.1911	5.4309
	83.13	349.44	.1296	4.2036
	45.05	232.27	.0862	5.1567
87	534.36	3685.94	1.3673	6.8998
	495.98	3281.24	1.2172	6.6163
	456.71	2919.73	1.0831	6.3943
	417.65	2544.67	.9439	6.0925
	259.75	1776.99	.6592	6.8428
	222.15	1402.27	.5202	6.3124
	186.04	1553.05	.5761	8.3497
	167.66	1110.41	.4119	6.6237
	152.30	945.50	.3507	6.2084
	114.23	595.91	.2211	5.2170
	94.34	482.97	.1792	5.1206
	83.06	342.57	.1271	4.1252
	45.05	204.52	.0759	4.5399
88	531.16	4236.90	1.5717	7.9799
	492.81	3752.33	1.3919	7.6171
	453.62	3459.92	1.2834	7.6306
	414.64	3072.94	1.1399	7.4109

INTERPOLATED HEAT CAPACITIES (cont.)

T (K)	N (STPCC)	C (STPCC-k_B)	C (J/K)	C/Nk_B
88	257.38	1837.30	.6815	7.1397
	219.98	1529.74	.5675	6.9565
	184.29	1580.48	.5863	8.5770
	166.24	1239.72	.4599	7.4592
	151.03	936.41	.3474	6.2029
	113.17	583.94	.2166	5.1612
	93.80	534.79	.1984	5.7039
	82.97	378.82	.1405	4.5665
	45.04	196.82	.0730	4.3688
89	527.60	6523.13	2.4197	12.3768
	489.29	6236.19	2.3133	12.7630
	450.16	5701.11	2.1148	12.6845
	411.24	4996.72	1.8535	12.1499
	254.77	1900.60	.7050	7.4623
	217.58	1553.32	.5762	7.1403
	182.42	1554.52	.5766	8.5223
	164.70	1143.58	.4242	6.9434
	149.61	923.95	.3427	6.1747
	112.02	633.50	.2350	5.6549
	93.25	505.38	.1875	5.4167
	82.87	413.84	.1535	4.9941
	45.04	135.92	.0504	3.0181
90	523.64	11085.36	4.1121	21.1859
	485.37	9216.44	3.4188	18.9839
	446.28	8092.44	3.0019	18.1200
	407.45	7527.53	2.7923	18.4686
	251.91	1972.57	.7317	7.8332
	214.89	1474.52	.5470	6.8617
	180.42	1456.49	.5403	8.0732
	163.03	1093.25	.4055	6.7066
	148.05	821.95	.3049	5.5536
	110.79	633.02	.2348	5.7138
	92.65	457.73	.1698	4.9431
	82.75	478.74	.1776	5.7855
	45.04	263.47	.0977	5.8481
91	519.29	7397.81	2.7442	14.2272
	481.12	6806.56	2.5249	14.1331
	442.09	5285.38	1.9606	11.9464
	403.34	3798.60	1.4091	9.4160
	248.77	2041.56	.7573	8.2072
	211.96	1471.37	.5458	6.9458
	178.31	1473.82	.5467	8.2658
	161.23	1044.20	.3873	6.4771
	146.33	843.29	.3128	5.7644
	109.48	620.88	.2303	5.6712
	92.01	576.56	.2139	6.2652
	82.57	490.50	.1820	5.9417

INTERPOLATED HEAT CAPACITIES (cont.)

T (K)	N (STPCC)	C (STPCC-k_B)	C (J/K)	C/Nk_B
91	45.04	171.01	.0634	3.7962
92	514.57	5104.60	1.8935	9.9178
	476.45	4485.41	1.6639	9.4075
	437.57	3889.16	1.4427	8.8850
	398.92	3097.46	1.1490	7.7639
	245.31	1991.96	.7389	8.1212
	208.73	1489.88	.5527	7.1392
	176.08	1369.55	.5080	7.7772
	159.28	1046.37	.3881	6.5736
	144.46	838.15	.3109	5.8019
	108.10	594.55	.2205	5.4997
	91.38	583.63	.2165	6.3859
	82.31	398.40	.1478	4.8412
	45.04	148.57	.0551	3.3006
93	509.42	4178.33	1.5499	8.2000
	471.43	3631.68	1.3472	7.7026
	432.66	3360.40	1.2465	7.7658
	394.10	2806.65	1.0411	7.1208
	241.56	2035.16	.7549	8.4251
	205.25	1467.34	.5443	7.1512
	173.75	1355.96	.5030	7.8053
	157.17	1065.30	.3952	6.7792
	142.43	814.07	.3020	5.7161
	106.68	612.63	.2273	5.7462
	90.76	618.94	.2296	6.8197
	81.93	258.10	.0957	3.1502
	45.03	218.99	.0812	4.8655
94	503.83	3858.88	1.4314	7.6583
	465.95	3377.88	1.2530	7.2480
	427.33	2899.48	1.0756	6.7815
	388.89	2604.48	.9661	6.6969
	237.43	1944.69	.7214	8.1895
	201.56	1386.33	.5143	6.8739
	171.31	1433.92	.5319	8.3736
	154.90	1009.18	.3744	6.5146
	140.23	766.27	.2842	5.4638
	105.20	649.30	.2409	6.1725
	90.12	576.43	.2138	6.3960
	81.43	162.42	.0603	1.9941
	45.03	220.79	.0819	4.9045
95	497.76	3460.31	1.2836	6.9502
	460.02	3140.12	1.1648	6.8257
	421.60	2896.00	1.0743	6.8759
	383.24	2463.93	.9140	6.4297
	232.94	1767.73	.6557	7.5880
	197.70	1253.11	.4648	6.3423

INTERPOLATED HEAT CAPACITIES (cont.)

T (K)	N (STPCC)	C (STPCC-k_B)	C (J/K)	C/Nk_B
95	168.79	1451.94	.5386	8.6033
	152.47	955.76	.3545	6.2708
	137.87	756.44	.2806	5.4886
	103.73	679.82	.2522	6.5554
	89.47	726.15	.2694	8.1228
	80.83	467.49	.1734	5.7908
	45.02	237.04	.0879	5.2646
96	491.18	3234.40	1.1998	6.5836
	453.60	2993.05	1.1103	6.5984
	415.30	2954.86	1.0961	7.1113
	377.16	2682.50	.9951	7.1112
	166.15	1458.61	.5411	8.7826
	88.77	810.13	.3005	9.1272
	80.42	652.14	.2419	8.1044
	45.02	250.33	.0929	5.5589
97	484.11	2929.28	1.0866	6.0489
	446.66	2861.76	1.0616	6.4066
	408.56	2911.26	1.0799	7.1307
	370.61	2424.06	.8992	6.5405
	45.01	265.38	.0984	5.8941
98	476.45	2785.83	1.0334	5.8472
	439.16	2781.01	1.0316	6.3343
	401.25	2733.60	1.0140	6.8079
	363.58	2399.35	.8900	6.6000
99	468.20	2823.64	1.0474	6.0320
	431.12	2795.67	1.0370	6.4827
	393.43	2447.32	.9078	6.2210
	356.15	2568.65	.9528	7.2142
100	459.32	2841.62	1.0541	6.1874
	422.47	2569.15	.9530	6.0838
	385.08	2403.31	.8915	6.2424
	348.29	2690.68	.9981	7.7252
101	449.84	2832.14	1.0506	6.2975
	413.27	2706.06	1.0038	6.5479
	376.23	2443.57	.9064	6.4981
	340.04	2664.72	.9885	7.8361
102	439.72	2762.54	1.0248	6.2830
	403.45	2654.28	.9846	6.5806
	366.87	2379.63	.8827	6.4857
	331.35	2557.71	.9488	7.7195
103	428.93	2601.99	.9652	6.0649
	393.02	2876.01	1.0668	7.3164

INTERPOLATED HEAT CAPACITIES (cont.)

T (K)	N (STPCC)	C (STPCC-k_B)	C (J/K)	C/Nk_B
103	356.95	2318.37	.8600	6.4982
	322.27	2497.06	.9263	7.7490
104	417.51	2589.92	.9607	6.2067
	382.02	2580.94	.9574	6.7559
	346.60	2222.10	.8243	6.4092
	312.84	2455.27	.9108	7.8497

References

[1] G. P. Matthews and E. B. Smith, Mol. Phys. **32**, 1719 (1976).

[2] A. D. Migone, M. H. W. Chan, and J. R. Boyer, Physica **108B**, 787 (1981) (Proceedings, LT-16).

[3] J. K. Kjems, L. Passell, H. Taub, J. G. Dash, and A. D. Novaco, Phys. Rev. B**13**, 1446 (1976).

[4] A. Thomy and X. Duval J. Chim. Phys.: (I) **66**, 1966 (1969); (II) **67**, 286 (1970); (III) **67**, 1101 (1970).

[5] Y. Larher, J. Chem. Phys. **68**, 2257 (1978)

[6] C. Bockel, A. Thomy, and X. Duval, Surf. Sci. **90**, 109 (1979)

[7] A. Thomy, X. Duval, and J. Regnier, Surf. Sci. Rpts. **1**, 1 (1981). This reference is a concise review of the technique of vapor pressure isotherm measurements.

[8] (a) J. P. Coulomb, R. Kahn, and M. Bienfait, Surf. Sci. **61**, 291 (1976)

(b) J. P. Coulomb, M. Bienfait, and P. Thorel, J. de Physique Colloq. **38** C4-31 (1977)

(c) J. P. Coulomb, M. Bienfait, and P. Thorel, Phys. Rev. Lett. **42**, 733 (1979)

(d) M. Bienfait, Surf. Sci. **89**, 13 (1979)

(e) A. Glachant, J. P. Coulomb, M. Bienfait, and J. G. Dash, J. de Physique Lett. **40**, L-543 (1979)

(f) J. P. Coulomb, M. Bienfait, and P. Thorel, J. de Physique **42**, 293 (1981).

[9] P. Vora, S. K. Sinha, and R. K. Crawford, Phys. Rev. Lett. **43**, 704 (1979).

[10] (a) I. Marlow, R. K. Thomas, T. D. Trewern, and J. W. White, J. de Physique Colloq **38**, C4-19 (1977)

(b) M. W. Newberry, et. al., Chem. Phys. Lett. **59**, 461 (1978)

(c) G. Bomchil, et. al., Phil. Trans. R. Soc. Lond. B **290**, 537 (1980).

[11] J. W. Riehl andK. Koch, J. Chem. Phys. **57**, 2199 (1972).

[12] J. H. Quateman and M. Bretz, Phys. Rev. Lett. **49**, 1503 (1982).

[13] R. Marx and E. F. Wasserman, Surf. Sci. **117**, 267 (1981); Sol. St. Commun. **40**, 959 (1981), and R. Marx, Z. Phys. B **46**, 237 (1982).

[14] A. G. Bezus, V. P. Dreving, and A. V. Kiselev, Russ. J. Phys. Chem. **38**, 1589 (1964).

[15] J. G. Dash and J. Siegwarth, Rev. Sci. Instrum. **34**, 1276 (1963).

[16] Datametrics, Inc., Wilmington, Massachussetts.

[17] R. Pandit, M. Schick, and M. Wortis, Phys. Rev. B **26**, 5112 (1982).

[18] R. L. Elgin and D. L. Goodstein Phys. Rev. A **9**, 2657 (1974).

[19] M. Bretz, J. G. Dash, D. C. Hickernell, E. O. McLean, and O. E. Vilches, Phys. Rev. A **8**, 1589 (1973).

[20] P. Taborek and D. L. Goodstein, Rev. Sci. Instrum. **50**, 227 (1979).

[21] Lake Shore Cryotronics, Inc., Westerville, Ohio.

[22] L. G. Rubin and Y. Golahny, Rev. Sci. Instrum. **43**, 1758 (1972).

[23] J. G. Dash, R. E. Peierls, and G. A. Stewart, Phys. Rev. A **2**, 932 (1970).

[24] Robert L. Elgin, thesis, California Institute of Technology (1973).

[25] L. D. Landau and E. M. Lifschitz, *Statistical Physics*, 3rd ed. Part 1, Pergamon Press (1980). See p. 72.

[26] David L. Goodstein, *States of Matter*, Prentice-Hall (1975). See p. 473.

[27] T. Takaishi and Y. Sensui, Trans. Faraday Soc. **59**, 2503 (1963).

[28] G. T. Armstrong, F. G. Brickwedde, and R. B. Scott, J. Res. NBS **55**, 39 (1955).

[29] Ref. 25, Chap. XV.

[30] J. G. Dash, Phys. Rev. B **15**, 3136 (1977); J. de Physique Colloq. **38**, C4-201 (1977).

[31] J. E. Avron, L. S. Balfour, C. G. Kuper, J. Landau, S. G. Lipson, and L. S. Schulman, Phys. Rev. Lett. **45**, 814 (1980).

[32] K. A. Jackson and C. E. Miller, J. Crystal Growth **40**, 169 (1977).

[33] M. W. Cole, J. Chem. Phys. **73**, 4012 (1980).

[34] M. J. de Oliveira and R. B. Griffiths, Surf. Sci. **71**, 687 (1978).

[35] R. Pandit and M. Wortis, Phys. Rev. B **25**, 3226 (1982).

[36] C. Ebner, Phys. Rev. A **22**, 2776 (1980).

[37] C. Ebner, Phys. Rev. A **23**, 1925 (1981).

[38] C. Ebner, to be published.

[39] J. D. Weeks, Phys. Rev. B **26**, 3998 (1982).

[40] I. M. Kim and D. P. Landau, Surf. Sci. **110**, 415 (1981).

[41] W. F. Saam, Surf. Sci. **125**, 253 (1983).

[42] H. Nakanishi and M. E. Fisher, Phys. Rev. Lett. **49**, 1565 (1982).

[43] O'D. Kwon, et. al., Phys. Rev. Lett. **48**, 185 (1982).

[44] D. W. Pohl and W. I. Goldberg, Phys. Rev. Lett. **48**, 1111 (1982).

[45] J. W. White, et. al., Surf. Sci. **76**, 13 (1978).

[46] J. Menaucourt, A. Thomy, and X. Duval, J. de Physique Colloq. **38**, C4-195 (1977).

[47] Y. Larher and D. Haranger, Surf. Sci. **39**, 100 (1973).

[48] J. G. Dash and R. D. Puff, Phys. Rev. B **24**, 295 (1981).

[49] F. A. Putnam and T. Fort, Jr., J. Phys. Chem. **79**, 459 (1975).

[50] S. Rauber, J. R. Klein, and M. W. Cole, Phys. Rev. B **27**, 1314 (1983).

[51] For a discussion of this point see R. E. Ecke and J. G. Dash, to be published.

[52] See, for example, K. Dennis, E. L. Pace, and C. S. Baughman, J. Amer. Chem. Soc. **75**, 3269 (1953), and J. A. Morrison, L. E. Drain, and J. S. Dugdale, Can. J. Chem. **30**, 890 (1952).

[53] M. Bretz, Phys. Rev. Lett. **31**, 1447 (1973).

[54] Recently, however, these experiments have been re-examined, and somewhat different results were obtained. See J. Yuyama and T. Watanabe, J. Low Temp. Phys. **48**, 331 (1982).

[55] T. T. Chung and J. G. Dash, J. Chem. Phys. **64**, 1855 (1976).

[56] The theory of Kosterlitz and Thouless, Halperin and Nelson, and Young is described in the following original papers: J. M. Kosterlitz and D. J. Thouless, J. Phys. C **6**, 1181 (1973); D. R. Nelson and B. I. Halperin, Phys. Rev. B **19**, 2457 (1979); A. P. Young, Phys. Rev. B **19**, 1855 (1979). See also W. F. Brinkman, D. S. Fisher, and M. E. Moncton, Science **217**, 693 (1982).

[57] R. L. Elgin, J. M. Greif, and D. L. Goodstein, Phys. Rev. Lett. **41**, 1723 (1978).

[58] J. Rouquerol, S. Partyka, and F. Rouquerol, J. Chem. Soc. Faraday Trans. I **73**, 306 (1977).